Dear Editor,

Please find below my responses to all comments (referee comments and short comment):

Title: Variation in brachiopod microstructure and isotope geochemistry under low pH–ocean acidification–conditions

Authors: Facheng Ye, Hana Jurikova, Lucia Angiolini, Uwe Brand, Gaia Crippa, Daniela Henkel, Jürgen Laudien, Claas Hiebenthal, and Danijela Šmajgl

MS No.: bg-2018-332

MS Type: Research article

The responses to referees are structured following this sequence using different colours:

(1) Comments from Referees;

(2) Author's response;

(3) Changes in the manuscript: original sentences/revised sentences

We want to thank very much Karem Azmy, the anonymous reviewer 2 and Emma Cross for the very constructive, helpful and valuable comments and corrections, which helped us to ameliorate the manuscript.

1. Comments from K. Azmy (Referee): Received and published: 13 August 2018

I have read the manuscript by Ye et al entitled "Variation in brachiopod microstructure and isotope geochemistry under low pH–ocean acidification–conditions", which test the ultrastructural and stable isotope geochemical variations in the shell of M. venosa shells that were partially cultured under different pH conditions. The subject of the manuscript fits well within the scope of BG and the paper present a novel application to brachiopods that are known to archive the climatic and oceanographic conditions of the ambient seawater.

The title reflects the paper contents and the abstract is concise and to the point. The authors used the proper methodology and utilized the most suitable tools to perform their investigation that lead to clear and reliable and good results that will contribute significantly to the subject of study. The experimental procedure is clear and the statistical analyses utilized are suitable. The references are up to date and the general structure of the manuscript is appropriate.

I have some minor comments that I list hereby below.

1) Page 7 Line 6: How were samples transported? in what type of containers and under what conditions of transportation. Provide couple of lines that describe the conditions during transportation and how they were maintained to simulate the original environment as close as possible.

Answer:

We agree with the referee's suggestion and we have added the requested information in the revised manuscript.

Page 7 Line 6:

In summary, *M. venosa* individuals sampled in Chile were transported to Germany and cultured under controlled environmental setting in a climate laboratory.

changed to

In summary, individuals of *M. venosa* were collected alive in Chile and transported to GEOMAR, Germany in plastic bags filled with seawater, and maintained under controlled conditions in a climate laboratory.

2) Page 11 Line 7: "Four sub-zones (C2, A1, A2, A3)", a figure is needed to be cited here to show the positions of those sub-zones.

Answer:

We have added the legend showing positions in the revised figure 4.

Page 11 Line 7:

Four sub-zones (C2, A1, A2, A3) were defined according to their position along the posterior-anterior direction,

changed to

Four sub-zones (C2, A1, A2, A3) were defined according to their position along the posterior-anterior direction (Figure 4),

3) Page 15 Line 3: after "microdrill" add here at "low speed"

Answer:

We have added it in the revised manuscript.

Page 15 Line 3:
microdrill with tungsten–carbide milling bit.
changed to
microdrill at low speed with tungsten–carbide milling bit.

4) Page 16 caption of Table 5: "are marked in bold style". There nothing is marked in bold font in the table. Mark those values in bold font. Also replace "style" by "font" or you can delete the entire word "style" and leave it as "marked in bold". Change to "N" into "n" in italic font and fix it in the rest of table headings. This way you do not need to repeat it in the following table captions
Answer:
We have made all these corrections in the caption and in Table 5.
Page 16 caption of Table 5:
are marked in bold style
changed to
are marked in bold

5) Page 17 Line 12: "worth noting" change to "noteworthy"
Answer:
We have changed it in the revised manuscript.
Page 17 Line 12:
However, it is worth noting that in the most anterior part
changed to
However, it is noteworthy that in the most anterior part

6) Caption of Table 6: What does this mean? " "â´S˘a: Specific zones see to Figure 7". Something is wrong. Delete "to" Also no specific zones marked on Figure 7. This is confusing and similarly in the Caption of Table 7.
Answer:
We have made this correction in the revised manuscript.
specific zones marked on Figure 7
changed to
position of zones before culturing: C2, and post culturing: A1, A2, A3 (cf. Figure 7)

7) Is STD 1 sigma or 2 sigma. Replace by the correct value and use the Greek proper letter. Fix it in the rest of the manuscript and table captions when applicable If you used exel for your calculations, then this is 1ïA¿s¸.
Answer:
We have made the correction in the table caption, and fixed it in the rest of the manuscript and table captions.
We have added this sentence in the captions of Tables 5, also changed STD to σ in the other tables (6-10):
Population standard deviation (σ) was calculated using the Excel STDEV.P function.

8) Page 28 Line 27: "which in", delete "in" and replace by "during". Also add "s" to "expansion"

Answer:

We have made this correction in the revised manuscript.

Page 28 Line 26:

Endopunctae, which in life are filled with mantle expansion,

changed to

Endopunctae, which during life are filled with mantle expansions,

9) Page 31 Line 6, add "," after "inconspicua"

Answer:

We have added it in the revised manuscript.

Page 31 Line 6:

For the Antarctic brachiopod *Liothyrella uva* and the New Zealand brachiopod *Calloria inconspicua* no ocean acidification effects on shell growth were detected by Cross et al. (2015, 2016, 2018),

changed to

For brachiopods, in the *Liothyrella uva* (Antarctic) and *Calloria inconspicua* (New Zealand), no ocean acidification effects on shell growth were detected by Cross et al. (2015, 2016, 2018),

10) Page 33 Line 22: replace "similarly" by "and similar"

Answer:

We have made this correction in the revised manuscript.

Page 33 Line 22:

Thus, in bivalves, similarly to our observations,

changed to

Thus, in bivalves, and similar to our observations,

11) Page 34 Line 9: "We exclude: : :: : :: : :: : :" The structure of this sentence is wrong. Rewrite it.

Answer:

We have rewritten this sentence:

Page 34 Line 9:

We exclude that this drop may be produced by shell material added later, during the during–culturing shell thickening, as the samples were taken from the mid-shell layer and not from the shell interior.

changed to

Since the samples were taken from the mid-shell layer and not from the shell interior, we can exclude that the isotope negative shift was produced by shell material added during the during–culturing shell thickening. This small drop may be an artefact of both sampling and analytical uncertainties. However, it does not distract from the isotopic drop observed with culturing.

12) Page 34 Line 11: add "a" before "similar"

Answer:

We have added it in the revised manuscript.

Page 34 Line 11:

negative isotope excursions of similar magnitude were recorded

changed to

negative isotope excursions of a similar magnitude were recorded

13) Page 34 Line 16: delete "also" and put it after "been" and delete the other "also in" after "observed"

Answer:

We have made these corrections in the revised manuscript.

Page 34 Line 16:

Negative shifts in both, δ^{13}C and δ^{18}O values during ontogeny have also been observed also in in the brachiopod *Terebratella dorsata*,

changed to

Negative shifts in both, δ^{13}C and δ^{18}O values during ontogeny have been also observed in the brachiopod *Terebratella dorsata*,

Comments from Anonymous Referee #2, Received and published: 19 September 2018

Dear Editor,

The manuscript 'Variation in brachiopod microstructure and isotope geochemistry under low pH–ocean acidification–conditions' examines the change to micro-structure and biogeochemistry of the shell of the brachiopod Magellania venosa in natural conditions versus experimentally cultured brachiopods under low pH environments. The authors apply scanning electron microscopy (SEM) to understand changes to the microstructure in the form of the distribution of endopunctae in the anterior margin and the thickness of the primary layer. In addition, the study applies stable carbon and oxygen isotopes (^{18}O, ^{13}C) to relate the shell growth to the surrounding seawater chemistry in which the brachiopods were grown. This is a thorough investigation of the changes to the brachiopod shell formation under low pH environments. The authors comment from a biogeochemistry point of view relating the changing microstructure and isotope geochemistry of the shell to environmental carbon isotopes therefore providing further evidence for brachiopods to be useful as an ocean acidification proxy in geological samples. A very good multi-disciplinary approach to determine the impacts on the brachiopods shell growth.

1) I do have a few concerns in the way the samples were prepared using 5% acid etching, and if this could possibly mask the impacts of the experimental acidification on the microstructure.

Answer:

The time of 5% acid etching was so rapid (3 seconds) that it did not affect the microstructure, as shown by a first screening and by previous published studies on preparation methods (e.g. Zaky et al., 2015; Crippa et al., 2016). In any case all the samples experienced the same treatment, with exactly the same possible effects; so for the comparative goals of the manuscript, this would have been negligible. Furthermore, if this treatment could have affected the microstructure- which was excluded by our screening and previous studies -, it could have only slightly affected the outline of the structural units (fibre), but not their size, and not the density of the endopunctae.

2) However, these are minor concerns outlined below for the authors. The use of calcein staining to mark the new growth of the shell distinguishes where natural and low pH environments impact the shell growth in the brachiopod. This should ensure that the authors can identify any similarities in the low pH treatment versus the acid etching. However, this should be discussed in the manuscript and perhaps guide the reader to the nice figures representing this. For example, can the authors provide figures 4 for each treatment for comparison? These are very nice visual representations of how the brachiopod microstructure is affected under low pH treatments versus the natural growth ahead of the calcein staining.

Answer:

There are: Figure 2 to show the growth lines marked with calcein, and Figure 11 to summarize the visible microstructure difference under different pH treatments. Also,

the onset of culturing could be seen by a 'break' in the shell structure-quite visible on the surface. Calcein has been widely used for staining calcium carbonate structures. Calcein has been shown to be incorporated passively into growing calcium carbonate of various taxa (e.g. Moran and Marko 2005; Riascos et al., 2007; Herrmann et al., 2009), including brachiopods (Rowley and Mackinnon 1995). None of the authors reported enhanced mortality or other negative influences on life histories or physiology.
Following the request of the reviewer, an additional plate was added in the supplementary material (supplementary figure 1) to show how the brachiopod microstructure is affected under different treatments.

The manuscript is appropriate and well-suited for publication in Biogeosciences Discussions, I would recommend for publication with minor edits as detailed below. Minor comments to the authors.
3) Introduction Please re-phrase, 'pH has dropped by 0.1 pH units and will probably drop another 0.3-0.5', these are projections based on modelling of historic data, I would suggest predicted or projected instead of probably.
Answer:
We have corrected them in the revised manuscript
Page 2 Line 2:
pH has dropped by 0.1 pH units and will probably drop another 0.3-0.5 units
changed to
pH has dropped by 0.1 units and predicted to drop another 0.3–0.5 units

4) Line 15 states 'calcifying organisms', the table 1 refers only to a few brachiopod studies, please change to brachiopods. I could not comment on the supplementary table here. I would instead suggest including a sentence referencing some of the key papers outlining the consequences of experimental acidification on biomineral formation in other calcifying organisms.
Answer:
Supplementary Table 1 contains all the information on calcifying organisms.
We are sorry that the reviewer could not find the supplementary table, which we report also here in the attached file.
The sentence referencing to some of the key-papers on experimental acidification on biominerals is already written in the manuscript, just below at Page 2 Line 18: Only a few studies deal with the effect of acidification on microstructure (Beniash et al., 2010; Hahn et al., 2012; Stemmer et al., 2013; Fitzer et al., 2014a, b; Milano et al., 2016), and all of them focused on bivalves and show that neither microstructure, nor shell hardness seem to be affected by seawater pH.

5) There are such studies examining acidification impact on the microstructure of the sea urchin spicules for example Bray et al., 2014 (Med. Mar. Sci.), PUPA Gilberts group including studies by Politi et al., the authors only list here studies applied to molluscs.

Answer:

We have added the suggested citations to the supplementary table 1: Bray et al., 2014; Wolfe et al., 2013.
However, the paper of Politi et al., 2008 is about the "Transformation mechanism of amorphous calcium carbonate into calcite in the sea urchin larval spicule" so it is not very relevant for this aim.

6) Materials and methods. Page 8, line 2, how long were the brachiopods acclimated for prior to calcein staining and CO_2 induced acidification?
Answer:
We have added the time of the acclimatisation and changed the sentence:
Brachiopods were first left to acclimatize,
changed to
The brachiopods were first acclimatized under control conditions for five weeks,

7) Low-pH culture of several brachiopods was done under two phases, what was the justification for this? Were these two phases comparable in their treatments?
Answer:
Regarding these two phases, basically we had a control and low pH aquarium. The two phases were comparable in their treatments. One reason for increasing the CO_2 treatment from 2000ppm to 4000ppm was that the brachiopods have been done obviously well under the 2000ppm treatment and we aimed to increase the chemical impact as much as possible but with considering the survival of the specimen. Before the 4000ppm treatment has been started individuals of *M. venosa* have been stained again with calcein in order to mark the new material grown under 4000ppm.

8) In general, the treatments appear clear in the table 2 and 3, however it is difficult to understand the experimental design without the details which are currently not obtainable from Jurikova et al., in review.
Answer:
Jurikova et al. manuscript (submitted to Geochimica et Cosmochimica Acta) was revised and sent to the Editor for final decision. We will update the information as soon as Hana Jurikova receives the notification about acceptance.

9) Microstructural analyses – this section is much easier to understand with sufficient detail for the reader to reproduce. The authors used 5% hydrochloric acid for etching the shell prior to SEM analyses. Although a standard protocol for SEM imaging, the authors should comment on how they can be sure that this has not affected the microstructure in comparison to the experimental acidification of the culture. How would the impact the microstructure be distinguishable compared to the acid etch of the microstructure of shells?
Answer:
As explained above, the time of 5% acid etching was so rapid (3 seconds) that it did not affect the microstructure, as shown by our screening as well as in previous

published studies on preparation methods (e.g. Zaky et al., 2015; Crippa et al., 2016). In any case, all the samples experienced the same treatment, with exactly the same possible effects; so for the comparative goals of the manuscript, this would have been negligible. Furthermore, if this treatment could have affected the microstructure-which was excluded by our screening and previous studies -, it could have only affected the outline of the structural units (fibre), but not their size, and not the density of the endopuncta.

In any case, in the revised manuscript we have added a sentence stating that the effect of 5% acid etching was negligible.

Page 10, line 5

The sectioned surfaces were manually smoothed with 1200 grit 5 sandpaper, then quickly (3 seconds) cleaned with 5% hydrochloric acid (HCl), immediately washed with tap water and air–dried.

changed to

The sectioned surfaces were manually smoothed with 1200 grit sandpaper, then quickly (3 seconds) cleaned with 5% hydrochloric acid (HCl), immediately washed with water and air–dried. The time of acid etching was kept short so not affect the microstructure (Crippa et al., 2016b).

10) Figure 4 and 5, can the authors please provide a specimen reference to which sample and treatment these images relate to?

Answer:

We have added the information to the figures in the revised manuscript.

Figure 4a: #9006dv; 4b: #8005dv

Figure 5: #43vv

11) The manuscript suggests just two specimens #8005 and #9006 were used for these analyses. Can the authors conclude that these are representable as a sample population? Are these images available in supplementary information for comparison?

Answer:

#43, #63, #158, #223, #8005 and #9006 were analysed for the microstructure of secondary layer, additionally, #8005 and #9006 were also analysed for the thickness of primary layer and the size/density of endopuncta. All the measurement data are available in the Appendix dataset.

12) Carbonate stable isotopes analyses Likewise, the authors use 5% hydrochloric acid to clean shell prior to sample preparation for stable isotopes. Please detail why this was used, for example to remove organic material? If so why was a bleach or plasma ash treatment not chosen for this purpose to avoid potential issues with comparing experimental acidification treatments with hydrochloric acid treated shells?

Answer:

As explained in the method description (paragraph 2.3), we used 10 % HCl to remove the primary shell layer and surface contaminants; then we immediately rinsed with

distilled water and air–dried. This is an important and fundamental step before doing isotope analyses. As already proved by previous studies (e.g., Veizer, 1992; Carpenter and Lohmann, 1995; Brand et al., 2003, 2013), the primary layer is not secreted in isotope equilibrium with the seawater in which the brachiopod lives, so we have to remove it in order to avoid contamination when sampling the shell. In this way we analysed only the in-equilibrium secondary layer (Parkinson et al., 2005; Cusack et al., 2012; Brand et al., 2013, 2015). To remove the organic material in the shell, as written in paragraph 2.1 we used 36 volume hydrogen peroxide. This in another important step to get clear images of recent brachiopods at the SEM (see Crippa et al., 2016b). We have added a sentence to explain wht we have removed the primary layer before isotope analyses.

.

Page 14 Line 10:
For specimens #8005 and #9006, the primary layer and surface contaminants were manually and chemically removed by leaching with 10 % HCl, rinsed with distilled water and air–dried

changed to

For specimens #8005 and #9006, surface contaminants and the primary layer were first manually and then chemically removed by leaching with 10 % HCl, rinsed with distilled water and air–dried. As the primary layer is not secreted in equilibrium with ambient seawater (e.g., Carpenter and Lohmann, 1995; Brand et al., 2003, 2013), it is important to chemically remove it in order to avoid cross-contamination of results.

13) Section 3.3.2 During culturing Page 23, the authors state that 'The results from specimens (#43 and #63) grown under low pH conditions (pH3 and pH4) for a short time interval of 214 days are difficult to interpret, as in this case, there is no direct control experiment sample to compare', can the authors confidently relate the changing microstructure and geochemistry here to acidification is the only comparison are those samples grown under natural conditions?
Answer:
As written in the manuscript, to assess the change in microstructure and geochemistry, we compared both the differences between parts produced before-culturing and during-culturing, as well as the differences between low-pH treated specimens and control specimens. For specimens (#43 and #63), a control specimen was not available so we were not confident in interpreting the results we obtained and we preferred to underline it in the manuscript

14) It appears that the experimental treatments here are similar despite the pH used (Figure 9). I would question the relevance of this section, perhaps omit or justify how this is comparable.
Answer:
We think that these data are very important to be represented as they show the results of the different methods used. Also this diagram answers to reviewer question 13 and it shows that specimen cultured under low–pH conditions had smaller fibres when

compared to that of control. It also shows the differences in fibre size among different subzones of the same specimens. In conclusion, this section clearly syntheses and displays the numerous measurements taken in this this study, so it is very important for the reader.

15) Section 3.4 Stable isotopes Nice figure 10, it is clear to see trends between three specimens for significantly lighter stable carbon isotopes with experimental low-pH treatment compared to natural versus control treatments. Did the authors compare these data statistically?
Answer:
We thank the reviewer for this suggestion. We have done additional t-tests to compare the data from different pH treatments, and added them in the revised manuscript (Supplementary table 2).

16) Discussion Page 28, 'electron back scattering diffraction' should be electron backscatter diffraction.
Answer:
We have corrected it in the revised manuscript
Page 28 Line 9
Analyses of electron back scattering diffraction
changed to
Analyses of electron backscatter diffraction

17) Line 20, 'May this indicate a greater amount of organic components in this part of the shell?' is this what the authors suggest? Please rephrase not as a question but a statement with references or omit.
Answer:
We have deleted this sentence in the revised manuscript, because there is no conclusive evidence about it in the literatures.

18) Lines 28, 'living organism' this should be living organisms.
Answer:
We have corrected it in the revised manuscript
Page 28 Lines 28:
living organism
Changed to
living organisms

19) Page 34-35. The discussion of the depleted ^{18}O, ^{13}C is related to changes in percentage, can the authors present the statistical significance here of the changing isotope values?
Answer:
We thank the reviewer for this suggestion. We have done additional t-tests to compare the data from different pH treatments, and added them in the revised manuscript

(Supplementary table 2).

20) The authors state that there is individual specimen variability, does this remove the significance of the low pH treatment over the isotope depleted values? Or are the authors suggesting here that there are insufficient specimen numbers to make significant statements relating to the isotope data? Page 35, line 11 'More measurements are however needed to fully answer this.'?
Answer:

We think that analyses on more specimens could help to understand in greater details the $d^{13}C$ variability, but this does not undermine that we have robust data to support the fact that brachiopod produce shells near brachiopod equilibrium even in changing external conditions. We have results from both dorsal and ventral valves, if there was uncertainty it might show up in one but hardly both, the matching and concurrent isotope results speak clearly to the robustness of the values and trends.

21) Page 35, line 16 'Thus, we think', perhaps the data suggest?
Answer:

We have changed it in the revised manuscript
Thus, we think that large part of the secondary layer isotope record
changed to
Thus, the data suggest that large part of the secondary layer isotope record

22) The authors end in the statement 'secondary layer isotope record may reflect the environmental conditions supporting the interpretation of brachiopod shells as good archives of geochemical proxies, even when stressed by ocean acidification.'. This is also stated in the abstract as one of the main implications of this study. Following the current discussion on page 34-35 I would question whether the authors can make this statement, and whether there is sufficient evidence to support this, although Figure 10 does suggest this is the case. Please directly refer to the data here; are there sufficient samples, what is the n-number? This will enable the reader to determine if the manuscripts data do support these conclusions. If this data is not available then the authors will need to remove this emphasis from the abstract and conclusion statements.
Answer:

We think that our data are robust because we have analysed 9 specimens, 6 specimens for microstructure analyses, 5 for isotope geochemistry. We measured the size and shape of 540 fibres plus 1392 fibre at the anterior margin, we selected and measured 388 sub-zones for boundary calculations; we took 170 measurements for primary layer thickness; we selected and measured 29 zones for endopunctae density, 227 for diameter of endopunctae; we analysed 79 samples for isotope geochemistry. Following the suggestions of the reviewer, we have added these numbers in the conclusions.
Page 35 lines 19-20:
This study combined the analysis of shell microstructure and stable isotope

geochemistry on brachiopods cultured at low pH conditions for different time intervals, and suggests the following conclusions.

changed to

This study combines the analysis of shell microstructures on 6 specimens consisting of 1932 fibre size measurements, 170 primary layer thickness measurements, 256 punctal density and diameter measurements and stable isotope geochemistry on 5 specimens of 79 sample analyses, on brachiopods cultured at low pH conditions for different time intervals. The results suggest the following conclusions.

23) Page 35 conclusions 'This was related to the source of carbon dioxide gas used in the culture setup', could this not be due to a change in the carbonate compositions as a result of adding CO_2 impacting the DIC? Did you test the carbon isotopes of the gas?
Answer:
We did not test the $d^{13}C$ of the gas, but we did measure the $d^{13}C$ in water, as we written in the manuscript Page 34 Line 31: the $\delta^{13}C_{DIC}$ in the water during the cultivation process of our specimens was low ($\delta^{13}C$ VPDB: -23.63 ‰ for the low pH conditions and -2.03 ‰ for the control conditions, which corresponds to the pH_2 phase), This is essentially the $d^{13}C$ of the DIC which comes from the source so it is pretty much almost the same.

24) I have seen this drop in carbon isotopes in the natural seawater samples where increasing CO_2 from run-off caused a lighter carbon isotope value. The authors should expand this discussion to the previous paragraph.
Answer:
As the main goal of the paper is to understand the impact of acidification on cultured specimens, we did not expand the discussion on what happened before culturing in the natural environment. However, this was the object of a paper by Romanin et al. (2018). In fact, as we have already written in manuscript at Page 34 Line 14, Romanin et al. (2018), who also analysed specimens collected from Comau Fjord, attributed the negative isotope excursion to environmental perturbations, in particular, to changes in seawater productivity and temperature, and/or to anthropogenic activities. Here, we follow the interpretation of Romanin et al. (2018) to explain the mid–shell excursion observed in our specimens.

Comments from E. Cross

e.l.cross@cantab.net Received and published: 27 September 2018

Firstly, it is great to read that other researchers are using living specimens of this highly calcium-carbonate-dependent group to address outstanding questions of biological responses to ocean acidification. I look forward to future publications from this lab. I have a few minor comments in relation to correctly citing previous research on ocean acidification impacts on brachiopods:

1) Page 2, Line 21-23: Please add to this sentence about previous findings of ocean acidification impacts on brachiopods that Cross et al. (2018) also found that punctae have become thinner over the last 120 years, which partially explained the increase in shell density over this time period.

Answer:

We have added this sentence in the revised manuscript.

Page 2, Line 21-23:

The few studies that examined brachiopods or brachiopod shells suggest that the latter suffered increased dissolution under lower seawater pH conditions, whereas the organism either exhibited no changes, or an increase in shell density [calculated as dry mass of the shell (g)/shell volume (cm^3)], but otherwise no changes in shell morphology and trace chemistry (Table 1).

changed to

The few studies that examined brachiopods or brachiopod shells suggest that the latter suffered increased dissolution under lower seawater pH. In other studies, the organism either exhibited no changes or an increase in shell density [calculated as dry mass of the shell (g)/shell volume (cm3)], but otherwise no changes in shell morphology and trace chemistry (Table 1). Cross et al. (2018) found that punctae became narrower over the past 120 years, which partially explained the increase in shell density over this period.

2) Page 2, Table 1: Please specify that shell growth rates and shell repair frequencies of *Calloria inconspicua* were not affected by low pH in the row related to Cross et al. (2016) in the column stating "not affected by lower pH".

Answer:

We have indicated it in the revised manuscript.

Page 2, Table 1 column 3 row 2:

not affected by lower pH

changed to

shell growth rates and shell repair frequencies were not affected by low pH

3) Page 3, Table 1: Please correct the number of specimens used in the row related to Cross et al. (2018). 389 adult specimens were used in the shell morphology analysis. A subsample of 40 brachiopods (2-5 specimens per decade over the last 120 years) were used for further shell analysis on shell density, punctal width, punctal density, shell dissolution, shell thickness and shell elemental composition.

Answer:

We have corrected it in the revised manuscript.
Page 2, Table 1 column 1 row 3:
N = 389 (adults)
changed to
N = 389 (adults) for shell morphology analyses*.
And we have added the note below the table:
*A subsample of 40 brachiopods (2-5 specimens per decade over the last 120 years) were used for further shell analysis of shell density, punctal width, punctal density, shell dissolution, shell thickness and shell elemental composition.

4) Please also add that no changes were found in shell dissolution over the last 120 years.
Answer:
We have added it in the revised manuscript.
Page 3, Table 1 column 3 row 3:
add:
no changes were found in shell dissolution over the last 120 years.

5) Page 3, Table 1: Please specify that shell growth rates and shell repair frequencies of *Liothyrella uva* were not affected by low pH and temperature in the row related to Cross et al. (2015) in the column stating "not affected by lower pH".
Answer:
We have specified it in the revised manuscript.
Page 3, Table 1 column 2 row 4:
not affected by lower pH
changed to
not affected by lower pH and temperature
Page 3, Table 1 column 3 row 4:
not affected by either low pH conditions or temperature
changed to
shell repair frequencies were not affected by low pH and temperature

6) Page 31, Line 9: To avoid confusion, please add in that these specimens are from the same locality in New Zealand (Paterson Inlet, Stewart Island, New Zealand).
Page 31, Line 10: Please also add that the pH decrease by 0.1 pH units occurred over the last two decades whilst the 2 ℃ increase in temperature occurred over the last 60 years.
Answer:
We have added it in the revised manuscript.
Page 31, Line 9:
One response, however, appears to reinforce the shells of C. inconspicua by laying down a denser shell compared to specimens from New Zealand over the last 120 years while subjected to a slight decrease in pH (by 0.1) and 2 ℃ increase in temperature over the last two decades (Cross et al., 2018).

changed to

However, C. inconspicua from the same locality in New Zealand (Paterson Inlet, Stewart Island) laid down a denser shell over the last 120 years, with nearby environmental conditions increased by 0.6 ℃ from 1953 to 2016, and slightly increased by 35.7 μatm in pCO2 from 1998 to 2016 (Cross et al., 2018). These changes are in line with global trends of ocean pH and temperature since the industrial revolution (Caldeira and Wickett, 2005; Orr et al., 2005; IPCC, 2013).

7) Page 32, Line 5-8: Majority of the studies listed here did not investigate brachiopod growth rates. To avoid confusion and strengthen the authors point that there is a limited database on ocean acidification impacts on brachiopods, only include studies here on brachiopods.

Answer:

As we mainly discussed the effects of acidification on the growth rates of marine calcifiers, we have corrected the word 'brachiopod' to 'marine calcifiers' in the revised manuscript.

Page 32, Line 5-8:

show no or little impact of acidification on brachiopod growth rates

changed to

show no or little impact of acidification on the growth rates of marine calcifiers

Variation in brachiopod microstructure and isotope geochemistry under low pH–ocean acidification–conditions

Facheng Ye[1], Hana Jurikova[2], Lucia Angiolini[1], Uwe Brand[3], Gaia Crippa[1], Daniela Henkel[2], Jürgen Laudien[4], Claas Hiebenthal[2], Danijela Šmajgl[5]

[1]Università degli Studi di Milano, Dipartimento di Scienze della Terra 'A. Desio', Milan, 20133, Italy
[2]GEOMAR Helmholtz–Zentrum für Ozeanforschung Kiel, 24148, Kiel, Germany
[3]Department of Earth Sciences, Brock University, St. Catharines, Ontario L2S 3A1, Canada
[4]Alfred-Wegener–Institut Helmholtz–Zentrum für Polar–und Meeresforschung, Bremerhaven, 27515, Germany
[5]ThermoFisher Scientific, Hanna–Kunath–Str. 11, Bremen, 28199, Germany

Correspondence to: Facheng Ye (facheng.ye@unimi.it)

Abstract. In the last few decades and in the near future CO_2–induced ocean acidification is potentially a big threat to marine calcite-shelled animals (e.g., brachiopods, bivalves, corals and gastropods). Despite the great number of studies focusing on the effects of acidification on shell growth, metabolism, shell dissolution and shell repair, the consequences on biomineral formation remain poorly understood. Only few studies have addressed the impact of ocean acidification on shell microstructure and geochemistry. In this study, a detailed microstructure and stable isotope geochemistry investigation was performed on nine adult brachiopod specimens of *Magellania venosa* (Dixon, 1789). These were grown in the natural environment as well as in controlled culturing experiments at different pH conditions (ranging from 7.35 to 8.15 ±0.05) over different time intervals (214 to 335 days). Details of shell microstructural features, such as thickness of the primary layer, density and size of endopunctae and morphology of the basic structural unit of the secondary layer were analysed using scanning electron microscopy. Stable isotope compositions ($\delta^{13}C$ and $\delta^{18}O$) were tested from the secondary shell layer along shell ontogenetic increments in both dorsal and ventral valves. Based on our comprehensive dataset, we observed that, under low pH conditions, *M. venosa* produced a more organic–rich shell with higher density of and larger endopunctae, and smaller secondary layer fibres. Also, increasingly negative $\delta^{13}C$ and $\delta^{18}O$ values are recorded by the shell produced during culturing and are related to the CO_2–source in the culture setup. Both the microstructural changes and the stable isotope results are similar to observations on brachiopods from the fossil record and strongly support the value of brachiopods as robust archives of proxies for studying ocean acidification events in the geologic past.

Key words:

Magellania venosa, biomineral, $\delta^{13}C$, $\delta^{18}O$, primary layer, secondary layer, endopunctae, culturing

1 Introduction

Since the industrial revolution the surface ocean pH has dropped by 0.1 units and predicted to drop another 0.3–0.5 units by 2100 (Caldeira and Wickett, 2005; Orr et al., 2005; IPCC, 2013). This is due to the increasing amount of atmospheric carbon dioxide (CO_2) absorbed by the ocean that extensively affects seawater carbonate chemistry (e.g., Caldeira and Wickett, 2003, 2005; Orr et al., 2005; Feely et al., 2004). Increased concentrations of anthropogenic CO_2 are reflected in an elevated concentration of hydrogen ions, which lowers the pH and the availability of carbonate ions. Effects on marine organisms is of great scientific interest, for understanding the geological past and the consequences in the immediate future (e.g., Ries et al., 2009), since the decrease in calcium carbonate saturation potentially threatens marine organisms forming biogenic calcium carbonate (e.g., Orr et al., 2005; Guinott et al., 2006; McCulloch et al., 2012; Jantzen et al., 2013a, b). This applies to calcium carbonate shell–forming species, such as brachiopods and mollusks, because they are considered excellent archives documenting changes in environmental conditions affecting marine organisms (e.g., Kurihara. 2008; Comeau et al., 2009; Hahn et al., 2012, 2014; Watson et al., 2012; Cross et al., 2015, 2016, 2018; Crippa et al., 2016a; Milano et al., 2016; Garbelli et al., 2017; Jurikova et al., in review).

Recently, several experiments were performed to investigate if a change of seawater pH may affect growth rate, shell repair and oxygen consumption of calcifying organisms, and how they respond, in general, to ocean acidification (Supplementary table 1). However, despite the great number of studies, the consequences on biomineral formation remain not well understood, as most studies focused mainly on growth, metabolic rates, shell dissolution and shell repair (Supplementary table 1, and references therein). Only a few studies deal with the effect of acidification on microstructure (Beniash et al., 2010; Hahn et al., 2012; Stemmer et al., 2013; Fitzer et al., 2014a, b; Milano et al., 2016), and most of them focused on bivalves and show that neither microstructure nor shell hardness seem to be affected by seawater pH.

The few studies that examined brachiopods or brachiopod shells suggest that the latter suffered increased dissolution under lower seawater pH. In other studies, the organism either exhibited no changes or an increase in shell density [calculated as dry mass of the shell (g)/shell volume (cm^3)], but otherwise no changes in shell morphology and trace chemistry (Table 1). Cross et al. (2018) found that punctae became narrower over the past 120 years, which partially explained the increase in shell density over this period. Overall, there appears to be little to no apparent effect on brachiopod morphology or chemistry with lower seawater pH (Cross et al., 2015, 2016, 2018).

Table 1. Culturing, dissolution experiments and natural variation on several brachiopod species and shells.

Species n (number of sample)	Growth Parameters	Shell repair/Microstructure/Oxygen consumption/Dissolution of shell/Microstructure	Method & Material	Environment/conditions T=Temperature (℃) S=Salinity (PSU) pCO_2 (µatm)	Duration of experiment	Source
Calloria inconspicua (Sowerby, 1846) n = 123	1) >3 mm in length undamaged individuals were not affected by lower pH; 2) <3 mm in length	Shell growth rates and shell repair frequencies were not affected by low pH (>80% of all damaged individuals repaired after 12 weeks)	Culture experiment	a) pH 8.16, T 16.5, S 33.9, pCO_2 465, $\Omega_{calcite}$ 3.5 b) pH 7.79, T 16.9, S 33.9, pCO_2 1130, $\Omega_{calcite}$ 1.6 c) pH 7.62, T 16.6, S 33.9, pCO_2 1536, $\Omega_{calcite}$ 1.3	12 weeks	Cross et al., 2016

2

	undamaged individuals grew faster at pH 7.62 than the control conditions					
Calloria inconspicua (Sowerby, 1846) n_{adult} = 389 for shell morphology analyses*	Punctae width decreased by 8.26%, shell density increased by 3.43%, no change in shell morphology, punctae density, shell thickness, and shell elemental composition (Ca, Mg, Na, Sr and P) No changes were found in shell dissolution over the last 120 years.	Collected every decade from one locality	Last two decades pH reduced 0.1 unit Temperature varied from 10.7–13.0 ℃ pCO_2 varied from 320–400 Salinity and $\Omega_{calcite}$ not provided	120–year record	Cross et al., 2018
Liothyrella uva (Broderip, 1833) n = 156	Not affected by lower pH and temperature	Shell repair frequencies were not affected by low pH and temperature (>83% of individuals repaired after 7 months)	Culture experiment	a) pH 7.98, T -0.3, S 35, pCO_2 417, $\Omega_{calcite}$ 1.20 b) pH 8.05, T 1.7, S 35, pCO_2 365, $\Omega_{calcite}$ 1.49 c) pH 7.75, T 1.9, S 35, pCO_2 725, $\Omega_{calcite}$ 0.78 d) pH 7.54, T 2.2, S 35, pCO_2 1221, $\Omega_{calcite}$ 0.50	7 months	Cross et al., 2015
Liothyrella uva (Broderip, 1833) $n_{post-mortem}$ = 5	Not applicable	Higher dissolution in gastropods and brachiopods at lower pH after 14 days	Empty shells	a) pH 7.4, T 4, S 35, $\Omega_{calcite}$ 0.74 b) pH 8.2, T 4, S 35, $\Omega_{calcite}$ 4.22 pCO_2 Not provided	14 to 63 days	McClintock et al., 2009

*A subsample of 40 brachiopods (2-5 specimens per decade over the last 120 years) were used for further shell analysis of shell density, punctal width, punctal density, shell dissolution, shell thickness and shell elemental composition.

Brachiopods possess a low–magnesium calcite shell, which should be more resistant compared to the more soluble forms of $CaCO_3$, such as aragonite and high-Mg calcite (Brand and Veizer, 1980; Morse et al., 2007). The shell microstructure of Rhynchonelliformean brachiopods has been used as a powerful tool to understand the biomineral's response to modern global ocean acidification and similar events in the geologic past (Payne and Clapham, 2012; Cross et al., 2015, 2016; Garbelli et al., 2017). A comprehensive study focusing on fossil brachiopods during the end-Permian mass extinction showed that brachiopods produce shells with increased organic matter content during ocean acidification events (Garbelli et al., 2017).

Here, we describe the microstructure and carbon and oxygen isotopic composition of brachiopod shells belonging to the cold-temperate water species *Magellania venosa* (Dixon, 1789) grown in natural environment as well as in pH-controlled culturing conditions. *M. venosa* represents the largest recent brachiopod species, is often locally abundant (e.g. in Chile; Försterra et al., 2008), and it has the highest growth rate recorded for recent brachiopods (Baumgarten et al., 2014). Its low-magnesium calcite shell consists of a microgranular primary layer and a fibrous secondary layer (Smirnova et al., 1991; Baumgarten et al., 2014; Casella et al., 2018; Romanin et al., 2018) crossed by perforations – endopunctae.

Since little is known about the microstructural and geochemical responses of brachiopods to increased ocean acidification, the main goal of this study is to document any changes in this highly important archival marine organism. It will be described, if and how, shell microstructural features such as the primary layer thickness, density of endopunctae and fibre

morphology, together with their stable carbon (δ^{13}C) and oxygen (δ^{18}O) isotope compositions respond to low seawater pH conditions.

2 Materials and methods

2.1 Brachiopod samples and culturing set–up

A full description of the brachiopod sampling and culturing procedure is provided in Jurikova et al. (in review), but we provide an abbreviated version and reiterate the key points. Nine adult individuals of *M. venosa* (Dixon, 1789) were chosen for microstructure investigation and evaluation of their δ^{13}C and δ^{18}O values. All specimens were collected by scientific SCUBA divers alive from 20 m water depth of Comau Fjord (Chile) at different localities (Figure 1). Specimens #158 and #223 did not experience any treatment after collection from Comau Fjord. The other specimens, #43, #63, #8004, #8005, #9004, #9005 and #9006, were cultured under different pH conditions at either AWI in Bremerhaven or GEOMAR (at KIMOCC–Kiel Marine Organisms Culture Centre) in Kiel, Germany, (Table 2 and 3).

Table 2.

Culture and sensor systems used in *M. venosa* culturing (specimens; #43, #63, #8004, #8005, #9004, #9005 and #9006). Operated under controlled experimental settings in climate–controlled laboratories at Alfred–Wegener–Institut Helmholtz–Zentrum für Polar–und Meeresforschung, Bremerhaven, Germany and at GEOMAR Helmholtz–Zentrum für Ozeanforschung Kiel, Germany.

	Culture system at AWI	Automated sensor Systems at AWI	Culture system at GEOMAR	Automated sensor Systems at GEOMAR
	Aquarium (150 L/each pH treatment)		Aquarium (150 L/each pH treatment)	
	Supplied from a reservoir tank (twice a week 20 % water was replaced)		Supplied from a reservoir tank (twice a month 10 % water was replaced)	
Temperature	Controlled in temperature constant room		Controlled using heaters or coolers	Temperature Sensor Pond
pCO$_2$	Bubbling of CO$_2$	COMPORT, Dennerle, Vinningen; IKS aquastar Aquarium computer V2.xx with Aquapilot 2011	Bubbling of CO$_2$ enriched air	CONTROS HydroC® underwater CO$_2$ sensor
Salinity	Mixing Reef commercial	Conductivity Electrode	Mixing Tropic Marin Pro–	Conductivity Electrode

4

	sea–salt (until October: Aqua Medic, Bissendorf, Germany, thereafter Dupla Marin Reef Salt, Dohse Aquaristik, Grafschaft–Gelsdorf, Germany) with deionized water	Reef commercial sea-salt with deionized water
Filtering	Biofilter, protein skimmer and UV sterilizer	Biofilter, protein skimmer and UV sterilizer
Food	Regularly fed (typically 5 times per week) with Dupla Rin, Coral Food, Reef Pearls 5–200 μm, alive *Thalassiosira weissflogii*, and 1d old nauplii of *Artemia salina*	Regularly fed (typically 5 times per week) with *Rhodomonas baltica*
Substrate	Sabia Corallina, 7–8mm, Dohse Aquaristik, Grafschaft–Gelsdorf, Germany	No

Table 3. Specimens of *M. venosa* sampled from Comau Fjord, Chile, and natural and experimental culturing conditions.

Sample ID	Sample locality at Comau Fjord (Chile)[1]	Sample seawater conditions[2]	Date of collection	Length of ventral valve (mm)	Duration of experiment	Experimental conditions
#43	Lilliguapi	pH: ~7.9 T: ~13 S: ~32 D: 20	Feb. 2012	37	214 days [3]	pCO$_2$: 1390, pH: 7.66 ±0.04 T: 11.6 ±0.5, S: 32.6 Ω_{cal}: 2.0
#63	Lilliguapi	pH: ~7.9 T: ~13 S: ~32 D: 20	Feb. 2012	23	214 days [3]	pCO$_2$: 2600, pH: 7.44 ±0.08 T: 11.7 ±0.5, S: 32.7 Ω_{cal}: 1.4
#158	Huinay Dock	pH: ~7.9 T: ~13 S: ~32 D: 20	Dec. 2011	36	no	
#223	Cahuelmó	pH: ~7.9 T: ~13 S: ~32 D: 23	Feb. 2012	30	no	
#8004	Comau Fjord	pH: ~7.9 T: ~13 S: ~32 D: 21	Apr. 2016	31	335 days [4]	pCO$_2$: 600 pH: 8.00 to 8.15 ±0.05 T: 10 ± 1, S: 30 Ω_{cal}: 2.0–3.5

		pH: ~7.9 T: ~13 S: ~32 D: 21				pCO$_2$: 600 pH: 8.00 to 8.15 ±0.05 T: 10 ± 1, S: 30 Ω_{cal}: 2.0–3.5
#8005	Comau Fjord	pH: ~7.9 T: ~13 S: ~32 D: 21	Apr. 2016	46	335 days[4]	pCO$_2$: 600 pH: 8.00 to 8.15 ±0.05 T: 10 ± 1, S: 30 Ω_{cal}: 2.0–3.5
#9004	Comau Fjord	pH: ~7.9 T: ~13 S: ~32 D: 21	Apr. 2016	41	335 days[4]	pCO$_2$: 2000–4000[5] pH: 7.60 to 7.35 ±0.05 T: 10 ± 1, S: 30 Ω_{cal}: 0.6–1.1
#9005	Comau Fjord	pH: ~7.9 T: ~13 S: ~32 D: 21	Apr. 2016	25	335 days[4]	pCO$_2$: 2000–4000[5] pH: 7.60 to 7.35 ±0.05 T: 10 ± 1, S: 30 Ω_{cal}: 0.6–1.1
#9006	Comau Fjord	pH: ~7.9 T: ~13 S: ~32 D: 21	Apr. 2016	43	335 days[4]	pCO$_2$: 2000–4000[5] pH: 7.60 to 7.35 ±0.05 T: 10 ± 1, S: 30 Ω_{cal}: 0.6–1.1

Note: D: Depth (m), T: temperature (℃), S: salinity (PSU – practical salinity units), pCO$_2$ (μatm).

[1] Cahuelmó 42 °15'23" S, 72 °26'42" W, Cross–Huinay 42 °23'28" S, 72 °27'27" W, Jetty (Huinay Dock) 42 °22'47" S, 72 °24'56" W, Lilliguapy 42 °9'43" S, 72 °35'55" W, samples #8004, #8005, #9004, #9005, #9006 were harvested from three sites in Comau Fjord (Cross–Huinay, Jetty, and Liliguapy), Chile

[2] Reference: Laudien et al. (2014) and Jantzen et al. (2017)

[3] Culture experiments conducted at Alfred–Wegener–Institut Helmholtz–Zentrum für Polar–und Meeresforschung, Bremerhaven, Germany

[4] Culture experiments conducted at GEOMAR Helmholtz–Zentrum für Ozeanforschung Kiel, Germany (Jurikova et al., in review)

[5] CO$_2$ concentration was changed during the experiment: to 2000 μatm from 4th August 2016 to 18th April 2017 and to 4000 μatm from 18th April 2017 till 5th July 2017.

Figure 1. Map of Comau Fjord. Upper left map: Overview of Chilean Patagonia. Lower left map: Gulf of Ancud with connections in the north and south to the Pacific Ocean. Right hand map: Fjord Comau with brachiopod sample collection localities. In both maps the rectangle marks the location of Comau Fjord.

In summary, individuals of *M. venosa* were collected alive in Chile and transported to GEOMAR, Germany in plastic bags filled with seawater, and maintained under controlled conditions in a climate laboratory. The brachiopods were first acclimatized under control conditions for five weeks, and prior to the start of the experiment were labelled with a fluorescent dye – calcein (Sigma, CAS 1461–15–0; 50 mg/l for 3 h) (e.g., Baumgarten et al., 2013; Jurikova et al., in review). As a culture medium we used artificial seawater, which was prepared by mixing a commercial salt with deionized water until the desired salinity and chemical composition was achieved (Atkinson and Bingman, 1998). Overview of the culturing setup at both laboratories is available in Table 2. Specimens #43 and #63 were cultured at AWI at pH = 7.66 (pCO$_2$ = 1390 µatm) and pH = 7.44 (pCO$_2$ = 2610 µatm) from 29th August 2013 to 31th March 2014, respectively. Specimens #8004, #8005, #9004, #9005 and #9006 were cultured concurrently at GEOMAR under control or low pH conditions. Specimens #8004 and #8005 were maintained under pH settings of 8.0–8.15 from 4th August 2016 to 5th July 2017, conditions similar to those of their fjord habitat. In contrast, specimens #9004, #9005 and #9006 were cultured under low–pH artificial seawater

7

conditions. Low–pH conditions were achieved by bubbling of CO_2 through the tanks at AWI, and by bubbling CO_2-enriched air through the tanks at GEOMAR (Table 2). The acidification experiment at GEOMAR was performed in two phases; the first one from 4th August 2016 to 18th April 2017 during which the pCO_2 was set to 2000 µatm (corresponding to a pH of 7.60), and the second one during which the pCO_2 was set to 4000 µatm (corresponding to a pH of 7.35) from 18th April 2017 to 5th July 2017 (Table 3). In order to distinguish between the shell parts precipitated under the specific pH conditions as well as to allow exact comparison to shells of the control treatment, calcein marking was also carried out prior to the second low–pH experiment of 4000 µatm. Parts of the shell grown under specific pH conditions are indicated in Figure 2. In addition to the calcein marking, newly grown shell parts may be distinguished from visible growth lines on the surface of the shell (Figure 2). The total length (maximum distance from the blue line to the anterior margin) of the curved dorsal and ventral valves grown during 11 months of culturing (Figure 2) varied from < 5 to 15.6 mm (Table 4).

Figure 2. Growth tracked with calcein and marked by blue and red lines on the surface of the brachiopod specimens (#9006).

Table 4. Shell length of specimens of *M. venosa* before and during the culture.

Sample ID	Valve	Initial length before culturing (mm)	New shell growth (a) 257 Days (mm)	pH	New shell growth (b) 78 Days (mm)	pH
#8004	ventral	15.4	14	8.00	1.6	8.15
#8005	ventral	40	5	8.00	<1	8.15
#8005	dorsal	36	4	8.00	<1	8.15
#9004	ventral	26.8	13	7.60	1.2	7.35
#9005	ventral	11.2	12	7.60	1.8	7.35
#9006	ventral	33	9	7.60	<1	7.35
#9006	dorsal	29	8	7.60	<1	7.35

Note: (a) Culturing from 4th August 2016 to 18th April 2017; (b) Culturing from 18th April 2017 to 5th July 2017; $pH_0 = 8.00$ and 8.15, $pH_1 = 7.60$, $pH_2 = 7.35$.

8

2.2 Microstructural Analysis

This study followed the sample preparation method shells suggested by Crippa et al. (2016b). In order to obtain more detailed data on microstructural changes, the samples were cut with a diamond blade along different axes and directions (Figure 3a). Subsequently, the samples were immersed in 36 volume hydrogen peroxide (H_2O_2) for 24/48 hours to remove the organic tissue. The sectioned surfaces were manually smoothed with 1200 grit sandpaper, then quickly (3 seconds) cleaned with 5% hydrochloric acid (HCl), immediately washed with water and air–dried. The time of acid etching was kept short so not affect the microstructure (Crippa et al., 2016b). Finally, the valve sections were gold–coated and analysed by a Cambridge S–360 scanning electron microscope with a lanthanum hexaboride (LaB_6) source operating at an acceleration voltage of 20 kV (Dipartimento di Scienze della Terra "A. Desio", Università di Milano).

Figure 3. Brachiopod shell sample cut along different axes. (a): longitudinal and transverse sections; (b): transverse sections at the anterior margin of the shell; (c): plane grinding of the external surface of the shell.

The methods described by Ye et al. (2018a) were followed to investigate the basic microstructural units (fibres) in SEM images. We focused primarily on the anterior margin of the valves, the part that was produced during culturing (hereinafter referred to as *during–culturing*) under different pH conditions. Therefore, additional transverse sections along the growth lines were obtained in the most anterior part (black lines in Figure 3b) by manually smoothing with 1200 grit sandpaper. Plane grinding was performed on the external surface of the shell (Figure 3) to investigate the distribution of endopunctae.

The thickness of the primary layer was measured on the SEM images of specimens #8005 and #9006 (Figure 4a) in different positions along the longitudinal growth axis (posterior, central and anterior regions). In the vicinity of the transition from natural growth to cultured growth, the region was further subdivided into four sub–zones.

To calculate and measure the density and diameter (max) of endopunctae, squares (800 µm $\times$ 800 µm) were located randomly over the smoothed external surface of the anterior shell (Figure 4b). Four sub-zones (C2, A1, A2, A3) were

9

defined according to their position along the posterior-anterior direction (Figure 4), while distinguishing the part of the shell produced *before–culturing* and that produced *during–culturing*.
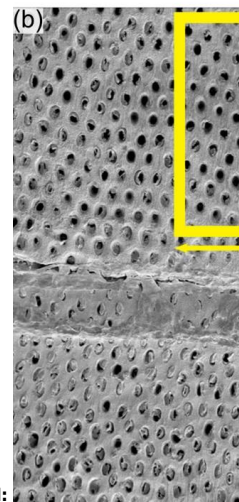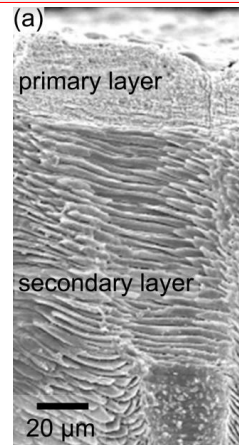

Figure 4. Measurement methods used for the thickness of primary layer (a) and the density of the endopunctae (b). Note that for the latter, endopunctae were counted when included for more than their half diameter inside the square. dv: dorsal valve.

For morphometric analyses, fibres were manually outlined using polygonal lasso in Adobe Photoshop CS6, and size and shape parameters were measured with Image-Pro Plus 6.0 and ImageJ (for convexity). In particular, following Ye et al. (2018a, b) we measured/calculated the Feret diameter (max), Area, Roundness [4Area/π × Feret diameter (max)^2] and Convexity (Convex Perimeter/Perimeter). The width of an individual fibre roughly corresponds to its Max Feret diameter, whereas its height corresponds to the Min Feret diameter (see Figure 6 in Ye et al., 2018a).

As individual fibres are irregular in shape in the most anterior section of brachiopods, the morphometric measurement method proposed by Ye et al. (2018a, b) is not always suitable. Thus, modifications had to be made to the Ye et al. (2018a, b) measurement method to make the comparative morphometric analysis of the fibres from anterior part (Figure 5a, b). First, all SEM images were oriented in the same direction with the base of the primary layer facing upwards. Then a uniformly sized zone (20 μm × 20 μm) was selected for additional measurements with the upper side of the square always placed at the boundary between the primary and the secondary layers (Figure 5c). Two new methods were developed and applied: for Method 1, the width of fibres crossed by two standard lines was measured, which were always located in the same position and at the same distance in all the selected zones (yellow and orange lines in Figure 5 method 1). For Method 2, we calculated the number of boundaries based on the number of fibres crossed by the two standard lines (Figure 5 method 2). Sub-zones were named according to the following nomenclature, the most anterior transection zone of the ventral valve was named Z1, the second most anterior transection zone of the ventral valve Z2 and so on, the most anterior transection zone of the dorsal valve was named Z4. The standard line facing towards the primary layer was named "1" and the second standard

10

line "2" (example: "Z1–1" is the sample of the standard line facing towards the primary layer at the most anterior transect zone of the ventral valve).
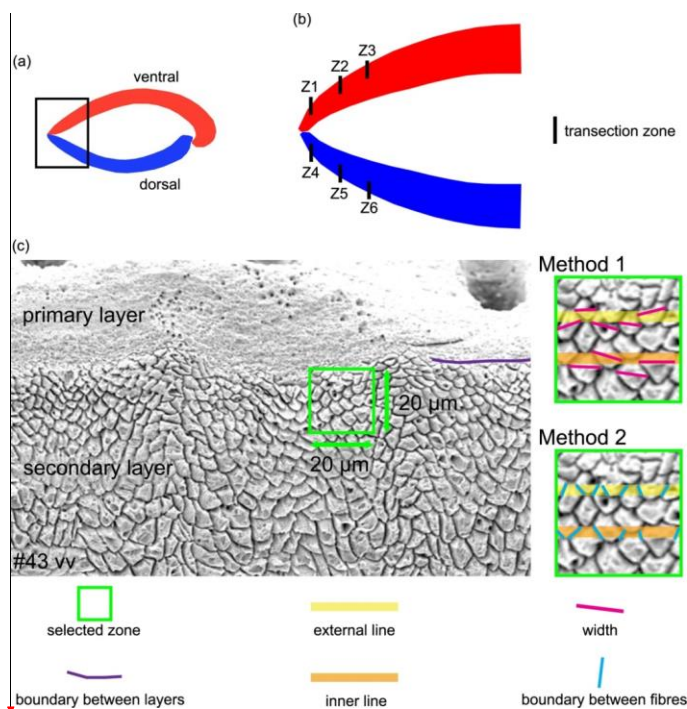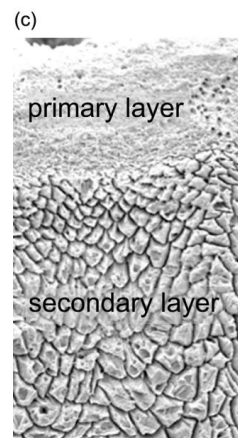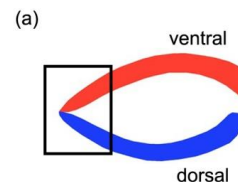

Figure 5. Methods of measurements used in the anterior transverse sections. All SEM images are oriented in the same direction: base of the primary layer facing upwards. A square (20 µm × 20 µm) was analysed with its upper side just overlapping the boundary between the primary and secondary layer. Method 1 refers to the measurement of the width of the fibres crossed by two standard lines, which were located in the same position and at the same distance in all 194 squares (yellow and orange lines); Method 2 involved the calculation of the numbers of boundaries between the fibres that are crossed by two standard lines. vv: ventral valve.

2.3 Stable isotope analyses of shells

Cleaned shells of specimens #8004, #8005, #9004, #9005 and #9006 were chosen for carbon and oxygen isotope analyses. For specimens #8005 and #9006, surface contaminants and the primary layer were first manually and then chemically removed by leaching with 10 % HCl, rinsed with distilled water and air–dried. As the primary layer is not secreted in equilibrium with ambient seawater (e.g., Carpenter and Lohmann, 1995; Brand et al., 2003, 2013), it is important to chemically remove it in order to avoid cross-contamination of results. Individual growth increments exclusively come from the secondary layer, and were separated from the shell in both dorsal and ventral valves using a WECHEER (WE 248)

11

microdrill at low speed with tungsten–carbide milling bit. Shell increment fragments, of similar width, were then powdered using an agate mortar and pestle. For carbon and oxygen isotope analyses about 250 μg of powdered calcite of each sample was analysed using an automated carbonate preparation device (GasBench II) connected to a Delta V Advantage (Thermo Fisher Scientific Inc.) isotopic ratio mass spectrometer at the Earth Sciences Department, University of Milan, Italy. The carbon and oxygen isotope compositions are expressed in the conventional delta notation calibrated to the Vienna Pee-Dee Belemnite (V-PDB) scale by the international standards IAEA 603 (International Atomic Energy Agency 603; $\delta^{18}O$: -2.37 ± 0.04 ‰, $\delta^{13}C$: +2.46 ± 0.01 ‰) and NBS 18 ($\delta^{18}O$: -23.2 ± 0.1 ‰, $\delta^{13}C$: -5.014 ± 0.035 ‰). Analytical reproducibility (1σ) for these analyses was better than ± 0.04‰ for $\delta^{13}C$ and ± 0.1‰ for $\delta^{18}O$ (Appendix). Another set of shells, #8004, #9004 and #9005, were gently rinsed with ultra pure water (Milli–Q) and dried for a few days on a hotplate at 40 °C in a clean flow hood. Targeted parts of the shell were sampled for powder under binoculars using a precision drill (Proxxon) with a mounted dental tip. Stable isotope analyses of powders of these specimens were performed at GEOMAR, Kiel on a Thermo Finnigan MAT 252 mass spectrometer coupled online to an automated Kiel carbonate preparation line. The external reproducibility (1σ) of in–house carbonate standards was better than ± 0.1 ‰ and ± 0.08 ‰ for $\delta^{13}C$ and $\delta^{18}O$, respectively (Appendix).

2.4 Stable isotope analyses of water samples

In addition to carbon and oxygen isotope analyses of shells, analyses were also carried out on seawater samples collected from the culturing tanks. Measurements of $\delta^{13}C_{DIC}$ and $\delta^{18}O_{H2O}$ were performed using Thermo Scientific™ Delta Ray™ IRIS with URI Connect.

Isotope values ($\delta^{13}C$, $\delta^{18}O$) are reported as per mil (‰) deviations of the isotopic ratios ($^{13}C/^{12}C$, $^{18}O/^{16}O$) calculated to the VPDB scale for $\delta^{13}C$ and VSMOW scale for $\delta^{18}O$ values. Analytical reproducibility (1σ) on 3 aliquots of each water sample, was ≤ 0.03‰ for both $\delta^{13}C$ and $\delta^{18}O$ values (Appendix).

3 Results

3.1 Primary layer thickness

The thickness of the primary layer was measured at different positions along the shell from the posterior (umbonal) region to the *before–culturing* portion and finally to the anterior valve margin (Figure 6). Generally, in the posterior part of *M. venosa,* the primary layer is missing, or it has the lowest recorded thickness. Then, the primary layer progressively thickens toward the central and anterior parts. The thickest primary layer within the same valve is always located just before the beginning of the culture (*before–culturing* portion, Table 5). During culturing the thickness of the primary layer decreases. A most distinct change was observed in specimen #9006 cultured at the lowest pH condition of 7.6, and of 7.35 followed by another progressive increase in both valves *during–culturing*. In contrast, the thickness of the primary layer of the control condition specimen (#8005) remained stable (dorsal valve) or slightly decreased (Figure 6, ventral valve; Table 5).

12

Table 5. Statistical comparison of thickness of the primary layer (µm) along the ontogenetic direction of both valves of specimens #8005 and #9006 before and during culturing. ①: position of zones before culturing: P, C1, C2; during culturing: A1, A2, A3 (cf. Figure 6). n = number of measurements. Population standard deviation (σ) was calculated using the Excel STDEV.P function. Significant values (p–value ≤ 0.05) are marked in bold.

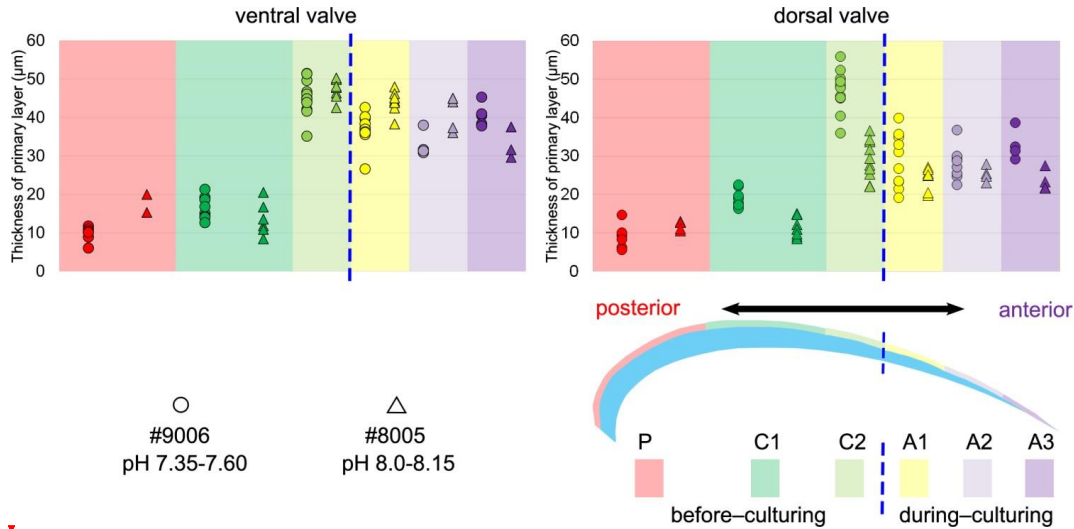| Sample	Position①	n	Mean	σ	Min	Max	p-values	p-values
#8005 dorsal	P	4	11.82	1.05	10.55	13.02	P vs C1 0.755	
	C1	8	11.40	2.29	8.50	15.05	C1 vs C2 **< 0.001**	
	C2	10	28.99	4.79	22.15	36.65	C2 vs A1 **0.033**	
	A1	8	24.36	2.52	19.80	27.06	A1 vs A2 0.726	
	A2	7	24.83	2.15	21.67	27.94	A2 vs A3 NA	
	A3	1	21.77	NA	NA	NA		#8005DP vs #9006DP 0.120
#8005 ventral	P	2	17.64	2.36	15.28	20		#8005DC1 vs #9006DC1 **< 0.001**
	C1	6	13.68	3.96	8.50	20.52	P vs C1 NA	
	C2	8	47.57	2.49	42.55	50.27	C1 vs C2 **< 0.001**	#8005DC2 vs #9006DC2 **< 0.001**
	A1	8	44.18	2.68	38.33	47.98	C2 vs A1 **0.028**	
	A2	6	42.09	3.85	36.06	45.04	A1 vs A2 0.289	#8005DA1 vs #9006DA1 0.088
	A3	4	34.09	3.51	29.63	37.52	A2 vs A3 **0.017**	#8005DA2 vs #9006DA2 0.101
#9006 dorsal	P	7	9.08	2.77	5.56	14.64		#8005DA3 vs #9006DA3 NA
	C1	10	18.78	2.04	16.90	22.50	P vs C1 **< 0.001**	#8005VP vs #9006VP NA
	C2	11	46.91	5.22	35.92	55.86	C1 vs C2 **< 0.001**	
	A1	10	28.83	6.65	19.04	39.93	C2 vs A1 **< 0.001**	#8005VC1 vs #9006VC1 0.123
	A2	8	28.06	4.03	22.50	36.69	A1 vs A2 0.779	
	A3	4	32.84	3.55	29.10	38.65	A2 vs A3 0.096	#8005VC2 vs #9006VC2 0.194
#9006 ventral	P	7	9.78	1.72	6.07	11.79		#8005VA1 vs #9006VA1 **< 0.001**
	C1	9	16.75	2.77	12.61	21.29	P vs C1 **< 0.001**	#8005VA2 vs #9006VA2 **0.007**
	C2	12	45.16	4.34	35.09	51.40	C1 vs C2 **< 0.001**	
	A1	11	36.92	3.82	26.62	42.54	C2 vs A1 **< 0.001**	#8005VA3 vs #9006VA3 **0.027**
	A2	4	32.95	2.91	30.84	37.95	A1 vs A2 0.102	
	A3	5	40.55	2.63	37.78	45.23	A2 vs A3 **0.008**	

Figure 6. Variation of the thickness of the primary layer (ventral and dorsal valve) of a *M. venosa* specimen cultured at pH 7.35 and 7.6 (#9006) and a specimen cultured at pH 8.0 and 8.15 (#8005).

3.2 Endopunctae density and size

On the externally–ground surface of the anterior part, the total number and the diameter (max) of endopunctae in a squared area of 800 μm × 800 μm was measured in four *before-culturing* and of the *during–culturing* parts of the shell (Figure 7). Generally, the density of endopunctae gradually increased along the selected transect from ca. 185 /mm^2 to ca. 305 /mm^2 in the ventral valve and from ca. 220 /mm^2 to ca. 280 /mm^2 in the dorsal valve (Table 6). The size of endopunctae increased along the selected transect in the ventral valve (from ca. 17 μm to 33 μm; Table 7), but it slightly decreases in the dorsal valve from ca. 36 μm to ca. 21 μm (Table 7). These density and size trends were observed in both specimens cultured at different pH conditions. However, it is noteworthy that in the most anterior part (*during–culturing*) of the ventral valve of #9006 (cultured at a pH of 7.35), the density of endopunctae sharply increases and their diameter reached a recorded maximum values (Table 6).

Table 6. Statistical comparison of the number of endopunctae (per mm^2) on both valves of #8005 and #9006. ①: position of zones before culturing: C2, and post culturing: A1, A2, A3 (cf. Figure 7).

Sample	Zone①	n	Mean	σ	Min	Max
	C2	3	236	10.4	225	250
#8005 dorsal	A1	1	280	NA	NA	NA
	A2	2	244	12.5	231	256

14

Sample	Zone	N	Mean	σ	Min	Max
	A3	2	281	14.1	267	295
#8005 ventral	C2	2	225	1.6	223	227
	A1	1	242	NA	NA	NA
	A2	2	241	5.5	236	247
	A3	2	269	6.3	263	275
#9006 dorsal	C2	2	221	8.6	213	230
	A1	1	269	NA	NA	NA
	A2	2	250	3.1	247	253
	A3	2	266	3.1	263	269
#9006 ventral	C2	2	186	3.1	183	189
	A1	1	234	NA	NA	NA
	A2	2	230	4.7	225	234
	A3	2	308	1.6	306	309

Table 7. Statistical comparison of the diameter (max) (µm) of endopunctae on valves of #8005 and #9006. ①: position of zones before culturing: C2, and during culturing: A1, A2, A3 (cf. Figure 7). Significant values (p-value ≤ 0.05) are marked in bold.

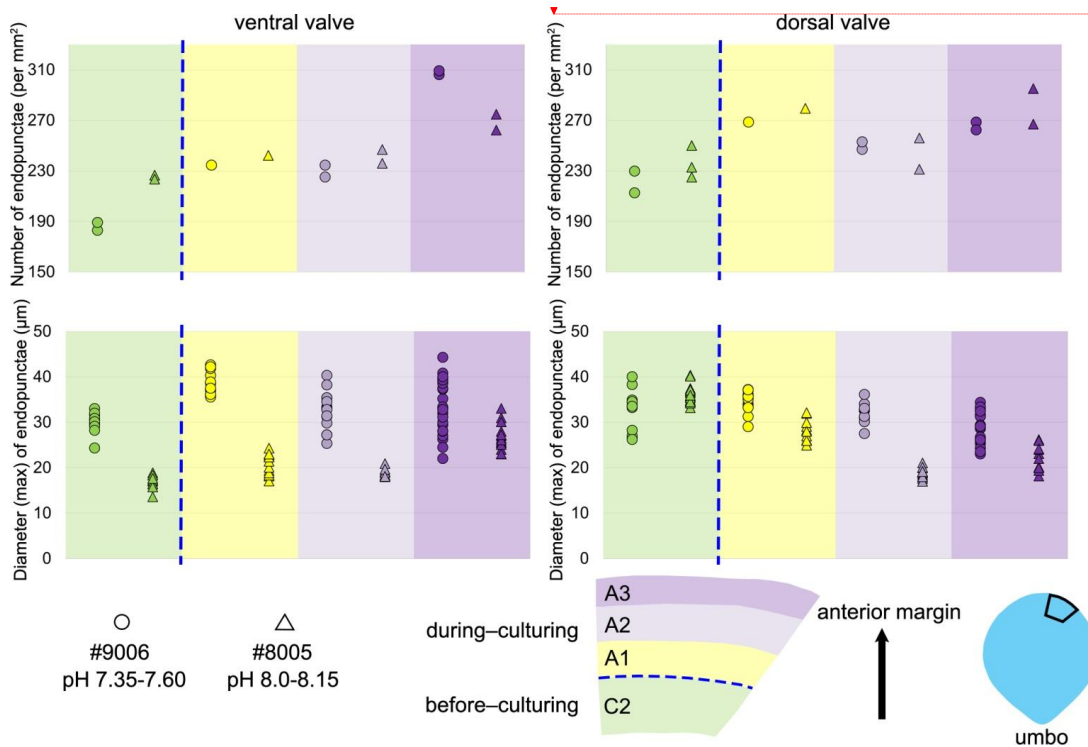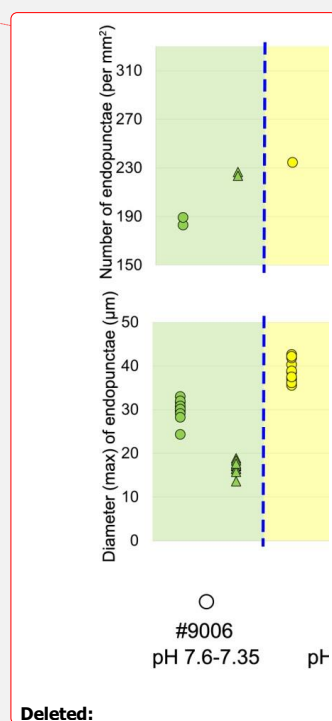| Sample	Zone①	n	Mean	σ	Min	Max	p-values	p-values
#8005D	C2	21	36.04	1.78	33.2	40.4	C2 vs A1 < **0.001**	#8005DC2 vs #9006DC2 **0.025**
	A1	10	28.36	2.33	25	32.1	A1 vs A2 < **0.001**	
	A2	15	18.77	1.10	17	21.1	A2 vs A3 **0.001**	
	A3	13	21.8	2.53	18.2	26.2		#8005DA1 vs #9006DA1 < **0.001**
#8005V	C2	11	17.07	1.42	13.6	18.9	C2 vs A1 < **0.001**	
	A1	13	20.88	2.22	17.1	24.3	A1 vs A2 **0.007**	#8005DA2 vs #9006DA2 < **0.001**
	A2	12	18.74	0.84	18	20.9	A2 vs A3 < **0.001**	
	A3	14	26.83	2.83	23	33.1		
#9006D	C2	12	32.54	4.39	26.2	40	C2 vs A1 0.178	#8005DA3 vs #9006DA3 < **0.001**
	A1	13	34.63	2.33	29	37.2	A1 vs A2 **0.012**	
	A2	11	32.02	2.12	27.5	36.1	A2 vs A3 **0.005**	
	A3	19	28.75	3.51	23	34.4		
#9006V	C2	13	29.98	2.04	24.3	33	C2 vs A1 < **0.001**	#8005VC2 vs #9006VC2 < **0.001**
	A1	12	38.66	2.41	35.5	42.6	A1 vs A2 < **0.001**	
	A2	14	32.51	4.08	25.3	40.3	A2 vs A3 0.516	
	A3	24	33.70	5.82	22	44.3		#8005VA1 vs #9006VA1 <

Figure 7. Variation in the number and diameter (max) of endopunctae in the dorsal and ventral valve from a specimen of *M. venosa* cultured at pH 7.35 and 7.6 (#9006) and a specimen cultured at pH 8.0 and 8.15 (#8005).

3.3 Shell morphometrics

3.3.1 Before–culturing

Ontogenetic variation in fibre morphometry is not obvious when all six adult specimens are considered (Table 8). However, clearer growth trends can be observed when considering the data from each single specimen separately, where *t*-tests on morphometric data from specimens #8005 and #9006 show that there are significant differences in Feret diameter (max) and Roundness between the posterior and the middle part of the shell (Table 9). Overall, in specimens #8005 and #9006 fibres become wider from the posterior to mid–shell. In contrast, #63 shows an opposite trend along the posterior to mid-shell direction (Figure 8). The fibre size and shape in the other specimens are rather constant.

Sidebar markup annotations:

Formatted: Font: 9 pt, Bold
Deleted: Variations
Formatted: Font: 9 pt, Bold
Formatted: Font: 9 pt, Bold
Formatted: Affiliation, None
Deleted: and dorsal
Formatted: Font: 9 pt, Bold
Deleted: –
Formatted: Font: 9 pt, Bold

Deleted:

Table 8. Statistical comparison of fibre size and shape of the posterior external vs central middle parts of the ventral and dorsal valves. NC: non-cultured samples #158, #223; CU: cultured samples #43, #63, #8005, #9006; Vpe: ventral posterior external, Vcm: ventral central middle, Dpe: dorsal posterior external, Dcm: dorsal central middle. Significant values (*p*–value ≤ 0.05) are marked in bold.

Sample	Position	*n*	Mean	*σ*	Min	Max	*p*-values
Feret diameter (max) (μm):							
NC	Vpe	7	13.79	3.22	6.97	17.33	NC Vpe vs CU Vpe 0.486
CU	Vpe	26	12.47	6.58	4.59	24.78	NC Vcm vs CU Vcm 0.633
NC	Vcm	32	12.98	2.91	7.09	20.61	NC Vpe vs NC Vcm 0.533
CU	Vcm	65	13.24	2.15	8.68	18.84	CU Vpe vs CU Vcm 0.572
NC	Dpe	8	18.36	4.22	13.30	24.46	NC Vpe vs CU Vpe 0.486
CU	Dpe	12	10.78	6.36	4.85	22.29	NC Vcm vs CU Vcm 0.633
NC	Dcm	12	12.14	1.13	9.84	14.42	NC Vpe vs NC Vcm 0.533
CU	Dcm	46	12.51	1.57	9.45	15.89	CU Vpe vs CU Vcm 0.572
Roundness:							
NC	Vpe	7	0.308	0.077	0.239	0.475	NC Vpe vs CU Vpe 0.717
CU	Vpe	26	0.296	0.074	0.172	0.446	NC Vcm vs CU Vcm 0.396
NC	Vcm	29	0.282	0.051	0.179	0.389	NC Vpe vs NC Vcm 0.296
CU	Vcm	65	0.272	0.051	0.180	0.421	CU Vpe vs CU Vcm 0.146
NC	Dpe	8	0.220	0.034	0.169	0.268	NC Dpe vs CU Dpe **0.003**
CU	Dpe	12	0.337	0.100	0.155	0.500	NC Dcm vs CU Dcm **0.028**
NC	Dcm	11	0.311	0.068	0.192	0.416	NC Dpe vs NC Dcm **0.005**
CU	Dcm	48	0.269	0.051	0.162	0.378	CU Dpe vs CU Dcm **0.048**
Convexity:							
NC	Vpe	7	0.985	0.004	0.979	0.991	NC Vpe vs CU Vpe 0.309
CU	Vpe	26	0.982	0.008	0.968	0.999	NC Vcm vs CU Vcm 0.655
NC	Vcm	32	0.984	0.005	0.975	1.000	NC Vpe vs NC Vcm 0.823
CU	Vcm	62	0.984	0.008	0.965	1.008	CU Vpe vs CU Vcm 0.257
NC	Dpe	8	0.987	0.006	0.979	0.998	NC Dpe vs CU Dpe 0.604
CU	Dpe	11	0.985	0.007	0.973	0.998	NC Dcm vs CU Dcm 0.273
NC	Dcm	12	0.984	0.008	0.973	1.000	NC Dpe vs NC Dcm 0.543
CU	Dcm	48	0.982	0.008	0.967	1.001	CU Dpe vs CU Dcm 0.207

Table 9. Statistical comparison of fibres size and shape data of the posterior external vs central middle area for #8005 and #9006, considering both valves together. pe: posterior external, cm: central middle. Significant values (*p*–value ≤ 0.05) are marked in bold.

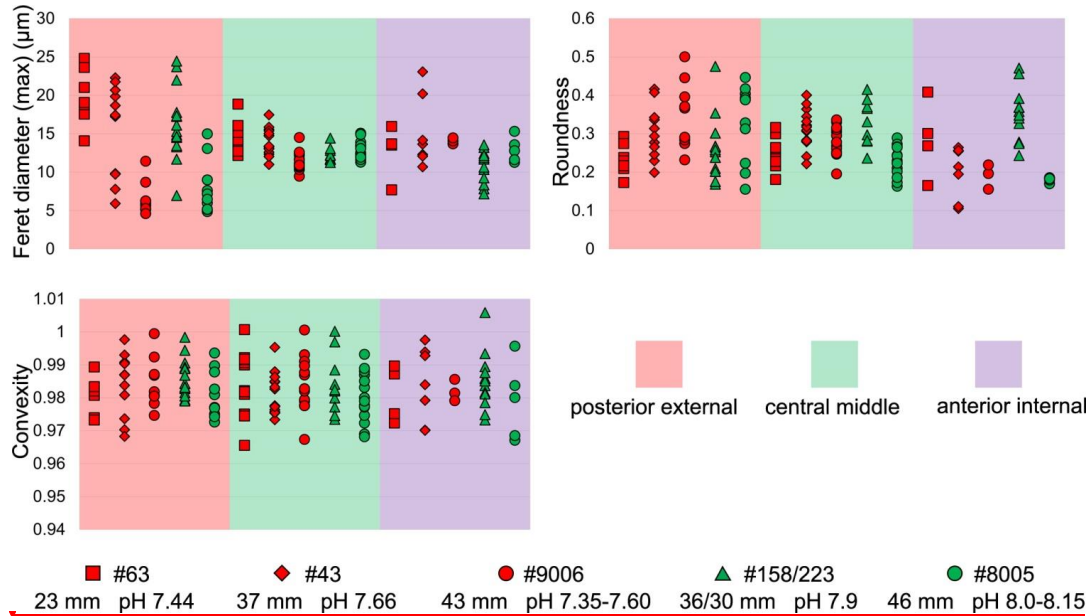| Sample	Position	N	Mean	σ	Min	Max	*p*-values
Feret diameter (max) (µm):							
#8005	pe	10	7.92	3.30	4.85	14.97	#8005 pe vs #9006 pe 0.265
#8005	cm	36	12.29	1.64	9.63	15.89	#8005 cm vs #9006 cm 0.171
#9006	pe	10	6.45	1.95	4.59	11.41	#8005 pe vs #8005 cm **0.003**
#9006	cm	25	11.73	1.39	8.68	15.24	#9006 pe vs #9006 cm **< 0.001**
Roundness:							
#8005	pe	10	0.33	0.097	0.155	0.446	#8005 pe vs #9006 pe 0.547
#8005	cm	36	0.25	0.045	0.162	0.374	#8005 cm vs #9006 cm **0.012**
#9006	pe	10	0.35	0.079	0.232	0.500	#8005 pe vs #8005 cm **0.040**
#9006	cm	26	0.28	0.043	0.195	0.369	#9006 pe vs #9006 cm **0.022**
Convexity:							
#8005	pe	10	0.981	0.007	0.973	0.994	#8005 pe vs #9006 pe 0.308
#8005	cm	35	0.982	0.008	0.968	1.001	#8005 cm vs #9006 cm 0.277
#9006	pe	9	0.985	0.007	0.975	0.999	#8005 pe vs #8005 cm 0.829
#9006	cm	26	0.984	0.007	0.967	1.001	#9006 pe vs #9006 cm 0.775

Figure 8. Comparisons of the fibre size and shape of *M. venosa* (ventral and dorsal valve) at different positions along the posterior-anterior axis; pH conditions of culturing or natural environment are reported. One circle point represents one measurement. Outliers have been removed, the latter were identified with Tukey's fences (Tukey, 1977), when falling outside the fences F1 and F2 [F1 = Q1 - 1.5IQR; F2 = Q3 + 1.5IQR; Q1/Q3 = first/third quartiles; IQR (interquartile range) = Q3 - Q1].
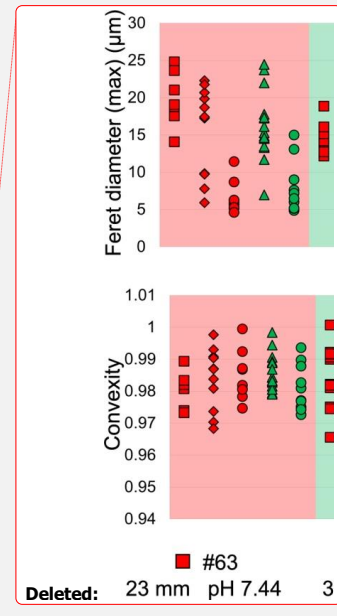
3.3.2 During–culturing

Transverse sections obtained by smoothing of the anterior part of the shell allowed to measure the width of 1392 fibres [Max Ferret diameter (max) see in Method 1], and select 388 sub–zones for fibre boundary calculation. In addition, they allowed us to focus on the parts that were produced under the different low–pH treatments (7.66, 7.60, 7.44, and 7.35 respectively).

In all six specimens, the width of fibres increases and the number of boundaries decreases along a transect from the more external subzone to the immediately inner subzone (e.g., Z1–1 to Z1–2; Z2–1 to Z2–2; and Z3–1 to Z3–2 in Figure 9a, b, c, d). That means, within a 10 μm distance the size of fibres become larger from the exterior to the interior part of the shell. Results from specimen #9006 (pH: 7.60 and 7.35) were compared to those of control specimen #8005 (pH: 8.00 and 8.15). Specimen #9006 cultured under low–pH conditions (pH: 7.60 and 7.35) had narrower fibres and a higher number of fibre boundaries when compared to that of control specimen #8005 (Figure 9a, c). It is worth noting that, in comparison between

19

the two specimens, the fibres from Z1–2 and Z2–2 of #9006 are significantly smaller than those of #8005. However, there is no significant difference in the size of fibres from subzone Z3–2 between the two specimens (Table 10).

The results from specimens (#43 and #63) grown under low pH conditions (pH: 7.66 and 7.44) for a short time interval of 214 days are difficult to interpret, as in this case, there is no direct control experiment sample to compare with the cultured specimens (Figure 9b, d). The specimens grown in the natural environment (#158, #223) have different sizes and ages and so different growth rates may affect the size of the fibres.

Table 10. Statistical comparison of fibres size of *M. venosa* (ventral and dorsal valve) in the anterior transverse sections (during culturing). ①: for the position of zones (Z1-1, Z2-1, Z3-1, Z1-2, Z2-2, Z3-2, Z4-1, Z5-1, Z4-2, Z5-2) see Figure 9. Significant values (p–value ≤ 0.05) are marked in bold.

Sample	position ①	N	Mean (µm)	STD	Min (µm)	Max (µm)	Difference between means (µm) and (p–values) #9006 vs #8005 for the same zone	Difference between means (µm) and (p–values) Z1 vs Z2, Z2 vs Z3 for the same vertical position in the same specimen	Difference between means (µm) and (p–values) Z1 vs Z2, Z2 vs Z3 for the same transverse position in the same specimen
#9006	Z1–1	26	4.43	1.06	2.86	6.74	0.23 (0.402)	#9006 Z1–1 vs Z2–1	
#8005	Z1–1	49	4.66	1.13	1.89	7.37		**0.60 (0.013)**	
#9006	Z2–1	53	3.83	0.66	2.76	5.30	0.12 (0.419)	#9006 Z2–1 vs Z3–1 0.07 (0.650)	#9006 Z1 vs Z2
#8005	Z2–1	65	3.95	1.03	2.06	6.46		#8005 Z1–1 vs Z2–1	**0.48 (0.011)**
#9006	Z3–1	38	3.76	0.80	2.32	5.55	0.32 (0.134)	**0.71 (0.001)**	#9006 Z2 vs Z3
#8005	Z3–1	44	4.08	1.05	2.22	7.53		#8005 Z2–1 vs Z3–1 0.13 (0.554)	0.14 (0.323)
#9006	Z1–2	26	4.71	1.27	2.76	8.38	**0.74 (0.024)**	#9006 Z1–2 vs Z2–2	#8005 Z1 vs Z2
#8005	Z1–2	46	5.45	1.29	2.94	10.43		0.33 (0.200)	**0.59 (< 0.001)**
#9006	Z2–2	48	4.38	0.90	2.87	7.00	**0.62 (0.001)**	#9006 Z2–2 vs Z3–2 0.30 (0.144)	#8005 Z2 vs Z3
#8005	Z2–2	59	5.00	0.97	2.94	7.16		#8005 Z1–2 vs Z2–2	0.09 (0.595)
#9006	Z3–2	40	4.68	1.01	2.57	7.76	0.40 (0.087)	**0.45 (0.048)**	
#8005	Z3–2	38	5.08	1.00	3.02	7.78		#8005 Z2–2 vs Z3–2 0.08 (0.720)	
#9006	Z4–1	23	3.79	0.71	2.72	4.99	**0.72 (0.003)**		
#8005	Z4–1	58	4.51	1.02	2.15	7.11		#9006 Z4–1 vs Z5–1 0.11 (0.594)	
#9006	Z5–1	24	3.68	0.72	2.54	5.19	NA		#9006 Z4 vs Z5 0.09 (0.615)
#9006	Z4–2	33	4.61	0.89	3.15	6.55	0.24 (0.272)	#9006 Z4–2 vs Z5–2	
#8005	Z4–2	52	4.85	1.01	3.07	6.90		0.06 (0.811)	
#9006	Z5–2	24	4.67	1.08	2.79	7.48	NA		

							#63 vs #43 vs #158/223 for the same zone	Z1 vs Z2 for the same vertical position in the same specimen	Z1 vs Z2 for the same transverse position in the same specimen
#63	Z1–1	36	3.37	0.59	2.39	4.97	#63 vs #158/223 **0.40 (0.013)**		
#43	Z1–1	70	3.73	0.98	1.63	6.94		#63 Z1–1 vs Z2–1 **0.72 (< 0.001)**	
#158/223	Z1–1	29	2.97	0.66	2.03	4.52	#43 vs #158/223 **0.76 (< 0.001)**		
#63	Z2–1	24	4.09	0.75	2.84	5.85	#63 vs #158/223 0.17 (0.404)	#43 Z1–1 vs Z2–1 0.26 (0.109)	
#43	Z2–1	61	3.99	0.82	1.95	5.88		#158/223 Z1–1 vs Z2–1 **0.95 (< 0.001)**	#63 Z1 vs Z2 **0.80 (< 0.001)**
#158/223	Z2–1	56	3.92	0.83	2.17	6.14	#43 vs #158/223 0.07 (0.691)		#43 Z1 vs Z2 **0.40 (0.001)**
#63	Z1–2	35	4.02	0.87	2.56	6.19	#63 vs #158/223 **0.73 (0.001)**		#158/223 Z1 vs Z2 **1.2 (< 0.001)**
#43	Z1–2	71	4.04	0.87	2.16	7.24		#63 Z1–2 vs Z2–2 **0.95 (< 0.001)**	
#158/223	Z1–2	25	3.29	0.67	2.04	4.73	#43 vs #158/223 **0.75 (< 0.001)**	#43 Z1–2 vs Z2–2 **0.58 (0.001)**	
#63	Z2–2	20	4.97	0.95	3.64	7.19	#63 vs #158/223 0.28 (0.234)	#158/223 Z1–2 vs Z2–2 **1.4 (< 0.001)**	
#43	Z2–2	56	4.62	1.10	2.68	7.67			
#158/223	Z2–2	55	4.69	0.85	3.02	7.09	#43 vs #158/223 0.07 (0.688)		

Formatted Table

Figure 9. Differences in sizes of fibres of *M. venosa* (ventral and dorsal valve) in the anterior transverse sections of specimens cultured at different pH conditions. (a) (b): The bottom/top of the box and the band inside the box are the first/third quartiles and the median of the data respectively; ends of the whiskers represent the minimums and maximums. **(c) (d):** Circle point represents average data, N_m: number of measurement.

3.4 Stable isotopes

The carbon and oxygen isotope compositions were measured along the shell growth increments in the dorsal and ventral valves (Figure 10). In the *before–culturing* part of the shell, $\delta^{13}C$ values varied between -2.02 and +0.45 ‰ in control group specimens #8004 and #8005, whereas they varied between -9.24 and -0.53 ‰ in the low pH group specimens #9004, #9005 and #9006. Similarly, in the before-culturing shell part, $\delta^{18}O$ values varied between -2.39 and +0.21 ‰ in the control group specimens #8004 and #8005, but varied between -4.92 and +0.05 ‰ in the low pH group specimens #9004, #9005 and #9006.

In the *during–culturing* part, $\delta^{13}C$ values varied between -6.80 and -1.34 ‰ in the control group specimens #8004 and #8005, whereas they varied between -27.09 and -9.69 ‰ in the low pH group specimens #9004, #9005 and #9006 (Figure 10). Concomitantly, $\delta^{18}O$ values varied between -6.80 and -1.34 ‰ in the control group specimens #8004 and #8005, but varied between -6.97 and -5.29 ‰ in the low pH group specimens #9004, #9005 and #9006 (Figure 10).

A marked drop in $\delta^{13}C$ and $\delta^{18}O$ is recorded in the shell increments produced *during–culturing*, particularly so in the specimens grown under low pH conditions of 7.60 and 7.35, where $\delta^{13}C$ values decreased to -27.09 ‰ (Figure 10).
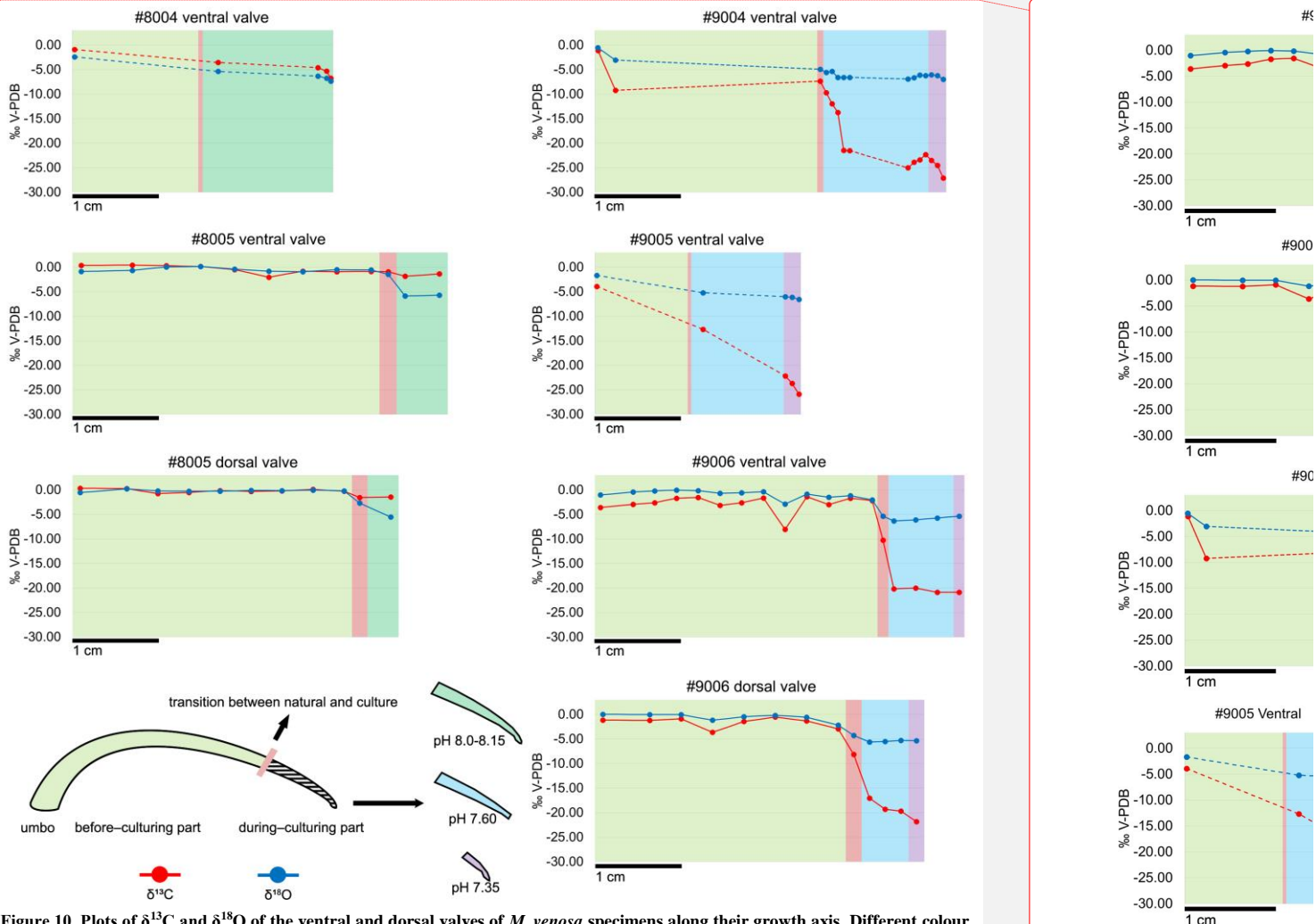
Figure 10. Plots of δ^{13}C and δ^{18}O of the ventral and dorsal valves of *M. venosa* specimens along their growth axis. Different colour backgrounds represent different pH conditions during growth. When few data were available, data-points were joined by dashed lines.

Deleted:

Formatted: Font: 9 pt, Bold

24

4 Discussion

4.1 Microstructure and organic components relationship

Before discussing whether and how acidification may affect the microstructure of the brachiopod shell, it is important to examine the relationship between the microstructure and the amount of organic components within the shell. It has already been stated that, in fossil and recent brachiopods, different shell microstructures have different amounts of shell organic components (Garbelli et al., 2014, 2017; Casella et al., 2018; Ye et al., 2018a).

This holds true for most rhynchonelliformean brachiopods, the primary layer of *M. venosa* consists of acicular and granular calcite (Williams, 1968, 1973, 1997; MacKinnon and Williams, 1974; Williams and Cusack, 2007; Casella et al., 2018). Analyses of electron backscatter diffraction show that the primary layer is a thin nanocrystalline layer with higher micro–hardness and smaller–sized calcite crystallites compared to those of the secondary layer (Griesshaber et al., 2004). In addition, each spherical and small unit is coated by a mixture of organics and amorphous calcium carbonate (Cusack et al., 2010). This, *per se*, may suggest a higher amount of organic components associated with the primary layer in contrast to other shell layers (i.e. secondary or in some species tertiary layer), but it has never been proven.

In fossils, the primary layer is likely absent or if present diagenetically altered and it will luminesce (Grossman et al., 1991), suggesting that higher amounts of organics may be present. However, this has been also ascribed to the incorporation of magnesium into the lattice (Popov, et al., 2007; Cusack et al., 2008). A report of higher sulphur concentration in the primary layer of the brachiopod *Terebratulina retusa* may suggest the presence of a sulphur-rich organic component, but backscatter electron imaging revealed contradictory results (England et al., 2007). Cusack et al. (2008) showed that, in the same species, the sulphate concentration is higher in the primary layer than in the secondary layer.

Since there is no conclusive evidence for this observation, we cannot relate the increase in thickness of the primary layer to changes in organics within the shell. With respect to previous findings (Williams, 1966; Parkinson et al., 2005), our results show that the thickness of the primary layer of *M. venosa* is much less uniform and shows an increase with growth, which is more evident during culturing at low pH conditions. However, disturbances (stress condition with handling before and at the start of the culturing) may also cause an abrupt change in thickness.

Endopunctae, which during life are filled with mantle expansions, are widely distributed in the shell of *M. venosa* and show the superficial hexagonal close-packing pattern documented by Cowen (1966). The biological function of endopunctae is still controversial, with some suggesting, that generally, in living organisms, they serve as support and protection structures (Williams, 1956, 1997), as sensors, or as storage and respiration features (Pérez–Huerta et al., 2009). With more endopunctae filled by mantle expansions, the amount of organic tissue would increase in the same volume of shell. The density of endopunctae has been related to temperature, as species living at higher temperatures have greater endopunctae density (Campbell, 1965; Foster, 1974; Peck et al., 1987; Ackerly et al., 1993). The present analyses support the concept that the increase in endopunctae density may be related in part to ontogeny, and to low pH condition. This may be expected, as organisms living under low pH conditions have to up-regulate their internal pH to be able to calcify as demonstrated in *M.*

venosa by Jurikova et al. (in review) and also observed in other calcifiers such as corals (McCulloch et al., 2012; Movilla et al., 2014). This would require a higher energy cost and a larger respiration/storage surface would satisfy this requirement. In addition to the thickness of the primary layer and the density of the endopunctae, the size changes of the individual fibres within the fibrous secondary layer may also contribute to the variability in organic components. Most of the recent rhynchonelliformean brachiopods, and *M. venosa* in particular, possess a shell mainly made of a fibrous secondary layer (Williams, 1997; Parkinson et al., 2005; Williams and Cusack, 2007). Each fibre of this layer is secreted by the mantle and it is ensheathed by an organic membrane (e.g., Jope, 1965; Williams, 1968; MacKinnon, 1974; Williams and Cusack, 2007; Cusack et al., 2008; Casella et al., 2018). Thus, with a decrease in size but within the same shell volume the surface area increases and with it the amount of organic components. Recently, the relationship between the size of fibres and shell organic components was discussed in detail (Garbelli, 2017; Garbelli et al., 2017; Ye et al., 2018a). The main conclusion is that the smaller the calcite fibres, the higher the organic component in the shell (cf. Figure 11). Thus, smaller fibres, and a greater endopunctae density may lead to higher organic content per shell volume (Figure 11).
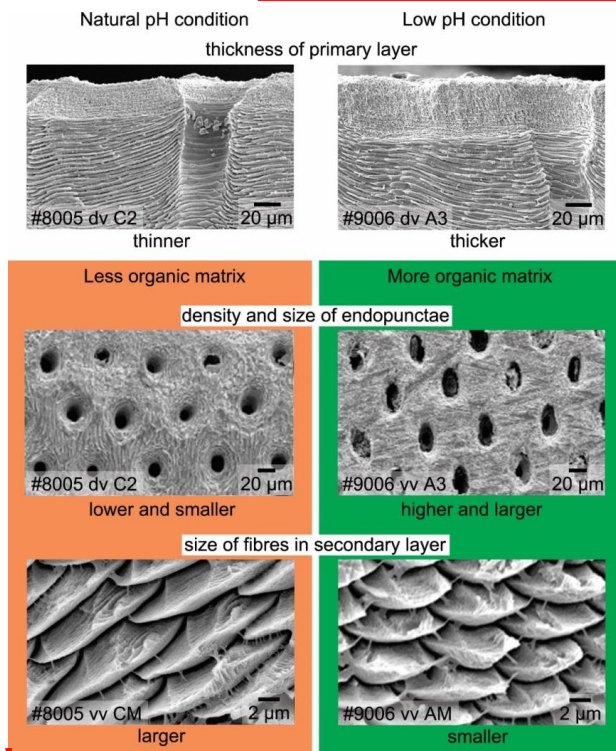

Figure 11. Relationship between the microstructure and the organic components of calcified shells of brachiopods. Position information see Figure 6 and Figure 7; dv: dorsal valve; vv: ventral valve; CM: central middle part; AM: anterior middle part.

26

4.2 Low pH and brachiopod microstructure

Several studies tried to understand how marine carbonate-shelled animals respond to ocean acidification, such as brachiopods (McClintock et al., 2009; Cross et al., 2015, 2016, 2018; Jurikova et al., in review), bivalves (e.g., Berge et al., 2006; McClintock et al., 2009; Beniash et al., 2010; Parker et al., 2010; Melzner et al., 2011; Talmage and Gobler, 2011; Amaral et al., 2012; Hiebenthal et al., 2013; Coleman et al., 2014; Gobler et al., 2014; Milano et al., 2016), cold–water scleractinian corals (e.g., Form and Riebesell, 2012; McCulloch et al., 2012; Jantzen et al., 2013b; Büscher et al., 2017) and sea urchins (Suckling et al., 2015) (Supplementary table 1). The results of these studies show that, in general, seawater acidification reduces the growth rate of marine calcifiers (Michaelidis et al., 2005; Shirayama and Thornton, 2005; Berge et al., 2006; Bibby et al., 2007; Beniash et al., 2010; Nienhuis et al., 2010; Thomsen and Melzner, 2010; Fernández–Reiriz et al., 2011; Melzner et al., 2011; Mingliang et al., 2011; Parker et al., 2011, 2012; Talmage and Gobler, 2011; Liu and He, 2012; Navarro et al., 2013; Milano et al., 2016).

For brachiopods, in the *Liothyrella uva* (Antarctic) and *Calloria inconspicua* (New Zealand), no ocean acidification effects on shell growth were detected by Cross et al. (2015, 2016, 2018), although the shells of the former species may rapidly dissolve in acidified waters (McClintock et al., 2009). However, *C. inconspicua* from the same locality in New Zealand (Paterson Inlet, Stewart Island) laid down a denser shell over the last 120 years, with nearby environmental conditions increased by 0.6 °C from 1953 to 2016, and slightly increased by 35.7 µatm in pCO_2 from 1998 to 2016 (Cross et al., 2018). These changes are in line with global trends of ocean pH and temperature since the industrial revolution (Caldeira and Wickett, 2005; Orr et al., 2005; IPCC, 2013). The present experiment showed that growth of specimen was not affected by the low pH conditions, instead their growth was similar to that of specimens cultured under control conditions (#9006, ~0.9 cm in the ventral valve, ~0.8 cm in the dorsal valve; 8005, ~0.5 cm in the ventral valve, ~0.4 cm in the dorsal valve). Based on the von Bertalanffy growth function, Baumgarten et al. (2013) calculated an expected growth increment and rate and we compared those parameters with the measured ones under control and low-pH conditions. The results in Figure 12 demonstrate that the measured individual growth rates are within the range of the ones of naturally growing individuals.

27

Figure 12. Projection of shell length of ventral valves on the von Bertalanffy growth function (grey line) $L_t = 71.53 [1 - e^{-0.336(t-t0)}]$, source from Baumgarten et al. (2013), L_b: shell length at the beginning of culturing; L_m: measured shell growth at the end of culturing; Le: expected shell growth.

A limiting factor is the small database, but in general, the present observations agree with studies that show no or little impact of acidification on the growth rates of marine calcifiers (cf., Marchant et al., 2010; Thomsen et al., 2010; Range et al., 2011, 2012; Talmage and Gobler, 2011; Dickinson et al., 2012; Fernández–Reiriz et al., 2012; Liu and He, 2012; Hiebenthal et al., 2013; Cross et al., 2015, 2016, 2018) or, even an increase in respiration, shell growth or metabolic rates after having experienced low pH condition (Wood et al., 2008; Cummings et al., 2011; Parker et al., 2012). We note however, that a combined effect of multiple stressors, such as low pH, lower dissolved oxygen and higher temperature or scarce food availability is more complex and potentially detrimental.. For instance, Steckbauer et al. (2015) reported that hypoxia and increased pCO$_2$ could significantly reduce the respiration rate of some marine invertebrates (Anthozoa, Gastropoda, Echinoidea and Crustacea). On the other hand, the highest growth rate in the bivalve *Macoma balthica* [= *Limecola balthica* (Linnaeus, 1758)] was observed in seawater with low O$_2$ and high pH (Jansson et al., 2015). Gobler et al. (2014) reported that juveniles of the bivalves *Argopecten irradians* (Lamarck, 1819) and *Mercenaria mercenaria* (Linnaeus, 1758) were not affected by and when hypoxia or acidification was applied individually, but the growth rate decreased when juveniles were exposed to both conditions simultaneously.

To explore the effects of acidification on brachiopod biomineralization, the microstructures of the specimens cultured for 214 days (#43, pH = 7.66 ± 0.04; and #63, pH = 7.44 ± 0.08) and the other population cultured for 335 days (#8005, pH =

28

8.0 to 8.15 ± 0.05; and #9006, pH = 7.6 to 7.35 ± 0.05) were investigated in detail. No conclusive consideration can be carried out on the specimens cultured for 214 days (#43 and #63), but in the other culturing experiments conducted for 335 days, the microstructure produced by the specimen cultured at low pH conditions was different from that produced under control condition: 1) the thickness of the primary layer increased with culturing (supplementary figure 1a-d); 2) the density and size of the endopunctae were higher (supplementary figure 1e-h); and 3) the fibres of the secondary layer were smaller. The punctal pattern detected here is different from that observed by Cross et al. (2018), who recorded no change in the punctal density of the ventral valve of *C. inconspicua* on specimens from the last 120 years. Also different is the trend in size of the endopunctae, which measured in the dorsal valve by Cross et al. (2018), seems to decrease. However, the slight environmental changes of the natural environment (refs. in Cross et al., 2018) are very different from those of our culturing experiments. Furthermore, the size of the endopunctae was measured from the dorsal valve only by Cross et al. (2018), whereas the increase in size we report was observed only from the ventral valve of *M. venosa*. A potential factor controlling this could be the duration of culturing under low-pH conditions. We note, however, that during the second phase of this acidification experiment (pH = 7.35), the seawater was strongly under-saturated with respect to calcite ($\Omega_{cal.}$ = 0.6), suggesting that the observed structural changes could be also linked to the saturation state. Conversely, the duration of low-pH conditions as a controlling factor is also in line with the few data available in the literature on microstructural changes during acidification. Milano et al. (2016) reported no significant difference in the prismatic microstructure of the cockle *Cerastoderma edule* when cultured under low pH conditions for about 2 months, except for dissolution of ontogenetically younger parts of the shell. Similarly, a study by Stemmer et al. (2013) on the clam *Arctica islandica* revealed that there was no effect on the shape and size of the crystals in the homogeneous microstructure after three months of culturing at low pH (Supplementary table 1). However, the experiments conducted by Fitzer et al. (2014a, b) for six months on the blue mussel *Mytilus edulis* showed that the animals exposed to low pH and high pCO$_2$ tend to produce less organised, disorientated calcite crystals and an unordered layer structure.

Thus, in bivalves, and similar to our observations, the duration of culturing may be crucial in recording significant effects. The present results lend support to the microstructure variation observed in brachiopods during the end-Permian extinction event and concomitant ocean acidification (Garbelli et al., 2017). During this event, both Strophomenata and Rhynchonellata produced more organic rich shells to cope with the long term and protracted seawater acidification effects (Garbelli et al., 2017).

4.3 Stable isotope variation at low pH condition

Brachiopod shells are commonly used as archives for deep-time paleoenvironmental reconstructions as they potentially record the original geochemical composition of the seawater they lived in (Grossman et al., 1993; Banner and Kaufman, 1994; Mii and Grossman, 1994; Mii et al., 2001; Brand et al., 2003, 2011, 2016; Jurikova et al., in review). Several studies suggest that carbon and oxygen isotope compositions of the secondary layer of brachiopod shells, especially slow-growing species – and particularly the innermost shell parts – tend to be close to equilibrium with the ambient seawater temperature

(e.g., Popp et al., 1986; Carpenter and Lohmann, 1995; Parkinson et al., 2005; Brand et al., 2013, 2015, 2016; Takayanagi et al., 2013; Yamamoto et al., 2013). Recently, Bajnai et al. (2018) documented that brachiopods do not incorporate oxygen isotopes in thermodynamic equilibrium with ambient seawater, and appear to be subjected to taxon-specific growth-rate induced kinetic effects. The documented isotopic offset appears to be relatively constant throughout the range of brachiopod shell production from cold to warm environments. Thus, the brachiopod oxygen isotope composition, when corrected for the seawater-^{18}O contribution records ambient water temperatures close to those observed for their ambient environment (Brand et al., 2013). Overall, the δ^{18}O values of brachiopods remain a mainstay and robust proxies of paleoenvironmental temperature conditions.

In general, the measured δ^{13}C (between -8.05 ‰ and +0.45 ‰) and δ^{18}O (between -3.04 ‰ and +0.21 ‰) values of the secondary layer produced during growth in the natural environment (Figure 10) are similar to previous results from the shells of *M. venosa* (Penman et al., 2013; Ullmann et al., 2017; Romanin et al., 2018). Furthermore, the present results show that there are no significant differences in δ^{13}C and δ^{18}O values between the dorsal and the ventral valves (*p*–values in δ^{13}C and δ^{18}O of #8005 are 0.437 and 0.491 respectively, *p*-values in δ^{13}C and δ^{18}O of #9006 are 0.862 and 0.910 respectively), which is in agreement with previous findings (e.g., Parkinson et al., 2005; Brand et al., 2015; Romanin et al., 2018).

In the naturally grown shell *before–culturing*, the δ^{13}C and δ^{18}O values are relatively stable along the ontogenetic direction (Supplementary table 2), except for the depleted values at approximately mid–shell length in both #8005 and #9006. In particular, in #9006, in this part of the shell values drop to about -6 ‰ for δ^{13}C and -2 ‰ for δ^{18}O values (Figure 10). Since the samples were taken from the mid-shell layer and not from the shell interior, we can exclude that the isotope negative shift was produced by shell material added during the *during–culturing* shell thickening. This small drop may be an artefact of both sampling and analytical uncertainties. However, it does not distract from the isotopic drop observed with culturing. Also, negative isotope excursions of a similar magnitude were recorded in *M. venosa* specimens from the South America shelf by Ullmann et al. (2017) and Romanin et al. (2018). Ullmann et al. (2017) implied that these variable δ^{13}C and δ^{18}O values indicate isotope disequilibrium with ambient waters in Terebratellids. In contrast, Romanin et al. (2018), who also analysed specimens collected from Comau Fjord, attributed the negative isotope excursion to environmental perturbations, in particular, to changes in seawater productivity and temperature, and/or to anthropogenic activities. Negative shifts in both, δ^{13}C and δ^{18}O values during ontogeny have been also observed in the brachiopod *Terebratella dorsata*, which co–occurs with *M. venosa* and have been explained by the effect of resorption in corresponding muscle scar areas (Carpenter and Lohmann, 1995). Here, we follow the interpretation of Romanin et al. (2018) to explain the mid–shell excursion observed in our specimens.

The most prominent change in δ^{13}C values was observed in the secondary layer produced *during–culturing* under low pH conditions, reflecting the composition of the δ^{13}C$_{DIC}$ (δ^{13}C VPDB: -23.63 ‰ for the low pH / high *p*CO$_2$ conditions and -2.03 ‰ for the control conditions, during the last culturing phase). The δ^{13}C values were significant depleted by more than 20 ‰ in the specimens cultured under low pH / high *p*CO$_2$ conditions (pH 7.60 and pH 7.35; #9004, #9005 and #9006) (Figure 10, Appendix, Supplementary table 2), whereas the depletion was lower and only a few per mil (about 0.9–1.2 ‰) in the control

specimens (pH 8.00 and 8.15; #8004 and #8005). This demonstrates that the δ^{13}C values of *M. venosa* to a large extent reflect the composition of the CO_2 source, and thus present a valuable geochemical archive. Similar observations have also been reported for other calcifiers cultured under controlled experimental settings with pH mediated by CO_2-bubbling. For a comparison, Hahn et al. (2014) reported a decreasing trend of about 10 ‰ in δ^{13}C values in the blue mussel *Mytilus edulis* when exposed to seawater conditions of pH 8.03 (pCO$_2$ 612 µatm) and pH of 7.21 (pCO$_2$ 4237 µatm). In corals, a species–specific δ^{13}C response to high pCO$_2$ conditions was reported by Krief et al. (2010) of more negative 2.3‰ and 1.5‰ δ^{13}C values in *Porites* sp. after 14 months of culturing at low pH conditions (pH 7.49, pCO$_2$ 1908 µatm and 7.19 pCO$_2$, 3976 µatm), whereas no significant difference was found in other coral species, such as *Stylophora pistillata* (Esper, 1797).

In our culturing experiments, oxygen isotope compositions of the shells record only a minor depletion *during* culturing at different pH conditions [δ^{18}O (VPDB): -6.4 ‰ to -7.9 ‰ / (VSMOW): ~ +23.6‰ to +24.3 ‰] in comparison to the values observed in the shell parts grown under natural conditions, following the changes in the $\delta^{18}O_{H2O}$.

The fractionation of carbon and oxygen isotopes between phases – brachiopod calcite and culture seawater – is defined as $\Delta^{13}C_{cal-DIC}$ or $\Delta^{18}O_{cal-sw}$ = 1000 × ln$\alpha_{cal-DIC/sw}$, where $\alpha_{cal-DIC/sw}$ = [^{13}C/^{12}C]$_{cal}$ / [^{13}C/^{12}C]$_{DIC}$ or [^{18}O/^{16}O]$_{cal}$ / [^{18}O/^{16}O]$_{sw}$, respectively. The calculated values based on our culture measurements are presented in Table 11.

Table 11. Calculated carbon and oxygen fractionation factors for brachiopods based on cultured *M. venosa* and culture seawater.

Sample #ID	Treatment	Avg. $\Delta^{13}C_{cal-DIC}$	Avg. $\Delta^{18}O_{cal-sw}$	Growth temperature
#8004	Control	-4.06	29.99	10 ℃
#9005	Acidification pH 7.35	-1.21	30.92	10 ℃
#9004	Acidification pH 7.35	-2.23	30.70	10 ℃

For carbon isotopes, we observe variable $\Delta^{13}C_{cal-DIC}$ between the different specimens and culturing treatments, and it is inconclusive if this is linked to culturing conditions, differences between individuals or involves an ontogenetic component. It appears that there is about a 2 ‰ difference between the control specimen and samples from the acidification treatments (pH 7.35), with the last one being, strikingly, closer to the equilibrium with seawater DIC. Possibly, this illustrates the variability in kinetic effects (Bajnai et al., 2018), but may also be linked to changes in the source $\delta^{13}C_{DIC}$ in the control treatment. More studies are needed to fully answer this question.

However, our brachiopod δ^{18}O values are offset from calcite equilibrium δ^{18}O (-4.4‰, relative to 10°C from Watkins et al., 2013) by -2.2‰ to -2.7‰, for the low-pH and the control specimen, respectively. This offset is comparable to that recorded by Bajnai et al. (2018). There, the *M. venosa* specimen showed apparent equilibrium δ^{18}O relative to Kim and O'Neil (1997) which translates to a ca. -1.5‰ offset, relative to Watkins et al. (2013). In addition, alike in the experiment of Watkins et al. (2013), we observed a slight trend in pH, with higher $\Delta^{18}O_{cal-sw}$ at lower pH.

Thus, the data suggest that large part of the secondary layer isotope record may reflect the environmental conditions supporting the interpretation of brachiopod shells as good archives of geochemical proxies, even when stressed by ocean acidification.

5 Conclusions

This study combines the analysis of shell microstructures on 6 specimens consisting of 1932 fibre size measurements, 170 primary layer thickness measurements, 256 punctal density and diameter measurements and stable isotope geochemistry on 5 specimens of 79 sample analyses, on brachiopods cultured at low pH conditions for different time intervals. The results suggest the following conclusions.

In brachiopod specimens cultured for a period of 11 months, the microstructure produced by the specimen cultured at low pH (from pH 7.60 to pH 7.35) is different from that produced under control conditions (pH 8.00 and 8.15). In particular, the microstructure of shells produced at low pH tends to be more organic rich. A result that lends strong support to brachiopod microstructure variations observed in fossil counterparts and the related effect of ocean acidification.

Brachiopod shell parts precipitated during culture conditions of low pH for about one year record a change in the microstructure but not in the growth rate.

Their δ^{13}C and δ^{18}O values are rather constant during growth but experience a sharp drop during culturing. In particular, the δ^{13}C values dropped abruptly in specimens cultured for one year at low pH conditions. This drop is related to the source of carbon dioxide gas used in the culture setup.

Brachiopods are thus faithful recorders of the ambient carbon and oxygen isotope compositions, even when stressed by environmental perturbations such as ocean acidification.

The present observations are invaluable in using proxies and shell morphologic features for studying ocean acidification events and changes in atmospheric CO_2 contents in the geologic past.

References:

Ackerly, S., Cisne, J. L., Railsback, L. B., and Anderson, T. F.: Punctal density in the Ordovician orthide brachiopod *Paucicrura rogata*: anatomical and paleoenvironmental variation, Lethaia, 26, 17–24, 1993.

Amaral, V., Cabral, H. N., and Bishop, M. J.: Moderate acidification affects growth but not survival of 6–month–old oysters, Aquatic Ecol., 46, 119–127, 2012.

Atkinson, M. J. and Bingman, C.: Elemental composition of commercial seasalts, J. Aquaricult. Aquat. Sci., 8, 39–43, 1998.

32

Bajnai, D., Fiebig, J., Tomašových, A., Milner G. S., Rollin-Bard, C., Raddztz, J., Löffler, N., Primo-Romos, C., and Brand, U.: Assessing kinetic fractionation in brachiopod calcite using clumped isotopes, Sci. Rep., 8, 533, 2018.

Banner, J. L. and Kaufman, J.: The isotopic record of ocean chemistry and diagenesis preserved in non-luminescent brachiopods from Mississippian carbonate rocks, Illinois and Missouri, Geol. Soc. Am. Bull., 106, 1074–1082, 1994.

Baumgarten, S., Laudien, J., Jantzen, C., Häussermann, V., and Försterra, G.: Population structure, growth and production of a recent brachiopod from the Chilean fjord region, Mar. Ecol., 35, 401–413, 2013.

Beniash, E., Ivanina, A., Lieb, N. S., Kurochkin, I., and Sokolova, I.: Elevated level of carbon dioxide affects metabolism and shell formation in oysters *Crassostrea virginica*, Mar. Ecol., 419, 95–108, 2010.

Berge, J. A., Bjerkeng, B., Pettersen, O., Schaanning, M. T., and Øxnevad, S.: Effects of increased sea water concentrations of CO_2 on growth of the bivalve *Mytilus edulis* L, Chemosphere, 62, 681–687, 2006.

Bibby, R., Cleall–Harding, P., Rundle, S., Widdicombe, S., and Spicer, J.: Ocean acidification disrupts induced defences in the intertidal gastropod *Littorina littorea*, Biol. Lett., 3, 699–701, 2007.

Brand, U. and Veizer, J.: Chemical diagenesis of a multicomponent carbonate system-1. Trace elements, J. Sediment. Petrol., 50, 1219–1236, 1980.

Brand, U., Logan, A., Hiller, N., and Richardson, J.: Geochemistry of modern brachiopods: applications and implications for oceanography and paleoceanography, Chem. Geol., 198, 305–334, 2003.

Brand, U., Logan, A., Bitner, M. A., Griesshaber, E., Azmy, K., and Buhl, D.: What is the ideal proxy of Palaeozoic seawater chemistry? Mem. Assoc. Australas., 41, 9–24, 2011.

Brand, U., Azmy, K., Bitner, M. A., Logan, A., Zuschin, M., Came, R., and Ruggiero, E., Oxygen isotopes and $MgCO_3$ in brachiopod calcite and a new paleotemperature equation, Chem. Geol., 359, 23–31, 2013.

Brand, U., Azmy, K., Griesshaber, E., Bitner, M. A., Logan, A., Zuschin, M., Ruggiero, E., and Colin, P. L.: Carbon isotope composition in modern brachiopod calcite: A case of equilibrium with seawater? Chem. Geol., 411, 81–96, 2015.

Brand, U., Blamey, N., Garbelli, C., Griesshaber, E., Posenato, R., Angiolini, L., Azmy, K., Farabegoli, E., and Came, R.: Methane Hydrate: Killer cause of Earth's greatest mass extinction, Palaeoworld, 25, 496–507, 2016.

Büscher, J. V., Form, A. U., and Riebesell, U.: Interactive effects of ocean acidification and warming on growth, fitness and survival of the cold–water coral *Lophelia pertusa* under different food availabilities, Front. Mar. Sci., 4, 101, 2017.

Caldeira, K. and Wickett, M. E.: Anthropogenic carbon and ocean pH, Nature, 425, 365, 2003.

Caldeira, K. and Wickett, M. E.: Ocean model predictions of chemistry changes from carbon dioxide emissions to the atmosphere and ocean, J. Geophys. Res., 110, C09S04, 2005.

Campbell, K. S. W.: Australian Permian terebratuloids, Bur. Min. Resour. Geol. Geophys. Aust. Bull., 68, l–113, 1965.

Carpenter, S. J., and Lohmann, K. C.: $\delta^{18}O$ and $\delta^{13}C$ values of modern brachiopod shells, Geochim. Cosmochim. Acta 59, 3749–3764, 1995.

Casella, L., Griesshaber, E., Simonet Roda, M., Ziegler, A., Mavromatis, V., Henkel, D., Laudien, J., Häussermann, V., Neuser, R. D., Angiolini, L., Dietzel, M., Eisenhauer, A., Immenhauser, A., Brand, U., and Schmahl, W. W.: Micro-

33

and nanostructures reflect the degree of diagenetic alteration in modern and fossil brachiopod shell calcite: a multi–analytical screening approach (CL, FE–SEM, AFM, EBSD), Palaeogeogr. Palaeoclimatol. Palaeoecol., 502, 13–30, 2018.

Coleman, D. W., Byrne, M., and Davis, A. R.: Molluscs on acid: gastropod shell repair and strength in acidifying oceans, Mar. Ecol. Prog. Ser., 509, 203–211, 2014.

Comeau, S., Gorsky, G., Jeffree, R., Teyssie, J. L., and Gattuso, J. P.: Impact of ocean acidification on a key Arctic pelagic mollusc (*Limacina helicina*), Biogeosciences, 6, 1877–1182, 2009.

Cowen, R.: The distribution of punctae on the brachiopod shell, Geol. Mag., 103, 269–275, 1966.

Cross, E. L., Peck, L. S., and Harper, E. M.: Ocean acidification does not impact shell growth or repair of the Antarctic brachiopod *Liothyrella uva* (Broderip, 1833), J. Exp. Mar. Biol. Ecol., 462, 29–35, 2015.

Cross, E. L., Peck, L. S., Lamare, M. D., and Harper, E. M.: No ocean acidification effects on shell growth and repair in the New Zealand brachiopod *Calloria inconspicua* (Sowerby, 1846), ICES J. Mar. Sci., 73, 920–926, 2016.

Cross, E. L., Harper, E. M., and Peck, L. S.: A 120-year record of resilience to environmental change in brachiopods, Glob. Chang. Biol., https://doi.org/10.1111/gcb.14085, 2018.

Cummings, V., Hewitt, J., Rooyen, A. V., Currie, K., Beard, S., Thrush, S., Norkko, J., Barr, N., Heath, P., Halliday, N. J., Sedcole, R., Gomez, A., McGraw, C., and Metcalf, V.: Ocean acidification at high latitudes: potential effects on functioning of the Antarctic bivalve *Laternula elliptica*, PLoS ONE, 6, e16069, 2011.

Cusack, M., Dauphin, Y., Cuif, J. P., Salomé, M., Freer, A., and Yin, H.: Micro–XANES mapping of sulphur and its association with magnesium and phosphorus in the shell of the brachiopod, *Terebratulina retusa*, Chem. Geol., 253, 172–179, 2008.

Cusack, M., Chung, P., Dauphin, Y., and Pérez–Huerta, A.: Brachiopod primary layer crystallography and nanostructure, in: Alvarez, F., and Curry, G. B., (Eds.): Evolution and Development of the Brachiopod Shell, Special Papers in Palaeontology, 84, Aberystwyth, Palaeontological Association, 99–105, 2010.

Crippa, G., Angiolini, L., Bottini, C., Erba, E., Felletti, F., Frigerio, C., Hennissen, J. A. I., Leng, M. J., Petrizzo, M. R., Raffi, I., Raineri, G., and Stephenson, M. H.: Seasonality fluctuations recorded in fossil bivalves during the early Pleistocene: Implications for climate change, Palaeogeogr. Palaeoclimatol. Palaeoecol., 446, 234–251, 2016a.

Crippa, G., Ye, F., Malinverno, C., and Rizzi, A.: Which is the best method to prepare invertebrate shells for SEM analysis? Testing different techniques on recent and fossil brachiopods, Boll. Soc. Paleontol. Ital., 55, 111–125, 2016b.

Dickinson, G. H., Ivanina, A. V., Matoo, O. B., Pörtner, H. O., Lannig, G., Bock, C., Beniash, E., and Sokolova, I. M.: Interactive effects of salinity and elevated CO_2 levels on juvenile Eastern oysters, *Crassostrea virginica*, J. Exp. Biol., 215, 29–43, 2012.

England, J., Cusack, M., and Lee, M. R.: Magnesium and sulphur in the calcite shells of two brachiopods, *Terebratulina retusa* and *Novocrania anomala*, Lethaia, 40, 2–10, 2007.

34

Deleted: Distribution

Deleted: Punctae

Deleted: Brachiopod Shell

Feely, R. A., Sabine, C. L., Lee, K., Berelson, W., Kleypas, J., Fabry, V.J., and Millero, F.J.: Impact of anthropogenic CO_2 on the $CaCO_3$ system in the oceans, Science, 305, 362–366, 2004.

Fernández–Reiriz, M. J., Range, P., Alvarez–Salgado, X. A., and Labarta, U.: Physiological energetics of juvenile clams *Ruditapes decussatus* in a high CO_2 coastal ocean, Mar. Ecol. Prog. Ser., 433, 97–105, 2011.

5 Fernández–Reiriz, M. J., Range, P., Alvarez–Salgado, X. A., Espinosa, J., and Labarta, U.: Tolerance of juvenile *Mytilus galloprovincialis* to experimental seawater acidification, Mar. Ecol. Prog. Ser., 454, 65–74, 2012.

Fitzer, S., Phoenix, V. R., Cusack, M., and Kamenos, N. A.: Ocean acidification impacts mussel control on biomineralisation, Sci. Rep., 4, doi:10.1038/srep06218, 2014a.

Fitzer, S., Cusack, M., Phoenix, V. R., and Kamenos, N. A.: Ocean acidification reduces the crystallographic control in

10 juvenile mussel shells, J. Struct. Biol., 188, 39–45, 2014b.

Form, A. U., and Riebesell, U.: Acclimation to ocean acidification during long–term CO_2 exposure in the cold–water coral *Lophelia pertusa*, Glob. Chang. Biol., 18, 843–3853, 2012. Försterra, G., Häussermann, V., and Lueter, C.: Mass occurrence of the recent brachiopod *Magellania venosa* (Terebratellidae) in the fjords Comau and Renihue, northern Patagonia, Chile, Mar. Ecol., 29, 342–347, 2008.

15 Foster, M. W.: Recent Antarctic and Subantarctic brachiopods, Antarctic Research Series, 21, American Geophysical Union, Washington, D.C., pp. 183, 1974.

Garbelli, C.: Shell microstructures in Upper Permian brachiopods: implication for fabric evolution and calcification, Boll. Soc. Paleontol. Ital., 123, 541–560, 2017.

Garbelli, C., Angiolini, L., Brand, U., and Jadoul, F., Brachiopod fabric, classes and biogeochemistry: Implications for the

20 reconstruction and interpretation of seawater carbon–isotope curves and records, Chem. Geol., 371, 60–67, 2014. Garbelli, C., Angiolini, L., and Shen, S. Z.: Biomineralization and global change: A new perspective for understanding the end–Permian extinction, Geology, 45, 19–12, 2017.

Gobler, C. J., DePasquale, E. L., Griffith, A. W., and Baumann, H.: Hypoxia and acidification have additive and synergistic negative effects on the growth, survival, and metamorphosis of early life stage bivalves, PLoS ONE, 9, e83648, 2014.

25 Griesshaber, E., Schmahl, W., Neuser, R., Job, R., Bluem, M., and Brand, U.: Microstructure of brachiopod shells−An inorganic/organic fibre composite with nanocrystalline protective layer, Mater. Res. Soc. Symp. Proc., 844, Y9.3.1– Y9.3.6, 2004.

Grossman, E. L., Zhang, C., and Yancey, T. E.: Stable–isotope stratigraphy of brachiopods from Pennsylvanian shales in Texas, Geol. Soc. Am. Bull., 103, 953–965, 1991.

30 Grossman, E. L., Mii, H., and Yancey, T. E.: Stable isotopes in Late Pennsylvanian brachiopods from the United Stated: Implications for Carboniferous paleoceanography, Geol. Soc. Am. Bull., 105, 1284–1296, 1993.

Guinotte, J. M., Orr, J., Cairns, S., Freiwald, A., Morgan, L., and George, R.: Will human–induced changes in sea water chemistry alter the distribution of deep-sea scleractinian corals? Front. Ecol. Environ., 1, 141–146, 2006.

35

Hahn, S., Rodolfo–Metalpa, R., Griesshaber, E., Schmahl, W. W., Buhl, D., Hall-Spencer, J. M., Baggini, C., Fehr, K. T., and Immenhauser, A.: Marine bivalve shell geochemistry and ultrastructure from modern low pH environments: environmental effect versus experimental bias, Biogeosciences, 9, 1897–1914, 2012.

Hahn, S., Griesshaber, E., Schmahl, W. W., Neuser, R. D., Ritter, A., Hoffmann, R., Buhl, D., Niedermayr, A., Geske, A., and Immenhauser, A.: Exploring aberrant bivalve shell ultrastructure and geochemistry as proxies for past sea water acidification, Sedimentology, 61, 1625–1658, 2014.

Hiebenthal, C., Philipp, E. E. R., Eisenhauer, A., and Wahl, M.: Effects of seawater pCO$_2$ and temperature on shell growth, shell stability, condition and cellular stress of Western Baltic Sea *Mytilus edulis* (L.) and *Arctica islandica* (L.), Mar. Biol., 160, 2073–2087, 2013.

IPCC: Climate change 2013: the physical science basis, in: Stocker, T. F., Qin, D., Plattner, G. –K., Tignor, M., Allen, S. K., Boschung, J., Nauels, A., Xia, Y., Bex, V., and Midgley, P. M. (Eds.): Contribution of working group I to the fifth assessment report of the intergovernmental panel on climate change, Cambridge University Press, Cambridge, United Kingdom and New York, NY, USA, pp. 1535, 2013.

Jansson. A., Norkko, J., Dupont, S., and Norkko, A.: Growth and survival in a changing environment: Combined effects of moderate hypoxia and low pH on juvenile bivalve *Macoma balthica*, J. Sea Res., 102, 41–47, 2015.

Jantzen, C., Laudien, J., Sokol, S., Försterra, G., Häussermann, V., Kupprat, F., and Richter, C.: In situ short-term growth rates of a cold–water coral, Mar. Freshw. Res., 64, 631–641, 2013a.

Jantzen, C., Häussermann, V., Försterra, G, Laudien, J., Ardelan, M., Maier, S., and Richter, C.: Occurrence of a cold-water coral along natural pH gradients (Patagonia, Chile), Mar. Biol., 160, 2597–2607, 2013b.

Jantzen, C., Laudien, J., Häussermann, V., Försterra, G., and Richter, C.: Seawater carbonate chemistry measured in fjord Comau, Patagonia, Chile (02-2011), Alfred Wegener Institute, Helmholtz Center for Polar and Marine Research, Bremerhaven, PANGAEA, https://doi.org/10.1594/PANGAEA.884131, 2017.

Jope, H. M.: Composition of brachiopod shell, in Moore, R. C. (Ed.): Treatise on Invertebrate Paleontology. Part H, Brachiopoda, Geological society of America and University of Kansas Press, New York and Lawrence, pp. 156–164, 1965.

Jurikova, H., Liebetrau, V., Gutjahr, M., Rollion–Bard, C., Hu, M. Y., Krause, S., Henkel, D., Hiebenthal, C., Schmidt, M., Laudien, J., and Eisenhauer, A.: Boron isotope systematics of cultured brachiopods: response to acidification, vital effects and implications for palaeo-pH reconstruction, Geochim. Cosmochim. Acta, in review.

Kim, S.T. and O'Neil, J.R.: Equilibrium and nonequilibrium oxygen isotope effects in synthetic carbonates, Geochim. Cosmochim. Acta, 61, 3461–3475, 1997.

Krief, S., Hendy, E. J., Fine, M., Yam, R., Meibom, A., Foster, G. L., and Shemesh, A.: Physiological and isotopic responses of scleractinian corals to ocean acidification, Geochim. Cosmochim. Acta, 74, 4988–5001, 2010.

Kurihara, H.: Effects of CO$_2$–driven ocean acidification on the early developmental stages of invertebrates, Mar. Ecol. Prog. Ser., 373, 274–284, 2008.

Deleted: pangaea.de/10.1594/PANGAEA.884131, https://doi.

Deleted: brachiopod calcite: the role of vital effects,

Deleted: paleo–

Deleted: reconstructions

Lannig, G., Eilers, S., Pörtner, H. O., Sokolova, I. M., and Bock, C.: Impact of ocean acidification on energy metabolism of oyster, *Crassostrea gigas*–changes in metabolic pathways and thermal response, Mar. Drugs, 8, 2318–2339, 2010.

Laudien, J., Häussermann, V., Försterra, G., and Göhlich, H.: Physical oceanographic profiles of seven CTD casts from Gulf of Ancud into Comau Fjord in 2014, Alfred Wegener Institute, Helmholtz Center for Polar and Marine Research, Bremerhaven, PANGAEA, https://doi.org/10.1594/PANGAEA.832187, 2014.

Liu, W. and He, M.: Effects of ocean acidification on the metabolic rated of three species of bivalve from southern coast of China, Chin. J. Oceanol. Limn., 30, 206–211, 2012.

MacKinnon, D. I.: The shell structure in spiriferide brachiopoda, Bull. Br. Mus. Nat. Hist., 5, 189–258, 1974.

MacKinnon, D. I. and Williams, A.: Shell structure of terebratulid brachiopods, Palaeontology, 17, 179–202, 1974.

Marchant, H. K., Calosi, P., and Spicer, J. I.: Short–term exposure to hypercapnia does not compromise feeding, acid–base balance or respiration of *Patella vulgata* but surprisingly is accompanied by radula damage, J. Mar. Biolog. Assoc. U.K., 90, 1379–1384, 2010.

McClintock, J. B., Angus, R. A., Mcdonald, M. R., Amsler, C. D., Catledge, S. A., and Vohra, Y. K.: Rapid dissolution of shells of weakly calcified Antarctic benthic macroorganisms indicates high vulnerability to ocean acidification, Antarct. Sci., 21, 449–456, 2009.

McCulloch, M., Trotter, J., Montagna, P., Falter, J., Dunbar, R., Freiwald, A., Försterra, G., Lopez Correa, M., Maier, C., Ruggeberg, A., and Taviani, M.: Resilience of cold–water scleractinian corals to ocean acidification: Boron isotopic systematics of pH and saturation state up–regulation, Geochim. Cosmochim. Acta, 87, 21–34, 2012.

Melzner, F., Stange, P., Trübenbach, K., Thomsen, J., Casties, I., Panknin, U., Gorb, S. N., and Gutowska, M. A.: Food supply and seawater pCO$_2$ impact calcification and internal shell dissolution in the blue mussel *Mytilus edulis*, PLoS ONE, 6, e24223, 2011.

Michaelidis, B., Ouzounis, C., Paleras, A., and Pörtner H. O.: Effects of long-term moderate hypercapnia on acid–base balance and growth rate in marine mussels *Mytilus galloprovincialis*, Mar. Ecol. Prog. Ser., 293, 109–118, 2005.

Mii, H. S., and Grossman, E. L.: Late Pennsylvanian seasonality reflected in the ^{18}O and elemental composition of a brachiopod shell, Geology, 22, 661–664, 1994.

Mii, H. S., Grossman, E. L., Yancey, T. E., Chuvashov, B., and Egorov, A.: Isotopic records of brachiopod shells from the Russian Platform–evidence for the onset of mid–Carboniferous glaciation, Chem. Geol., 175, 133–147, 2001.

Milano, S., Schöne, B. R., Wang, S., and Müller, W. E.: Impact of high pCO$_2$ on shell structure of the bivalve *Cerastoderma edule*, Mar. Environ. Res., 119, 144–155, 2016.

Mingliang, Z., Jianguang, F., Jihong, Z., Bin, L., Shengmin, R., Yuze, M., and Yaping, G.: Effect of marine acidification on calcification and respiration of *Chlamys farreri*, J. Shellfish Res., 30, 267–271, 2011.

Morse, J. W., Arvidson, R. S., and Luttge, A.: Calcium carbonate formation and dissolution, Chem. Rev., 107, 342–381, 2007.

Deleted: .,

Deleted: .,

Deleted: McConnaughey, T.A., and Gillikin, D.P.: Carbon isotopes in mollusk shell carbonates, Geo–Mar. Lett., 28, 287–299, 2008. ¶

37

Movilla, J., Orejas, C., Calvo, E., Gori, A., López Sanz, Á., Grinyó, J., Dominguez–Carrió, C., and Pelejero, C.: Differential response of two Mediterranean cold–water coral species to ocean acidification, Coral reefs, 33, 675–686, 2014.

Navarro, J. M., Torres, R., Acuna, K., Duarte, C., Manriquez, P. H., Lardies, M., Lagos, N. A., Vargas, C., and Aguilera, V.: Impact of medium–term exposure to elevated pCO_2 levels on the physiological energetics of the mussel *Mytilus chilensis*, Chemosphere, 90, 1242–1248, 2013.

Nienhuis, S., Palmer, A. R., and Harley, C. D. G.: Elevated CO_2 affects shell dissolution rate but not calcification rate in a marine snail, Philos. Trans. R. Soc. Lond., B, Biol. Sci., 277, 2553–2558, 2010.

Orr, J. C., Fabry, V. J., Aumont, O., Bopp, L., Doney, S. C., Feely, R. A., Gnanadesikan, A., Gruber, N., Ishida, A., Joos, F., Key, R. M., Lindsay, K., Maier-Reimer, E., Matear, R., Monfray, P., Mouchet, A., Najjar, R. G., Plattner, G. K., Rodgers, K. B., Sabine, C. L., Sarmiento, J. L., Schlitzer, R., Slater, R. D., Totterdell, I. J., Weirig, M. F., Yamanaka, Y., and Yool, A.: Anthropogenic ocean acidification over the twenty–first century and its impact on calcifying organisms, Nature, 437, 681–686, 2005.

Parker, L. M., Ross, P. M., and O'Connor, W. A.: Comparing the effect of elevated pCO_2 and temperature on the fertilization and early development of two species of oysters, Mar. Biol., 157, 2435–2452, 2010.

Parker, L. M., Ross, P. M., and O'Connor, W. A.: Populations of the Sydney rock oyster, *Saccostrea glomerata*, vary in response to ocean acidification, Mar. Biol., 158, 689–697, 2011.

Parker, L. M., Ross, P. M., O'Connor, W. A., Borysko, L., Raftos, D. A., and Pörtner, H. –O.: Adult exposure influences offspring response to ocean acidification in oysters, Glob. Chang. Biol., 18, 82–92, 2012.

Parkinson, D., Curry, G. B., Cusack, M., and Fallick, A. E.: Shell structure, patterns and trends of oxygen and carbon stable isotopes in modern brachiopod shells, Chem. Geol., 219, 193–235, 2005.

Payne, J. L, and Clapham, M. E.: End–Permian mass extinction in the oceans: an ancient analog for the twenty-first century? Annu. Rev. Earth Planet. Sci., 40, 89–111, 2012.

Peck, L. S., Clarke, A., and Holmes, L. J.: Size, shape and the distribution of organic matter in the Recent Antarctic brachiopod *Liothyrella uva*, Lethaia, 20, 33–40, 1987.

Penman, D. E., Hönisch, B., Rasbury, E. T., Hemming, N. G., and Spero, H. J.: Boron, carbon, and oxygen isotopic composition of brachiopod shells: Intra–shell variability, controls, and potential as a paleo–pH recorder, Chem. Geol., 340, 32–39, 2013.

Pérez-Huerta, A., Cusack, M., McDonald, S., Marone, F., Stampanoni, M., and MacKay, S.: Brachiopod punctae: a complexity in shell biomineralisation, J. Struct. Biol., 167, 62–67, 2009 Popov, L. E., Egerquist, E., and Holmer, L. E.: Earliest ontogeny of Middle Ordovician rhynchonelliform brachiopods (Clitambonitoidea and Polytoechioidea): implications for brachiopod phylogeny, Lethaia, 40, 85–96, 2007.

Popp, B. N., Anderson, T. F., and Sandberg, P. A.: Brachiopods as indicators of original isotopic compositions in some Paleozoic limestones, Geol. Soc. Am. Bull., 97, 1262–1269, 1986.

Range, P., Chícharo, M._A., Ben-Hamadou, R., Piló, D., Matias, D., Joaquim, S., Oliveira, A._P., and Chícharo, L.: Calcification, growth and mortality of juvenile clams *Ruditapes decussatus* under increased pCO_2 and reduced pH: Variable responses to ocean acidification at local scales? J. Exp. Mar. Biol. Ecol., 396, 177–184, 2011.

Range, P., Piló, D., Ben-Hamadou, R., Chícharo, M._A., Matias, D., Joaquim, S., Oliveira, A._P., and Chícharo, L.: Seawater acidification by CO_2 in a coastal lagoon environment: Effects on life history traits of juvenile mussels *Mytilus galloprovincialis*, J. Exp. Mar. Biol. Ecol., 424–425, 89–98, 2012.

Ries, J._B., Cohen, A._L., and McCorkle, D._C.: Marine calcifiers exhibit mixed responses to CO_2–induced ocean acidification, Geology, 37, 1131–1134, 2009.

Romanin, M., Crippa, G., Ye, F., Brand, U., Bitner, M._A., Gaspard, D., Häussermann, V., and Laudien J.: A sampling strategy for recent and fossil brachiopods: selecting the optimal shell segment for geochemical analyses, Riv. Ital. Paleontol. Stratigr., 124, 343–359, 2018.

Shirayama, Y. and Thornton, H.: Effect of increased atmospheric CO_2 on shallow water marine benthos, J. Geophys. Res. Oceans, 110, C09S08, doi:10.1029/2004jc002618, 2005.

Smirnova, T._N. and Popiel–Barczyk, E.: Characteristics of the shell ultrastructure in Terebratellacea, in: Brachiopods through time, MacKinnon, D. I., Lee, D. E., and Campbell, J. D. (Eds.): Brachiopods through time, Balkema, Rotterdam, pp. 159–165, 1991.

Steckbauer, A., Ramajo, L., Hendriks, I._R., Fernandez, M., Lagos, N._A., Prado, L., and Duarte, C._M.: Synergistic effects of hypoxia and increasing CO_2 on benthic invertebrates of the central Chilean coast, Front. Mar. Sci., 2, https://doi.org/10.3389/fmars.2015.00049, 2015.

Stemmer, K., Nehrke, G., and Brey, T.: Elevated CO_2 levels do not affect the shell structure of the bivalve *Arctica islandica* from the Western Baltic, PLoS ONE, 8, e70103, 2013.

Suckling, C._C., Clark, M._M., Richard, J., Morley, S._A., Thorne, M._A., Harper, E._M., and Peck, L._S.: Adult acclimation to combined temperature and pH stressors significantly enhances reproductive outcomes compared to short–term exposures, J. Anim. Ecol., 84, 773–784, 2015.

Takayanagi, H., Asami, R., Abe, O., and Miyajima, T.: Intraspecific variations in carbon–isotope and oxygen–isotope compositions of a brachiopod *Basiliola lucida* collected off Okinawa–jima, southwestern Japan, Geochim. Cosmochim. Acta, 115, 115–136, 2013.

Talmage, S._C., and Gobler, C._J.: Effects of elevated temperature and carbon dioxide on the growth and survival of larvae and juveniles of three species of northwest Atlantic bivalves, PLoS ONE, 6, e26941, 2011.

Thomsen, J., and Melzner, F.: Moderate seawater acidification does not elicit long-term metabolic depression in the blue mussel *Mytilus edulis*, Mar. Biol., 157, 2667–2676, 2010.

Thomsen, J., Gutowska, M._A., Saphörster, J., Heinemann, A., Trübenbach, K., Fietzke, J., Hiebenthal, C., Eisenhauer, A., Körtzinger, A., Wahl, M., and Melzner, F.: Calcifying invertebrates succeed in a naturally CO_2–rich coastal habitat but are threatened by high levels of future acidification, Biogeosciences, 7, 3879–3891, 2010.

Deleted: Poulain, C., Lorrain, A., Mas, R., Gillikin, D.P., Dehairs, F., Robert, R., and Paulet, Y.M.: Experimental shift of diet and DIC stable carbon isotopes: influence on shell δ13C values in the manila clam *Ruditapes philippinarum*, Chem. Geol., 272, 75–82, 2010. ¶

Deleted: .,

Deleted: .,

Tukey, J. W.: Exploratory data analysis. Reading, PA: Addison–Wesley, 1977.

Ullmann, C. V., Frei, R., Korte, C., and Lüter, C.: Element/Ca, C and O isotope ratios in modern brachiopods: Species–specific signals of biomineralization, Chem. Geol., 460, 15–24, 2017.

Watkins, J. M., Nielsen, L. C., Ryerson, F. J., and DePaolo, D. J.: The influence of kinetics on the oxygen isotope composition of calcium carbonate, Earth Planet. Sci. Lett., 375, 349–360, 2013.

Watson, S., Peck, L. S., Tyler, P. A., Southgate, P. C., Tan, K. S., Day, R. W., and Morley, S. A.: Marine invertebrate skeleton size varies with latitude, temperature and carbonate saturation: implications for global change and ocean acidification, Glob. Chang. Biol., 18, 3026–3038, 2012.

Williams, A.: The calcareous shell of the Brachiopoda and its importance to their classification, Biol. Rev., 31, 243–287, 1956.

Williams, A.: Growth and structure of the shell of living articulate brachiopods, Nature, 211, 1146–1148, 1966.

Williams, A.: Evolution of the shell structure of articulate brachiopods, Spec. Pap. Palaeontol., 2, 1–55, 1968.

Williams, A.: The secretion and structural evolution of the shell of thecideidine brachiopods, Philos. Trans. R. Soc. Lond., B, Biol. Sci., 264, 439–478, 1973.

Williams, A.: Shell structure, in: Kaesler, R. L. (Ed.): Treatise on Invertebrate Paleontology, Part H, Revised, Brachiopoda, vol. 1, Geological Society of America Inc., and The University of Kansas, Boulder, Colorado, USA, pp. 267–320, 1997.

Williams, A. and Cusack, M.: Chemicostructural diversity of the brachiopod shell, in: Selden, P. A. (Ed.): Treatise on Invertebrate Paleontology, Part H, Brachiopoda Revised, vol. 6, Geological Society of America Inc., and The University of Kansas, Boulder, Colorado, USA, pp. 2396–2521, 2007.

Wood, H. L., Spicer, J. I., and Widdicombe, S.: Ocean acidification may increase calcification rates, but at a cost, Proc. R. Soc. Lond., B, Biol. Sci., 275, 1767–1773, 2008.

Yamamoto, K., Asami, R., and Iryu, Y.: Correlative relationships between carbon–and oxygen–isotope records in two cool-temperate brachiopod species off Otsuchi Bay, northeastern Japan, Paleontol. Res., 17, 12–26, 2013.

Ye, F., Crippa, G., Angiolini, L., Brand, U., Capitani, G., Cusack, M., Garbelli, C., Griesshaber, E., Harper, E., and Schmahl, W.: Mapping of recent brachiopod microstructure: a tool for environmental studies, J. Struct. Biol., 201, 221–236, 2018a.

Ye, F., Crippa, G., Garbelli, C., and Griesshaber, E.: Microstructural data of six recent brachiopod species: SEM, EBSD, morphometric and statistical analyses, Data in Brief, 18, 300–318, 2018b.

40

Variation in brachiopod microstructure and isotope geochemistry under low pH–ocean acidification–conditions

Facheng Ye[1], Hana Jurikova[2], Lucia Angiolini[1], Uwe Brand[3], Gaia Crippa[1], Daniela Henkel[2], Jürgen Laudien[4], Claas Hiebenthal[2], Danijela Šmajgl[5]

[1]Università degli Studi di Milano, Dipartimento di Scienze della Terra 'A. Desio', Milan, 20133, Italy
[2]GEOMAR Helmholtz–Zentrum für Ozeanforschung Kiel, 24148, Kiel, Germany
[3]Department of Earth Sciences, Brock University, St. Catharines, Ontario L2S 3A1, Canada
[4]Alfred-Wegener–Institut Helmholtz–Zentrum für Polar–und Meeresforschung, Bremerhaven, 27515, Germany
[5]ThermoFisher Scientific, Hanna–Kunath–Str. 11, Bremen, 28199, Germany

Correspondence to: Facheng Ye (facheng.ye@unimi.it)

Abstract. In the last few decades and in the near future CO_2–induced ocean acidification is potentially a big threat to marine calcite-shelled animals (e.g., brachiopods, bivalves, corals and gastropods). Despite the great number of studies focusing on the effects of acidification on shell growth, metabolism, shell dissolution and shell repair, the consequences on biomineral formation remain poorly understood. Only few studies have addressed the impact of ocean acidification on shell microstructure and geochemistry. In this study, a detailed microstructure and stable isotope geochemistry investigation was performed on nine adult brachiopod specimens of *Magellania venosa* (Dixon, 1789). These were grown in the natural environment as well as in controlled culturing experiments at different pH conditions (ranging from 7.35 to 8.15 ± 0.05) over different time intervals (214 to 335 days). Details of shell microstructural features, such as thickness of the primary layer, density and size of endopunctae and morphology of the basic structural unit of the secondary layer were analysed using scanning electron microscopy. Stable isotope compositions ($\delta^{13}C$ and $\delta^{18}O$) were tested from the secondary shell layer along shell ontogenetic increments in both dorsal and ventral valves. Based on our comprehensive dataset, we observed that, under low pH conditions, *M. venosa* produced a more organic–rich shell with higher density of and larger endopunctae, and smaller secondary layer fibres. Also, increasingly negative $\delta^{13}C$ and $\delta^{18}O$ values are recorded by the shell produced during culturing and are related to the CO_2–source in the culture setup. Both the microstructural changes and the stable isotope results are similar to observations on brachiopods from the fossil record and strongly support the value of brachiopods as robust archives of proxies for studying ocean acidification events in the geologic past.

Key words:

Magellania venosa, biomineral, $\delta^{13}C$, $\delta^{18}O$, primary layer, secondary layer, endopunctae, culturing

1 Introduction

Since the industrial revolution the surface ocean pH has dropped by 0.1 units and predicted to drop another 0.3–0.5 units by 2100 (Caldeira and Wickett, 2005; Orr et al., 2005; IPCC, 2013). This is due to the increasing amount of atmospheric carbon dioxide (CO_2) absorbed by the ocean that extensively affects seawater carbonate chemistry (e.g., Caldeira and Wickett, 2003,

5 2005; Orr et al., 2005; Feely et al., 2004). Increased concentrations of anthropogenic CO_2 are reflected in an elevated concentration of hydrogen ions, which lowers the pH and the availability of carbonate ions. Effects on marine organisms is of great scientific interest, for understanding the geological past and the consequences in the immediate future (e.g., Ries et al., 2009), since the decrease in calcium carbonate saturation potentially threatens marine organisms forming biogenic calcium carbonate (e.g., Orr et al., 2005; Guinott et al., 2006; McCulloch et al., 2012; Jantzen et al., 2013a, b). This applies

10 to calcium carbonate shell–forming species, such as brachiopods and mollusks, because they are considered excellent archives documenting changes in environmental conditions affecting marine organisms (e.g., Kurihara. 2008; Comeau et al., 2009; Hahn et al., 2012, 2014; Watson et al., 2012; Cross et al., 2015, 2016, 2018; Crippa et al., 2016a; Milano et al., 2016; Garbelli et al., 2017; Jurikova et al., in review).

Recently, several experiments were performed to investigate if a change of seawater pH may affect growth rate, shell repair

15 and oxygen consumption of calcifying organisms, and how they respond, in general, to ocean acidification (Supplementary table 1). However, despite the great number of studies, the consequences on biomineral formation remain not well understood, as most studies focused mainly on growth, metabolic rates, shell dissolution and shell repair (Supplementary table 1, and references therein). Only a few studies deal with the effect of acidification on microstructure (Beniash et al., 2010; Hahn et al., 2012; Stemmer et al., 2013; Fitzer et al., 2014a, b; Milano et al., 2016), and most of them focused on

20 bivalves and show that neither microstructure nor shell hardness seem to be affected by seawater pH.

The few studies that examined brachiopods or brachiopod shells suggest that the latter suffered increased dissolution under lower seawater pH. In other studies, the organism either exhibited no changes or an increase in shell density [calculated as dry mass of the shell (g)/shell volume (cm^3)], but otherwise no changes in shell morphology and trace chemistry (Table 1). Cross et al. (2018) found that punctae became narrower over the past 120 years, which partially explained the increase in

25 shell density over this period. Overall, there appears to be little to no apparent effect on brachiopod morphology or chemistry with lower seawater pH (Cross et al., 2015, 2016, 2018).

Table 1. Culturing, dissolution experiments and natural variation on several brachiopod species and shells.

Species n (number of sample)	Growth Parameters	Shell repair/Microstructure/Oxygen consumption/Dissolution of shell/Microstructure	Method & Material	Environment/conditions T=Temperature (°C) S=Salinity (PSU) pCO_2 (μ atm)	Duration of experiment	Source
Calloria inconspicua (Sowerby, 1846) n = 123	1) >3 mm in length undamaged individuals were not affected by lower pH; 2) <3 mm in length	Shell growth rates and shell repair frequencies were not affected by low pH (>80% of all damaged individuals repaired after 12 weeks)	Culture experiment	a) pH 8.16, T 16.5, S 33.9, pCO_2 465, $\Omega_{calcite}$ 3.5 b) pH 7.79, T 16.9, S 33.9, pCO_2 1130, $\Omega_{calcite}$ 1.6 c) pH 7.62, T 16.6, S 33.9, pCO_2 1536, $\Omega_{calcite}$ 1.3	12 weeks	Cross et al., 2016

	undamaged individuals grew faster at pH 7.62 than the control conditions					
Calloria inconspicua (Sowerby, 1846) n_{adult} = 389 for shell morphology analyses*		Punctae width decreased by 8.26%, shell density increased by 3.43%, no change in shell morphology, punctae density, shell thickness, and shell elemental composition (Ca, Mg, Na, Sr and P) No changes were found in shell dissolution over the last 120 years.	Collected every decade from one locality	Last two decades pH reduced 0.1 unit Temperature varied from 10.7–13.0 ℃ pCO_2 varied from 320–400 Salinity and $\Omega_{calcite}$ not provided	120–year record	Cross et al., 2018
Liothyrella uva (Broderip, 1833) n = 156	Not affected by lower pH and temperature	Shell repair frequencies were not affected by low pH and temperature (>83% of individuals repaired after 7 months)	Culture experiment	a) pH 7.98, T -0.3, S 35, pCO_2 417, $\Omega_{calcite}$ 1.20 b) pH 8.05, T 1.7, S 35, pCO_2 365, $\Omega_{calcite}$ 1.49 c) pH 7.75, T 1.9, S 35, pCO_2 725, $\Omega_{calcite}$ 0.78 d) pH 7.54, T 2.2, S 35, pCO_2 1221, $\Omega_{calcite}$ 0.50	7 months	Cross et al., 2015
Liothyrella uva (Broderip, 1833) $n_{post-mortem}$ = 5	Not applicable	Higher dissolution in gastropods and brachiopods at lower pH after 14 days	Empty shells	a) pH 7.4, T 4, S 35, $\Omega_{calcite}$ 0.74 b) pH 8.2, T 4, S 35, $\Omega_{calcite}$ 4.22 pCO_2 Not provided	14 to 63 days	McClintock et al., 2009

*A subsample of 40 brachiopods (2-5 specimens per decade over the last 120 years) were used for further shell analysis of shell density, punctal width, punctal density, shell dissolution, shell thickness and shell elemental composition.

Brachiopods possess a low–magnesium calcite shell, which should be more resistant compared to the more soluble forms of CaCO$_3$ such as aragonite and high-Mg calcite (Brand and Veizer, 1980; Morse et al., 2007). The shell microstructure of Rhynchonelliformean brachiopods has been used as a powerful tool to understand the biomineral's response to modern global ocean acidification and similar events in the geologic past (Payne and Clapham, 2012; Cross et al., 2015, 2016; Garbelli et al., 2017). A comprehensive study focusing on fossil brachiopods during the end-Permian mass extinction showed that brachiopods produce shells with increased organic matter content during ocean acidification events (Garbelli et al., 2017).

Here, we describe the microstructure and carbon and oxygen isotopic composition of brachiopod shells belonging to the cold-temperate water species *Magellania venosa* (Dixon, 1789) grown in natural environment as well as in pH-controlled culturing conditions. *M. venosa* represents the largest recent brachiopod species, is often locally abundant (e.g. in Chile; Försterra et al., 2008), and it has the highest growth rate recorded for recent brachiopods (Baumgarten et al., 2014). Its low-magnesium calcite shell consists of a microgranular primary layer and a fibrous secondary layer (Smirnova et al., 1991; Baumgarten et al., 2014; Casella et al., 2018; Romanin et al., 2018) crossed by perforations – endopunctae.

Since little is known about the microstructural and geochemical responses of brachiopods to increased ocean acidification, the main goal of this study is to document any changes in this highly important archival marine organism. It will be described, if and how, shell microstructural features such as the primary layer thickness, density of endopunctae and fibre

morphology, together with their stable carbon (δ^{13}C) and oxygen (δ^{18}O) isotope compositions respond to low seawater pH conditions.

2 Materials and methods

2.1 Brachiopod samples and culturing set–up

5   A full description of the brachiopod sampling and culturing procedure is provided in Jurikova et al. (in review), but we provide an abbreviated version and reiterate the key points. Nine adult individuals of *M. venosa* (Dixon, 1789) were chosen for microstructure investigation and evaluation of their δ^{13}C and δ^{18}O values. All specimens were collected by scientific SCUBA divers alive from 20 m water depth of Comau Fjord (Chile) at different localities (Figure 1). Specimens #158 and #223 did not experience any treatment after collection from Comau Fjord. The other specimens, #43, #63, #8004, #8005, #9004, #9005 and #9006, were cultured under different pH conditions at either AWI in Bremerhaven or GEOMAR (at KIMOCC–Kiel Marine Organisms Culture Centre) in Kiel, Germany (Table 2 and 3).

Table 2. Culture and sensor systems used in *M. venosa* culturing (specimens: #43, #63, #8004, #8005, #9004, #9005 and #9006). Operated under controlled experimental settings in climate-controlled laboratories at Alfred–Wegener–Institut Helmholtz–Zentrum für Polar–und Meeresforschung, Bremerhaven, Germany and at GEOMAR Helmholtz–Zentrum für Ozeanforschung Kiel, Germany.

	Culture system at AWI	Automated sensor Systems at AWI	Culture system at GEOMAR	Automated sensor Systems at GEOMAR
	Aquarium (150 L/each pH treatment)		Aquarium (150 L/each pH treatment)	
	Supplied from a reservoir tank (twice a week 20 % water was replaced)		Supplied from a reservoir tank (twice a month 10 % water was replaced)	
Temperature	Controlled in temperature constant room		Controlled using heaters or coolers	Temperature Sensor Pond
pCO$_2$	Bubbling of CO$_2$	COMPORT, Dennerle, Vinningen; IKS aquastar Aquarium computer V2.xx with Aquapilot 2011	Bubbling of CO$_2$ enriched air	CONTROS HydroC® underwater CO$_2$ sensor
Salinity	Mixing Reef commercial sea–salt (until October: Aqua Medic, Bissendorf, Germany, thereafter Dupla Marin Reef Salt, Dohse Aquaristik, Grafschaft–Gelsdorf, Germany) with deionized water	Conductivity Electrode	Mixing Tropic Marin Pro–Reef commercial sea-salt with deionized water	Conductivity Electrode

Filtering	Biofilter, protein skimmer and UV sterilizer		Biofilter, protein skimmer and UV sterilizer
Food	Regularly fed (typically 5 times per week) with Dupla Rin, Coral Food, Reef Pearls 5–200 μm, alive *Thalassiosira weissflogii,* and 1d old nauplii of *Artemia salina*		Regularly fed (typically 5 times per week) with *Rhodomonas baltica*
Substrate	Sabia Corallina, 7–8mm, Dohse Aquaristik, Grafschaft–Gelsdorf, Germany		No

Table 3. Specimens of *M. venosa* sampled from Comau Fjord, Chile, and natural and experimental culturing conditions.

Sample ID	Sample locality at Comau Fjord (Chile)[①]	Sample seawater conditions[②]	Date of collection	Length of ventral valve (mm)	Duration of experiment	Experimental conditions
#43	Lilliguapi	pH: ~7.9 T: ~13 S: ~32 D: 20	Feb. 2012	37	214 days[③]	pCO$_2$: 1390, pH: 7.66 $\pm$0.04 T: 11.6 $\pm$0.5, S: 32.6 Ω_{cal}: 2.0
#63	Lilliguapi	pH: ~7.9 T: ~13 S: ~32 D: 20	Feb. 2012	23	214 days[③]	pCO$_2$: 2600, pH: 7.44 $\pm$0.08 T: 11.7 $\pm$0.5, S: 32.7 Ω_{cal}: 1.4
#158	Huinay Dock	pH: ~7.9 T: ~13 S: ~32 D: 20	Dec. 2011	36	no	
#223	Cahuelmó	pH: ~7.9 T: ~13 S: ~32 D: 23	Feb. 2012	30	no	
#8004	Comau Fjord	pH: ~7.9 T: ~13 S: ~32 D: 21	Apr. 2016	31	335 days[④]	pCO$_2$: 600 pH: 8.00 to 8.15 $\pm$0.05 T: 10 $\pm$ 1, S: 30 Ω_{cal}: 2.0–3.5
#8005	Comau Fjord	pH: ~7.9 T: ~13 S: ~32 D: 21	Apr. 2016	46	335 days[④]	pCO$_2$: 600 pH: 8.00 to 8.15 $\pm$0.05 T: 10 $\pm$1, S: 30 Ω_{cal}: 2.0–3.5
#9004	Comau Fjord	pH: ~7.9 T: ~13 S: ~32 D: 21	Apr. 2016	41	335 days[④]	pCO$_2$: 2000–4000[⑤] pH: 7.60 to 7.35 $\pm$0.05 T: 10 $\pm$1, S: 30 Ω_{cal}: 0.6–1.1

#9005	Comau Fjord	pH: ~7.9 T: ~13 S: ~32 D: 21	Apr. 2016	25	335 days[4]	pCO$_2$: 2000–4000[5] pH: 7.60 to 7.35 $\pm$0.05 T: 10 $\pm$1, S: 30 Ω_{cal}: 0.6–1.1
#9006	Comau Fjord	pH: ~7.9 T: ~13 S: ~32 D: 21	Apr. 2016	43	335 days[4]	pCO$_2$: 2000–4000[5] pH: 7.60 to 7.35 $\pm$0.05 T: 10 $\pm$1, S: 30 Ω_{cal}: 0.6–1.1

Note: D: Depth (m), T: temperature (°C), S: salinity (PSU – practical salinity units), pCO$_2$ (μatm).

[1]Cahuelmó 42°15'23" S, 72°26'42" W, Cross–Huinay 42°23'28" S, 72°27'27" W, Jetty (Huinay Dock) 42°22'47" S, 72°24'56" W, Lilliguapy 42°9'43" S, 72°35'55" W, samples #8004, #8005, #9004, #9005, #9006 were harvested from three sites in Comau Fjord (Cross–Huinay, Jetty, and Liliguapy), Chile

[2]Reference: Laudien et al. (2014) and Jantzen et al. (2017)

[3] Culture experiments conducted at Alfred–Wegener–Institut Helmholtz–Zentrum für Polar–und Meeresforschung, Bremerhaven, Germany

[4]Culture experiments conducted at GEOMAR Helmholtz–Zentrum für Ozeanforschung Kiel, Germany (Jurikova et al., in review)

[5]CO$_2$ concentration was changed during the experiment: to 2000 μatm from 4th August 2016 to 18th April 2017 and to 4000 μatm from 18th April 2017 till 5th July 2017.

Figure 1. Map of Comau Fjord. Upper left map: Overview of Chilean Patagonia. Lower left map: Gulf of Ancud with connections in the north and south to the Pacific Ocean. Right hand map: Fjord Comau with brachiopod sample collection localities. In both maps the rectangle marks the location of Comau Fjord.

5

In summary, individuals of *M. venosa* were collected alive in Chile and transported to GEOMAR, Germany in plastic bags filled with seawater, and maintained under controlled conditions in a climate laboratory. The brachiopods were first acclimatized under control conditions for five weeks, and prior to the start of the experiment were labelled with a fluorescent dye – calcein (Sigma, CAS 1461–15–0; 50 mg/l for 3 h) (e.g., Baumgarten et al., 2013; Jurikova et al., in review). As a

10 culture medium we used artificial seawater, which was prepared by mixing a commercial salt with deionized water until the desired salinity and chemical composition was achieved (Atkinson and Bingman, 1998). Overview of the culturing setup at both laboratories is available in Table 2. Specimens #43 and #63 were cultured at AWI at pH = 7.66 (pCO$_2$ = 1390 µatm) and pH = 7.44 (pCO$_2$ = 2610 µatm) from 29th August 2013 to 31th March 2014, respectively. Specimens #8004, #8005, #9004, #9005 and #9006 were cultured concurrently at GEOMAR under control or low pH conditions. Specimens #8004 and

15 #8005 were maintained under pH settings of 8.0-8.15 from 4th August 2016 to 5th July 2017, conditions similar to those of their fjord habitat. In contrast, specimens #9004, #9005 and #9006 were cultured under low–pH artificial seawater

7

conditions. Low–pH conditions were achieved by bubbling of CO_2 through the tanks at AWI, and by bubbling CO_2-enriched air through the tanks at GEOMAR (Table 2). The acidification experiment at GEOMAR was performed in two phases; the first one from 4th August 2016 to 18th April 2017 during which the pCO_2 was set to 2000 µatm (corresponding to a pH of 7.60), and the second one during which the pCO_2 was set to 4000 µatm (corresponding to a pH of 7.35) from 18th April 2017 to 5th July 2017 (Table 3). In order to distinguish between the shell parts precipitated under the specific pH conditions as well as to allow exact comparison to shells of the control treatment, calcein marking was also carried out prior to the second low–pH experiment of 4000 µatm. Parts of the shell grown under specific pH conditions are indicated in Figure 2. In addition to the calcein marking, newly grown shell parts may be distinguished from visible growth lines on the surface of the shell (Figure 2). The total length (maximum distance from the blue line to the anterior margin) of the curved dorsal and ventral valves grown during 11 months of culturing (Figure 2) varied from < 5 to 15.6 mm (Table 4).

Figure 2. Growth tracked with calcein and marked by blue and red lines on the surface of the brachiopod specimens (#9006).

Table 4. Shell length of specimens of *M. venosa* before and during the culture.

Sample ID	Valve	Initial length before culturing (mm)	New shell growth (a) 257 Days (mm)	pH	New shell growth (b) 78 Days (mm)	pH
#8004	ventral	15.4	14	8.00	1.6	8.15
#8005	ventral	40	5	8.00	<1	8.15
#8005	dorsal	36	4	8.00	<1	8.15
#9004	ventral	26.8	13	7.60	1.2	7.35
#9005	ventral	11.2	12	7.60	1.8	7.35
#9006	ventral	33	9	7.60	<1	7.35
#9006	dorsal	29	8	7.60	<1	7.35

Note: (a) Culturing from 4th August 2016 to 18th April 2017; (b) Culturing from 18th April 2017 to 5th July 2017; $pH_0 = 8.00$ and 8.15, $pH_1 = 7.60$, $pH_2 = 7.35$.

8

2.2 Microstructural Analysis

This study followed the sample preparation method shells suggested by Crippa et al. (2016b). In order to obtain more detailed data on microstructural changes, the samples were cut with a diamond blade along different axes and directions (Figure 3a). Subsequently, the samples were immersed in 36 volume hydrogen peroxide (H_2O_2) for 24/48 hours to remove the organic tissue. The sectioned surfaces were manually smoothed with 1200 grit sandpaper, then quickly (3 seconds) cleaned with 5% hydrochloric acid (HCl), immediately washed with water and air–dried. The time of acid etching was kept short so not affect the microstructure (Crippa et al., 2016b). Finally, the valve sections were gold–coated and analysed by a Cambridge S–360 scanning electron microscope with a lanthanum hexaboride (LaB_6) source operating at an acceleration voltage of 20 kV (Dipartimento di Scienze della Terra "A. Desio", Università di Milano).

Figure 3. Brachiopod shell sample cut along different axes. (a): longitudinal and transverse sections; (b): transverse sections at the anterior margin of the shell; (c): plane grinding of the external surface of the shell.

The methods described by Ye et al. (2018a) were followed to investigate the basic microstructural units (fibres) in SEM images. We focused primarily on the anterior margin of the valves, the part that was produced during culturing (hereinafter referred to as *during–culturing*) under different pH conditions. Therefore, additional transverse sections along the growth lines were obtained in the most anterior part (black lines in Figure 3b) by manually smoothing with 1200 grit sandpaper. Plane grinding was performed on the external surface of the shell (Figure 3) to investigate the distribution of endopunctae.

The thickness of the primary layer was measured on the SEM images of specimens #8005 and #9006 (Figure 4a) in different positions along the longitudinal growth axis (posterior, central and anterior regions). In the vicinity of the transition from natural growth to cultured growth, the region was further subdivided into four sub–zones.

To calculate and measure the density and diameter (max) of endopunctae, squares (800 μm × 800 μm) were located randomly over the smoothed external surface of the anterior shell (Figure 4b). Four sub-zones (C2, A1, A2, A3) were

defined according to their position along the posterior-anterior direction (Figure 4), while distinguishing the part of the shell produced *before–culturing* and that produced *during–culturing*.

Figure 4. Measurement methods used for the thickness of primary layer (a) and the density of the endopunctae (b). Note that for the latter, endopunctae were counted when included for more than their half diameter inside the square. dv: dorsal valve.

For morphometric analyses, fibres were manually outlined using polygonal lasso in Adobe Photoshop CS6, and size and shape parameters were measured with Image-Pro Plus 6.0 and ImageJ (for convexity). In particular, following Ye et al. (2018a, b) we measured/calculated the Feret diameter (max), Area, Roundness [$4Area/\pi \times$ Feret diameter (max)^2] and Convexity (Convex Perimeter/Perimeter). The width of an individual fibre roughly corresponds to its Max Feret diameter, whereas its height corresponds to the Min Feret diameter (see Figure 6 in Ye et al., 2018a).

As individual fibres are irregular in shape in the most anterior section of brachiopods, the morphometric measurement method proposed by Ye et al. (2018a, b) is not always suitable. Thus, modifications had to be made to the Ye et al. (2018a, b) measurement method to make the comparative morphometric analysis of the fibres from anterior part (Figure 5a, b). First, all SEM images were oriented in the same direction with the base of the primary layer facing upwards. Then a uniformly sized zone (20 μm × 20 μm) was selected for additional measurements with the upper side of the square always placed at the boundary between the primary and the secondary layers (Figure 5c). Two new methods were developed and applied: for Method 1, the width of fibres crossed by two standard lines was measured, which were always located in the same position and at the same distance in all the selected zones (yellow and orange lines in Figure 5 method 1). For Method 2, we calculated the number of boundaries based on the number of fibres crossed by the two standard lines (Figure 5 method 2). Sub-zones were named according to the following nomenclature, the most anterior transection zone of the ventral valve was named Z1, the second most anterior transection zone of the ventral valve Z2 and so on, the most anterior transection zone of the dorsal valve was named Z4. The standard line facing towards the primary layer was named "1" and the second standard

line "2" (example: "Z1–1" is the sample of the standard line facing towards the primary layer at the most anterior transect zone of the ventral valve).

Figure 5. Methods of measurements used in the anterior transverse sections. All SEM images are oriented in the same direction: base of the primary layer facing upwards. A square (20 µm × 20 µm) was analysed with its upper side just overlapping the boundary between the primary and secondary layer. Method 1 refers to the measurement of the width of the fibres crossed by two standard lines, which were located in the same position and at the same distance in all 194 squares (yellow and orange lines); Method 2 involved the calculation of the numbers of boundaries between the fibres that are crossed by two standard lines. vv: ventral valve.

2.3 Stable isotope analyses of shells

Cleaned shells of specimens #8004, #8005, #9004, #9005 and #9006 were chosen for carbon and oxygen isotope analyses. For specimens #8005 and #9006, surface contaminants and the primary layer were first manually and then chemically removed by leaching with 10 % HCl, rinsed with distilled water and air–dried. As the primary layer is not secreted in equilibrium with ambient seawater (e.g., Carpenter and Lohmann, 1995; Brand et al., 2003, 2013), it is important to chemically remove it in order to avoid cross-contamination of results. Individual growth increments exclusively come from the secondary layer, and were separated from the shell in both dorsal and ventral valves using a WECHEER (WE 248)

11

microdrill at low speed with tungsten–carbide milling bit. Shell increment fragments, of similar width, were then powdered using an agate mortar and pestle. For carbon and oxygen isotope analyses about 250 µg of powdered calcite of each sample was analysed using an automated carbonate preparation device (GasBench II) connected to a Delta V Advantage (Thermo Fisher Scientific Inc.) isotopic ratio mass spectrometer at the Earth Sciences Department, University of Milan, Italy. The

5 carbon and oxygen isotope compositions are expressed in the conventional delta notation calibrated to the Vienna Pee-Dee Belemnite (V-PDB) scale by the international standards IAEA 603 (International Atomic Energy Agency 603; $\delta^{18}O$: -2.37 ± 0.04 ‰, $\delta^{13}C$: +2.46 ± 0.01 ‰) and NBS 18 ($\delta^{18}O$: -23.2 ± 0.1 ‰, $\delta^{13}C$: -5.014 ± 0.035 ‰). Analytical reproducibility (1σ) for these analyses was better than ± 0.04‰ for $\delta^{13}C$ and ± 0.1‰ for $\delta^{18}O$ (Appendix). Another set of shells, #8004, #9004 and #9005, were gently rinsed with ultra pure water (Milli–Q) and dried for a few days on a hotplate at 40 ℃ in a clean flow

10 hood. Targeted parts of the shell were sampled for powder under binoculars using a precision drill (Proxxon) with a mounted dental tip. Stable isotope analyses of powders of these specimens were performed at GEOMAR, Kiel on a Thermo Finnigan MAT 252 mass spectrometer coupled online to an automated Kiel carbonate preparation line. The external reproducibility (1σ) of in–house carbonate standards was better than ± 0.1 ‰ and ± 0.08 ‰ for $\delta^{13}C$ and $\delta^{18}O$, respectively (Appendix).

2.4 Stable isotope analyses of water samples

15 In addition to carbon and oxygen isotope analyses of shells, analyses were also carried out on seawater samples collected from the culturing tanks. Measurements of $\delta^{13}C_{DIC}$ and $\delta^{18}O_{H2O}$ were performed using Thermo Scientific™ Delta Ray™ IRIS with URI Connect.

Isotope values ($\delta^{13}C$, $\delta^{18}O$) are reported as per mil (‰) deviations of the isotopic ratios ($^{13}C/^{12}C$, $^{18}O/^{16}O$) calculated to the VPDB scale for $\delta^{13}C$ and VSMOW scale for $\delta^{18}O$ values. Analytical reproducibility (1σ) on 3 aliquots of each water sample,

20 was ≤ 0.03‰ for both $\delta^{13}C$ and $\delta^{18}O$ values (Appendix).

3 Results

3.1 Primary layer thickness

The thickness of the primary layer was measured at different positions along the shell from the posterior (umbonal) region to the *before–culturing* portion and finally to the anterior valve margin (Figure 6). Generally, in the posterior part of *M. venosa,*

25 the primary layer is missing, or it has the lowest recorded thickness. Then, the primary layer progressively thickens toward the central and anterior parts. The thickest primary layer within the same valve is always located just before the beginning of the culture (*before–culturing* portion, Table 5). During culturing the thickness of the primary layer decreases. A most distinct change was observed in specimen #9006 cultured at the lowest pH condition of 7.6, and of 7.35 followed by another progressive increase in both valves *during–culturing*. In contrast, the thickness of the primary layer of the control condition

30 specimen (#8005) remained stable (dorsal valve) or slightly decreased (Figure 6, ventral valve; Table 5).

Table 5. Statistical comparison of thickness of the primary layer (μm) along the ontogenetic direction of both valves of specimens #8005 and #9006 before and during culturing. ①: position of zones before culturing: P, C1, C2; during culturing: A1, A2, A3 (cf. Figure 6). *n* = number of measurements. Population standard deviation (σ) was calculated using the Excel STDEV.P function. Significant values (*p*–value ≤ 0.05) are marked in bold.

Sample	Position[①]	*n*	Mean	σ	Min	Max	*p*-values	*p*-values
#8005 dorsal	P	4	11.82	1.05	10.55	13.02		
	C1	8	11.40	2.29	8.50	15.05	P vs C1 0.755	
	C2	10	28.99	4.79	22.15	36.65	C1 vs C2 < **0.001**	
	A1	8	24.36	2.52	19.80	27.06	C2 vs A1 **0.033**	
	A2	7	24.83	2.15	21.67	27.94	A1 vs A2 0.726	
	A3	1	21.77	NA	NA	NA	A2 vs A3 NA	
								#8005DP vs #9006DP 0.120
#8005 ventral	P	2	17.64	2.36	15.28	20		#8005DC1 vs #9006DC1 < **0.001**
	C1	6	13.68	3.96	8.50	20.52	P vs C1 NA	
	C2	8	47.57	2.49	42.55	50.27	C1 vs C2 < **0.001**	#8005DC2 vs #9006DC2 < **0.001**
	A1	8	44.18	2.68	38.33	47.98	C2 vs A1 **0.028**	#8005DA1 vs #9006DA1 0.088
	A2	6	42.09	3.85	36.06	45.04	A1 vs A2 0.289	
	A3	4	34.09	3.51	29.63	37.52	A2 vs A3 **0.017**	#8005DA2 vs #9006DA2 0.101
								#8005DA3 vs #9006DA3 NA
#9006 dorsal	P	7	9.08	2.77	5.56	14.64		#8005VP vs #9006VP NA
	C1	10	18.78	2.04	16.90	22.50	P vs C1 < **0.001**	
	C2	11	46.91	5.22	35.92	55.86	C1 vs C2 < **0.001**	#8005VC1 vs #9006VC1 0.123
	A1	10	28.83	6.65	19.04	39.93	C2 vs A1 < **0.001**	
	A2	8	28.06	4.03	22.50	36.69	A1 vs A2 0.779	#8005VC2 vs #9006VC2 0.194
	A3	4	32.84	3.55	29.10	38.65	A2 vs A3 0.096	
								#8005VA1 vs #9006VA1 < **0.001**
#9006 ventral	P	7	9.78	1.72	6.07	11.79		#8005VA2 vs #9006VA2 **0.007**
	C1	9	16.75	2.77	12.61	21.29	P vs C1 < **0.001**	
	C2	12	45.16	4.34	35.09	51.40	C1 vs C2 < **0.001**	#8005VA3 vs #9006VA3 **0.027**
	A1	11	36.92	3.82	26.62	42.54	C2 vs A1 < **0.001**	
	A2	4	32.95	2.91	30.84	37.95	A1 vs A2 0.102	
	A3	5	40.55	2.63	37.78	45.23	A2 vs A3 **0.008**	
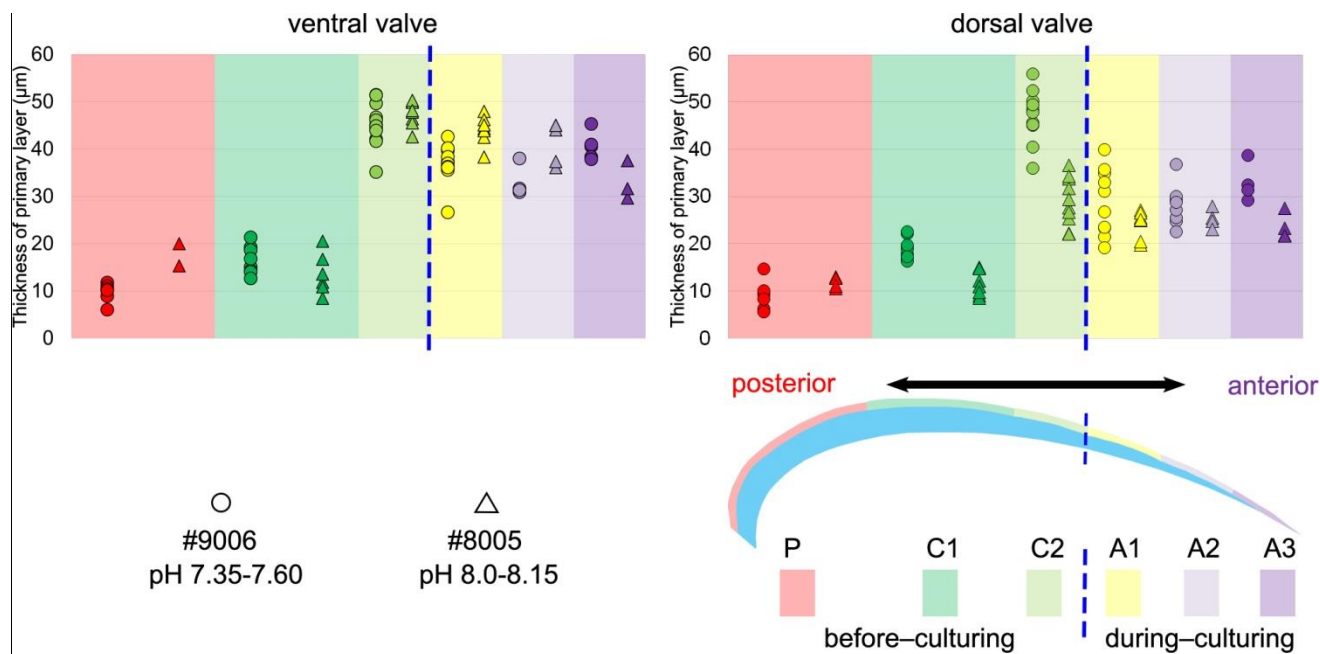
Figure 6. Variation of the thickness of the primary layer (ventral and dorsal valve) of a *M. venosa* specimen cultured at pH 7.35 and 7.6 (#9006) and a specimen cultured at pH 8.0 and 8.15 (#8005).

5 **3.2 Endopunctae density and size**

On the externally–ground surface of the anterior part, the total number and the diameter (max) of endopunctae in a squared area of 800 μm × 800 μm was measured in four *before-culturing* and of the *during–culturing* parts of the shell (Figure 7). Generally, the density of endopunctae gradually increased along the selected transect from ca. 185 /mm² to ca. 305 /mm² in the ventral valve and from ca. 220 /mm² to ca. 280 /mm² in the dorsal valve (Table 6). The size of endopunctae increased

10 along the selected transect in the ventral valve (from ca. 17 μm to 33 μm; Table 7), but it slightly decreases in the dorsal valve from ca. 36 μm to ca. 21 μm (Table 7). These density and size trends were observed in both specimens cultured at different pH conditions. However, it is noteworthy that in the most anterior part (*during–culturing*) of the ventral valve of #9006 (cultured at a pH of 7.35), the density of endopunctae sharply increases and their diameter reached a recorded maximum values (Table 6).

15

Table 6. Statistical comparison of the number of endopunctae (per mm²) on both valves of #8005 and #9006. ①: position of zones before culturing: C2, and post culturing: A1, A2, A3 (cf. Figure 7).

Sample	Zone①	*n*	Mean	σ	Min	Max
	C2	3	236	10.4	225	250
#8005 dorsal	A1	1	280	NA	NA	NA
	A2	2	244	12.5	231	256

14

	A3	2	281	14.1	267	295
	C2	2	225	1.6	223	227
#8005 ventral	A1	1	242	NA	NA	NA
	A2	2	241	5.5	236	247
	A3	2	269	6.3	263	275
	C2	2	221	8.6	213	230
#9006 dorsal	A1	1	269	NA	NA	NA
	A2	2	250	3.1	247	253
	A3	2	266	3.1	263	269
	C2	2	186	3.1	183	189
#9006 ventral	A1	1	234	NA	NA	NA
	A2	2	230	4.7	225	234
	A3	2	308	1.6	306	309

Table 7. Statistical comparison of the diameter (max) (µm) of endopunctae on valves of #8005 and #9006. ①: position of zones before culturing: C2, and during culturing: A1, A2, A3 (cf. Figure 7). Significant values (p–value ≤ 0.05) are marked in bold.

Sample	Zone①	n	Mean	σ	Min	Max	p-values	p-values
#8005D	C2	21	36.04	1.78	33.2	40.4	C2 vs A1 < **0.001**	#8005DC2 vs #9006DC2
	A1	10	28.36	2.33	25	32.1	A1 vs A2 < **0.001**	**0.025**
	A2	15	18.77	1.10	17	21.1	A2 vs A3 **0.001**	
	A3	13	21.8	2.53	18.2	26.2		#8005DA1 vs #9006DA1 <
#8005V	C2	11	17.07	1.42	13.6	18.9	C2 vs A1 < **0.001**	**0.001**
	A1	13	20.88	2.22	17.1	24.3	A1 vs A2 **0.007**	
	A2	12	18.74	0.84	18	20.9	A2 vs A3 < **0.001**	#8005DA2 vs #9006DA2 <
	A3	14	26.83	2.83	23	33.1		**0.001**
#9006D	C2	12	32.54	4.39	26.2	40	C2 vs A1 0.178	
	A1	13	34.63	2.33	29	37.2	A1 vs A2 **0.012**	#8005DA3 vs #9006DA3 <
	A2	11	32.02	2.12	27.5	36.1	A2 vs A3 **0.005**	**0.001**
	A3	19	28.75	3.51	23	34.4		
#9006V	C2	13	29.98	2.04	24.3	33	C2 vs A1 < **0.001**	#8005VC2 vs #9006VC2
	A1	12	38.66	2.41	35.5	42.6	A1 vs A2 < **0.001**	< **0.001**
	A2	14	32.51	4.08	25.3	40.3	A2 vs A3 0.516	
	A3	24	33.70	5.82	22	44.3		#8005VA1 vs #9006VA1 <

Figure 7. Variation in the number and diameter (max) of endopunctae in the dorsal and ventral valve from a specimen of *M. venosa* cultured at pH 7.35 and 7.6 (#9006) and a specimen cultured at pH 8.0 and 8.15 (#8005).

3.3 Shell morphometrics

3.3.1 Before–culturing

Ontogenetic variation in fibre morphometry is not obvious when all six adult specimens are considered (Table 8). However, clearer growth trends can be observed when considering the data from each single specimen separately, where *t*-tests on morphometric data from specimens #8005 and #9006 show that there are significant differences in Feret diameter (max) and Roundness between the posterior and the middle part of the shell (Table 9). Overall, in specimens #8005 and #9006 fibres become wider from the posterior to mid–shell. In contrast, #63 shows an opposite trend along the posterior to mid-shell direction (Figure 8). The fibre size and shape in the other specimens are rather constant.

Table 8. Statistical comparison of fibre size and shape of the posterior external vs central middle parts of the ventral and dorsal valves. NC: non-cultured samples #158, #223; CU: cultured samples #43, #63, #8005, #9006; Vpe: ventral posterior external, Vcm: ventral central middle, Dpe: dorsal posterior external, Dcm: dorsal central middle. Significant values (p–value ≤ 0.05) are marked in bold.

Sample	Position	n	Mean	σ	Min	Max	p-values
Feret diameter (max) (μm):							
NC	Vpe	7	13.79	3.22	6.97	17.33	NC Vpe vs CU Vpe 0.486
CU	Vpe	26	12.47	6.58	4.59	24.78	NC Vcm vs CU Vcm 0.633
							NC Vpe vs NC Vcm 0.533
NC	Vcm	32	12.98	2.91	7.09	20.61	CU Vpe vs CU Vcm 0.572
CU	Vcm	65	13.24	2.15	8.68	18.84	
NC	Dpe	8	18.36	4.22	13.30	24.46	NC Vpe vs CU Vpe 0.486
CU	Dpe	12	10.78	6.36	4.85	22.29	NC Vcm vs CU Vcm 0.633
							NC Vpe vs NC Vcm 0.533
NC	Dcm	12	12.14	1.13	9.84	14.42	CU Vpe vs CU Vcm 0.572
CU	Dcm	46	12.51	1.57	9.45	15.89	
Roundness:							
NC	Vpe	7	0.308	0.077	0.239	0.475	NC Vpe vs CU Vpe 0.717
CU	Vpe	26	0.296	0.074	0.172	0.446	NC Vcm vs CU Vcm 0.396
							NC Vpe vs NC Vcm 0.296
NC	Vcm	29	0.282	0.051	0.179	0.389	CU Vpe vs CU Vcm 0.146
CU	Vcm	65	0.272	0.051	0.180	0.421	
NC	Dpe	8	0.220	0.034	0.169	0.268	NC Dpe vs CU Dpe **0.003**
CU	Dpe	12	0.337	0.100	0.155	0.500	NC Dcm vs CU Dcm **0.028**
							NC Dpe vs NC Dcm **0.005**
NC	Dcm	11	0.311	0.068	0.192	0.416	CU Dpe vs CU Dcm **0.048**
CU	Dcm	48	0.269	0.051	0.162	0.378	
Convexity:							
NC	Vpe	7	0.985	0.004	0.979	0.991	NC Vpe vs CU Vpe 0.309
CU	Vpe	26	0.982	0.008	0.968	0.999	NC Vcm vs CU Vcm 0.655
							NC Vpe vs NC Vcm 0.823
NC	Vcm	32	0.984	0.005	0.975	1.000	CU Vpe vs CU Vcm 0.257
CU	Vcm	62	0.984	0.008	0.965	1.008	
NC	Dpe	8	0.987	0.006	0.979	0.998	NC Dpe vs CU Dpe 0.604
CU	Dpe	11	0.985	0.007	0.973	0.998	NC Dcm vs CU Dcm 0.273
							NC Dpe vs NC Dcm 0.543
NC	Dcm	12	0.984	0.008	0.973	1.000	CU Dpe vs CU Dcm 0.207
CU	Dcm	48	0.982	0.008	0.967	1.001	

Table 9. Statistical comparison of fibres size and shape data of the posterior external vs central middle area for #8005 and #9006, considering both valves together. pe: posterior external, cm: central middle. Significant values (_p_–value ≤ 0.05) are marked in bold.

Sample	Position	_n_	Mean	σ	Min	Max	_p_-values
Feret diameter (max) (µm):							
#8005	pe	10	7.92	3.30	4.85	14.97	#8005 pe vs #9006 pe 0.265
#8005	cm	36	12.29	1.64	9.63	15.89	#8005 cm vs #9006 cm 0.171
#9006	pe	10	6.45	1.95	4.59	11.41	#8005 pe vs #8005 cm **0.003**
#9006	cm	25	11.73	1.39	8.68	15.24	#9006 pe vs #9006 cm **< 0.001**
Roundness:							
#8005	pe	10	0.33	0.097	0.155	0.446	#8005 pe vs #9006 pe 0.547
#8005	cm	36	0.25	0.045	0.162	0.374	#8005 cm vs #9006 cm **0.012**
#9006	pe	10	0.35	0.079	0.232	0.500	#8005 pe vs #8005 cm **0.040**
#9006	cm	26	0.28	0.043	0.195	0.369	#9006 pe vs #9006 cm **0.022**
Convexity:							
#8005	pe	10	0.981	0.007	0.973	0.994	#8005 pe vs #9006 pe 0.308
#8005	cm	35	0.982	0.008	0.968	1.001	#8005 cm vs #9006 cm 0.277
#9006	pe	9	0.985	0.007	0.975	0.999	#8005 pe vs #8005 cm 0.829
#9006	cm	26	0.984	0.007	0.967	1.001	#9006 pe vs #9006 cm 0.775

Figure 8. Comparisons of the fibre size and shape of *M. venosa* (ventral and dorsal valve) at different positions along the posterior-anterior axis; pH conditions of culturing or natural environment are reported. One circle point represents one measurement. Outliers have been removed, the latter were identified with Tukey's fences (Tukey, 1977), when falling outside the fences F1 and F2 [F1 = Q1 - 1.5IQR; F2 = Q3 + 1.5IQR; Q1/Q3 = first/third quartiles; IQR (interquartile range) = Q3 - Q1].

3.3.2 During–culturing

Transverse sections obtained by smoothing of the anterior part of the shell allowed to measure the width of 1392 fibres [Max Ferret diameter (max) see in Method 1], and select 388 sub–zones for fibre boundary calculation. In addition, they allowed us to focus on the parts that were produced under the different low–pH treatments (7.66, 7.60, 7.44, and 7.35 respectively).

In all six specimens, the width of fibres increases and the number of boundaries decreases along a transect from the more external subzone to the immediately inner subzone (e.g., Z1–1 to Z1–2; Z2–1 to Z2–2; and Z3–1 to Z3–2 in Figure 9a, b, c, d). That means, within a 10 μm distance the size of fibres become larger from the exterior to the interior part of the shell.

Results from specimen #9006 (pH: 7.60 and 7.35) were compared to those of control specimen #8005 (pH: 8.00 and 8.15). Specimen #9006 cultured under low–pH conditions (pH: 7.60 and 7.35) had narrower fibres and a higher number of fibre boundaries when compared to that of control specimen #8005 (Figure 9a, c). It is worth noting that, in comparison between

the two specimens, the fibres from Z1–2 and Z2–2 of #9006 are significantly smaller than those of #8005. However, there is no significant difference in the size of fibres from subzone Z3–2 between the two specimens (Table 10).

The results from specimens (#43 and #63) grown under low pH conditions (pH: 7.66 and 7.44) for a short time interval of 214 days are difficult to interpret, as in this case, there is no direct control experiment sample to compare with the cultured specimens (Figure 9b, d). The specimens grown in the natural environment (#158, #223) have different sizes and ages and so different growth rates may affect the size of the fibres.

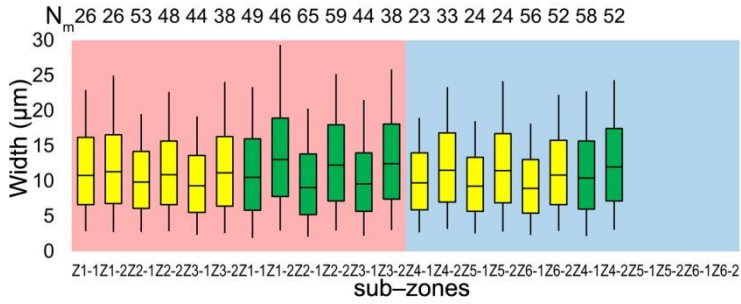**Table 10. Statistical comparison of fibres size of *M. venosa* (ventral and dorsal valve) in the anterior transverse sections (during culturing). ①: for the position of zones (Z1-1, Z2-1, Z3-1, Z1-2, Z2-2, Z3-2, Z4-1, Z5-1, Z4-2, Z5-2) see Figure 9. Significant values (p–value ≤ 0.05) are marked in bold.**

Sample	position ①	n	Mean (µm)	σ	Min (µm)	Max (µm)	Difference between means (µm) and (p–values)	Difference between means (µm) and (p–values)	Difference between means (µm) and (p–values)
							#9006 vs #8005 for the same zone	Z1 vs Z2, Z2 vs Z3 for the same vertical position in the same specimen	Z1vs Z2, Z2 vs Z3 for the same transverse position in the same specimen
#9006	Z1–1	26	4.43	1.06	2.86	6.74	0.23 (0.402)	#9006 Z1–1 vs Z2–1	
#8005	Z1–1	49	4.66	1.13	1.89	7.37		**0.60 (0.013)**	
#9006	Z2–1	53	3.83	0.66	2.76	5.30	0.12 (0.419)	#9006 Z2–1 vs Z3–1 0.07 (0.650)	#9006 Z1 vs Z2 **0.48 (0.011)**
#8005	Z2–1	65	3.95	1.03	2.06	6.46			
#9006	Z3–1	38	3.76	0.80	2.32	5.55	0.32 (0.134)	#8005 Z1–1 vs Z2–1 **0.71 (0.001)**	#9006 Z2 vs Z3 0.14 (0.323)
#8005	Z3–1	44	4.08	1.05	2.22	7.53		#8005 Z2–1 vs Z3–1 0.13 (0.554)	
#9006	Z1–2	26	4.71	1.27	2.76	8.38	**0.74 (0.024)**	#9006 Z1–2 vs Z2–2 0.33 (0.200)	#8005 Z1 vs Z2 **0.59 (< 0.001)**
#8005	Z1–2	46	5.45	1.29	2.94	10.43			
#9006	Z2–2	48	4.38	0.90	2.87	7.00	**0.62 (0.001)**	#9006 Z2–2 vs Z3–2 0.30 (0.144)	#8005 Z2 vs Z3 0.09 (0.595)
#8005	Z2–2	59	5.00	0.97	2.94	7.16			
#9006	Z3–2	40	4.68	1.01	2.57	7.76	0.40 (0.087)	#8005 Z1–2 vs Z2–2 **0.45 (0.048)**	
#8005	Z3–2	38	5.08	1.00	3.02	7.78		#8005 Z2–2 vs Z3–2 0.08 (0.720)	
#9006	Z4–1	23	3.79	0.71	2.72	4.99	**0.72 (0.003)**		
#8005	Z4–1	58	4.51	1.02	2.15	7.11		#9006 Z4–1 vs Z5–1 0.11 (0.594)	
#9006	Z5–1	24	3.68	0.72	2.54	5.19	NA		#9006 Z4 vs Z5 0.09 (0.615)
#9006	Z4–2	33	4.61	0.89	3.15	6.55	0.24 (0.272)		
#8005	Z4–2	52	4.85	1.01	3.07	6.90		#9006 Z4–2 vs Z5–2 0.06 (0.811)	
#9006	Z5–2	24	4.67	1.08	2.79	7.48	NA		

							#63 vs #43 vs #158/223 for the same zone	Z1 vs Z2 for the same vertical position in the same specimen	Z1 vs Z2 for the same transverse position in the same specimen
#63	Z1–1	36	3.37	0.59	2.39	4.97	#63 vs #158/223 **0.40 (0.013)**	#63 Z1–1 vs Z2–1 **0.72 (< 0.001)**	
#43	Z1–1	70	3.73	0.98	1.63	6.94			
#158/223	Z1–1	29	2.97	0.66	2.03	4.52	#43 vs #158/223 **0.76 (< 0.001)**	#43 Z1–1 vs Z2–1 0.26 (0.109)	
#63	Z2–1	24	4.09	0.75	2.84	5.85	#63 vs #158/223 0.17 (0.404)	#158/223 Z1–1 vs Z2–1 **0.95 (< 0.001)**	#63 Z1 vs Z2 **0.80 (< 0.001)**
#43	Z2–1	61	3.99	0.82	1.95	5.88			
#158/223	Z2–1	56	3.92	0.83	2.17	6.14	#43 vs #158/223 0.07 (0.691)		#43 Z1 vs Z2 **0.40 (0.001)**
#63	Z1–2	35	4.02	0.87	2.56	6.19	#63 vs #158/223 **0.73 (0.001)**		#158/223 Z1 vs Z2 **1.2 (< 0.001)**
#43	Z1–2	71	4.04	0.87	2.16	7.24		#63 Z1–2 vs Z2–2 **0.95 (< 0.001)**	
#158/223	Z1–2	25	3.29	0.67	2.04	4.73	#43 vs #158/223 **0.75 (< 0.001)**	#43 Z1–2 vs Z2–2 **0.58 (0.001)**	
#63	Z2–2	20	4.97	0.95	3.64	7.19	#63 vs #158/223 0.28 (0.234)	#158/223 Z1–2 vs Z2–2 **1.4 (< 0.001)**	
#43	Z2–2	56	4.62	1.10	2.68	7.67			
#158/223	Z2–2	55	4.69	0.85	3.02	7.09	#43 vs #158/223 0.07 (0.688)		

Figure 9. Differences in sizes of fibres of *M. venosa* (ventral and dorsal valve) in the anterior transverse sections of specimens cultured at different pH conditions. (a) (b): The bottom/top of the box and the band inside the box are the first/third quartiles and the median of the data respectively; ends of the whiskers represent the minimums and maximums. (c) (d): Circle point represents average data, N_m: number of measurement.

3.4 Stable isotopes

The carbon and oxygen isotope compositions were measured along the shell growth increments in the dorsal and ventral valves (Figure 10). In the *before–culturing* part of the shell, $\delta^{13}C$ values varied between -2.02 and +0.45 ‰ in control group specimens #8004 and #8005, whereas they varied between -9.24 and -0.53 ‰ in the low pH group specimens #9004, #9005 and #9006. Similarly, in the before-culturing shell part, $\delta^{18}O$ values varied between -2.39 and +0.21 ‰ in the control group specimens #8004 and #8005, but varied between -4.92 and +0.05 ‰ in the low pH group specimens #9004, #9005 and #9006.

In the *during–culturing* part, $\delta^{13}C$ values varied between -6.80 and -1.34 ‰ in the control group specimens #8004 and #8005, whereas they varied between -27.09 and -9.69 ‰ in the low pH group specimens #9004, #9005 and #9006 (Figure 10). Concomitantly, $\delta^{18}O$ values varied between -6.80 and -1.34 ‰ in the control group specimens #8004 and #8005, but varied between -6.97 and -5.29 ‰ in the low pH group specimens #9004, #9005 and #9006 (Figure 10).

A marked drop in $\delta^{13}C$ and $\delta^{18}O$ is recorded in the shell increments produced *during–culturing*, particularly so in the specimens grown under low pH conditions of 7.60 and 7.35, where $\delta^{13}C$ values decreased to -27.09 ‰ (Figure 10).

23

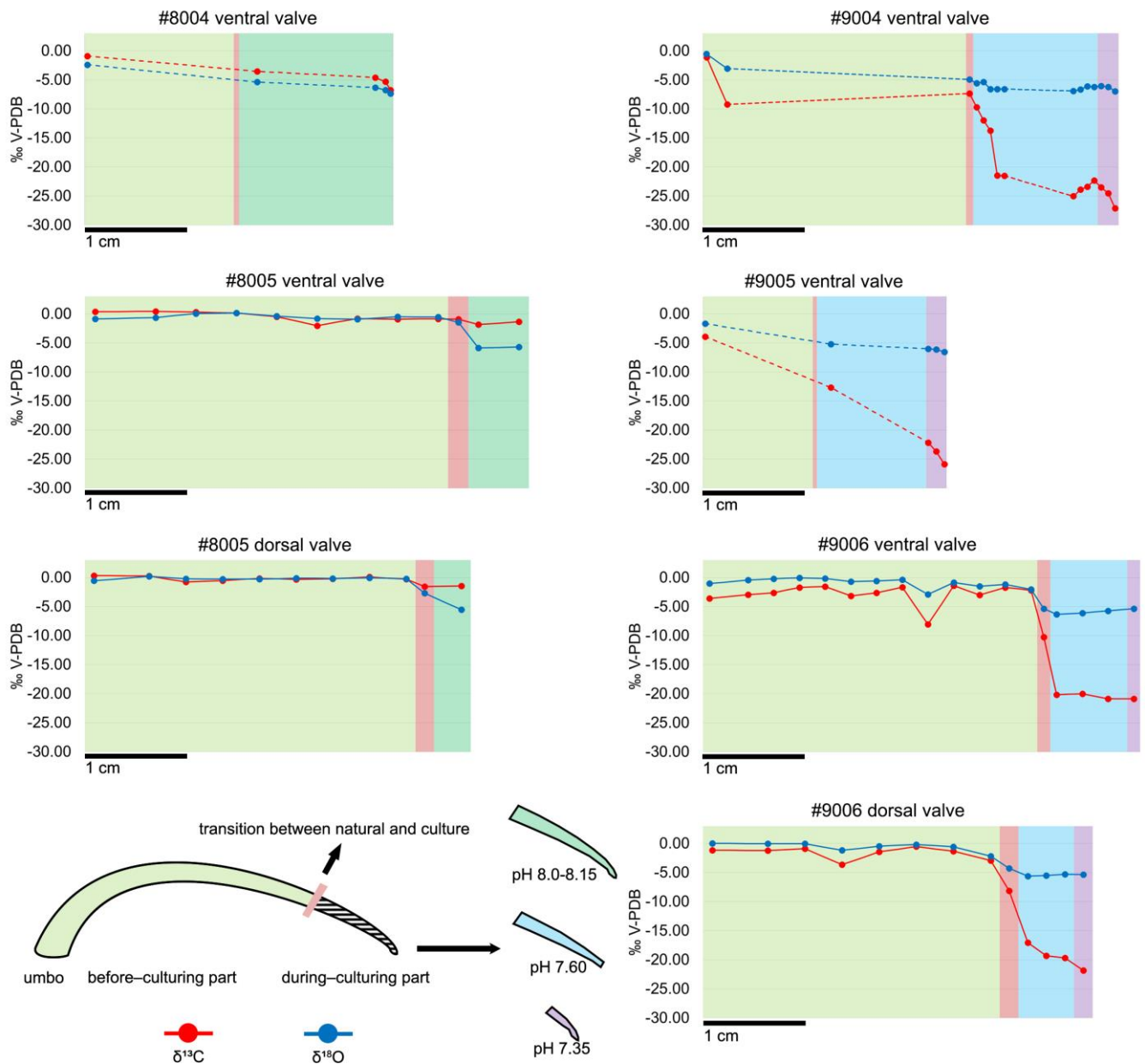**Figure 10. Plots of δ¹³C and δ¹⁸O of the ventral and dorsal valves of *M. venosa* specimens along their growth axis. Different colour backgrounds represent different pH conditions during growth. When few data were available, data-points were joined by dashed lines.**

24

4 Discussion

4.1 Microstructure and organic components relationship

Before discussing whether and how acidification may affect the microstructure of the brachiopod shell, it is important to examine the relationship between the microstructure and the amount of organic components within the shell. It has already been stated that, in fossil and recent brachiopods, different shell microstructures have different amounts of shell organic components (Garbelli et al., 2014, 2017; Casella et al., 2018; Ye et al., 2018a).

This holds true for most rhynchonelliformean brachiopods, the primary layer of *M. venosa* consists of acicular and granular calcite (Williams, 1968, 1973, 1997; MacKinnon and Williams, 1974; Williams and Cusack, 2007; Casella et al., 2018). Analyses of electron backscatter diffraction show that the primary layer is a thin nanocrystalline layer with higher micro–hardness and smaller–sized calcite crystallites compared to those of the secondary layer (Griesshaber et al., 2004). In addition, each spherical and small unit is coated by a mixture of organics and amorphous calcium carbonate (Cusack et al., 2010). This, *per se*, may suggest a higher amount of organic components associated with the primary layer in contrast to other shell layers (i.e. secondary or in some species tertiary layer), but it has never been proven.

In fossils, the primary layer is likely absent or if present diagenetically altered and it will luminesce (Grossman et al., 1991), suggesting that higher amounts of organics may be present. However, this has been also ascribed to the incorporation of magnesium into the lattice (Popov, et al., 2007; Cusack et al., 2008). A report of higher sulphur concentration in the primary layer of the brachiopod *Terebratulina retusa* may suggest the presence of a sulphur-rich organic component, but backscatter electron imaging revealed contradictory results (England et al., 2007). Cusack et al. (2008) showed that, in the same species, the sulphate concentration is higher in the primary layer than in the secondary layer.

Since there is no conclusive evidence for this observation, we cannot relate the increase in thickness of the primary layer to changes in organics within the shell. With respect to previous findings (Williams, 1966; Parkinson et al., 2005), our results show that the thickness of the primary layer of *M. venosa* is much less uniform and shows an increase with growth, which is more evident during culturing at low pH conditions. However, disturbances (stress condition with handling before and at the start of the culturing) may also cause an abrupt change in thickness.

Endopunctae, which during life are filled with mantle expansions, are widely distributed in the shell of *M. venosa* and show the superficial hexagonal close-packing pattern documented by Cowen (1966). The biological function of endopunctae is still controversial, with some suggesting, that generally in living organisms, they serve as support and protection structures (Williams, 1956, 1997), as sensors, or as storage and respiration features (Pérez–Huerta et al., 2009). With more endopunctae filled by mantle expansions, the amount of organic tissue would increase in the same volume of shell. The density of endopunctae has been related to temperature, as species living at higher temperatures have greater endopunctae density (Campbell, 1965; Foster, 1974; Peck et al., 1987; Ackerly et al., 1993). The present analyses support the concept that the increase in endopunctae density may be related in part to ontogeny and to low pH condition. This may be expected, as organisms living under low pH conditions have to up-regulate their internal pH to be able to calcify as demonstrated in *M.*

venosa by Jurikova et al. (in review) and also observed in other calcifiers such as corals (McCulloch et al., 2012; Movilla et al., 2014). This would require a higher energy cost and a larger respiration/storage surface would satisfy this requirement.

In addition to the thickness of the primary layer and the density of the endopunctae, the size changes of the individual fibres within the fibrous secondary layer may also contribute to the variability in organic components. Most of the recent rhynchonelliformean brachiopods, and *M. venosa* in particular, possess a shell mainly made of a fibrous secondary layer (Williams, 1997; Parkinson et al., 2005; Williams and Cusack, 2007). Each fibre of this layer is secreted by the mantle and it is ensheathed by an organic membrane (e.g., Jope, 1965; Williams, 1968; MacKinnon, 1974; Williams and Cusack, 2007; Cusack et al., 2008; Casella et al., 2018). Thus, with a decrease in size but within the same shell volume the surface area increases and with it the amount of organic components. Recently, the relationship between the size of fibres and shell organic components was discussed in detail (Garbelli, 2017; Garbelli et al., 2017; Ye et al., 2018a). The main conclusion is that the smaller the calcite fibres, the higher the organic component in the shell (cf. Figure 11). Thus, smaller fibres, and a greater endopunctae density may lead to higher organic content per shell volume (Figure 11).
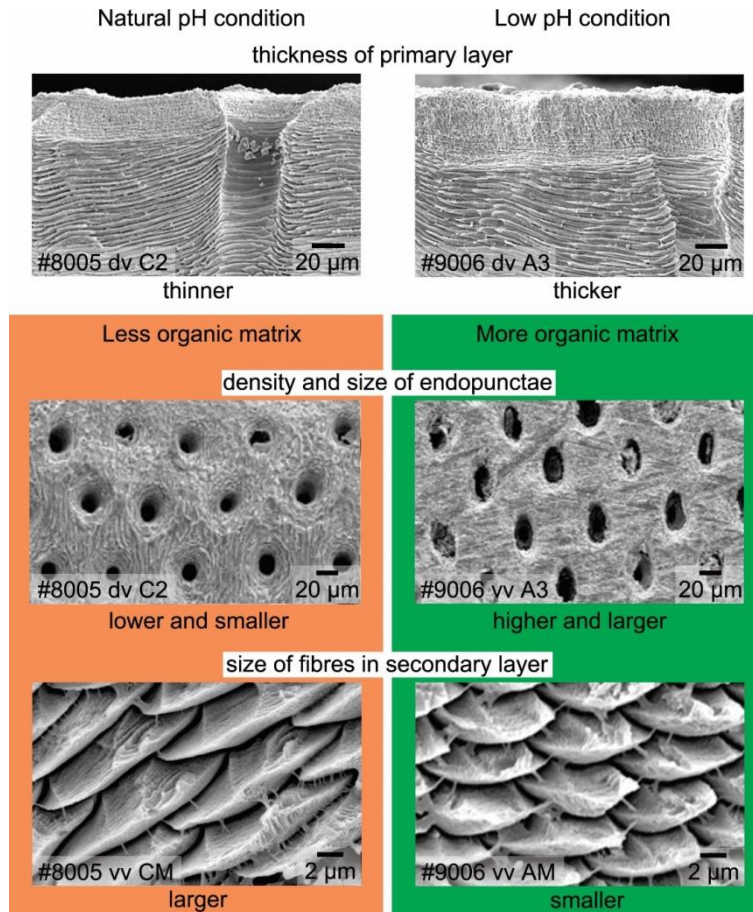

Figure 11. Relationship between the microstructure and the organic components of calcified shells of brachiopods. Position information see Figure 6 and Figure 7; dv: dorsal valve; vv: ventral valve; CM: central middle part; AM: anterior middle part.

26

4.2 Low pH and brachiopod microstructure

Several studies tried to understand how marine carbonate-shelled animals respond to ocean acidification, such as brachiopods (McClintock et al., 2009; Cross et al., 2015, 2016, 2018; Jurikova et al., in review), bivalves (e.g., Berge et al., 2006; McClintock et al., 2009; Beniash et al., 2010; Parker et al., 2010; Melzner et al., 2011; Talmage and Gobler, 2011; Amaral et al., 2012; Hiebenthal et al., 2013; Coleman et al., 2014; Gobler et al., 2014; Milano et al., 2016), cold–water scleractinian corals (e.g., Form and Riebesell, 2012; McCulloch et al., 2012; Jantzen et al., 2013b; Büscher et al., 2017) and sea urchins (Suckling et al., 2015) (Supplementary table 1). The results of these studies show that, in general, seawater acidification reduces the growth rate of marine calcifiers (Michaelidis et al., 2005; Shirayama and Thornton, 2005; Berge et al., 2006; Bibby et al., 2007; Beniash et al., 2010; Nienhuis et al., 2010; Thomsen and Melzner, 2010; Fernández–Reiriz et al., 2011; Melzner et al., 2011; Mingliang et al., 2011; Parker et al., 2011, 2012; Talmage and Gobler, 2011; Liu and He, 2012; Navarro et al., 2013; Milano et al., 2016).

For brachiopods, in the *Liothyrella uva* (Antarctic) and *Calloria inconspicua* (New Zealand), no ocean acidification effects on shell growth were detected by Cross et al. (2015, 2016, 2018), although the shells of the former species may rapidly dissolve in acidified waters (McClintock et al., 2009). However, *C. inconspicua* from the same locality in New Zealand (Paterson Inlet, Stewart Island) laid down a denser shell over the last 120 years, with nearby environmental conditions increased by 0.6 °C from 1953 to 2016, and slightly increased by 35.7 µatm in $p\text{CO}_2$ from 1998 to 2016 (Cross et al., 2018). These changes are in line with global trends of ocean pH and temperature since the industrial revolution (Caldeira and Wickett, 2005; Orr et al., 2005; IPCC, 2013).The present experiment showed that growth of specimen was not affected by the low pH conditions, instead their growth was similar to that of specimens cultured under control conditions (#9006, ~0.9 cm in the ventral valve, ~0.8 cm in the dorsal valve; 8005, ~0.5 cm in the ventral valve, ~0.4 cm in the dorsal valve). Based on the von Bertalanffy growth function, Baumgarten et al. (2013) calculated an expected growth increment and rate and we compared those parameters with the measured ones under control and low-pH conditions. The results in Figure 12 demonstrate that the measured individual growth rates are within the range of the ones of naturally growing individuals.
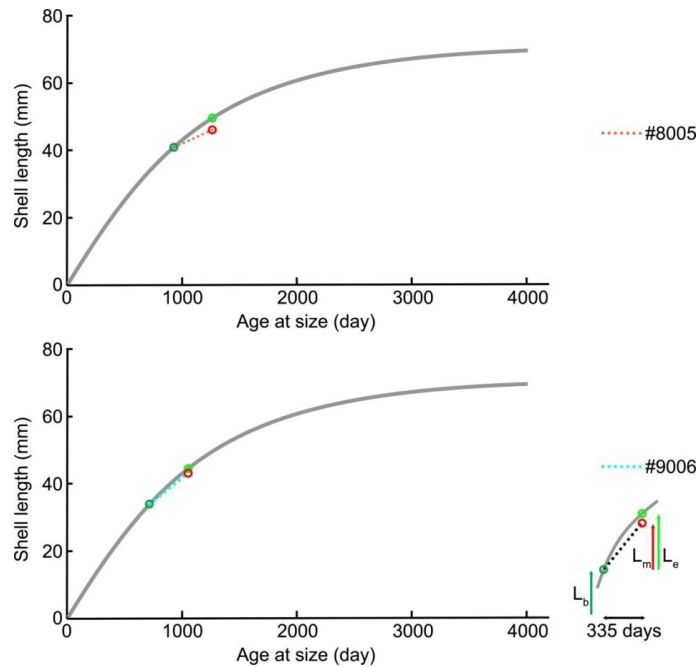
Figure 12. Projection of shell length of ventral valves on the von Bertalanffy growth function (grey line) $L_t = 71.53 [1 - e^{-0.336(t-t0)}]$, source from Baumgarten et al. (2013), L_b: shell length at the beginning of culturing; L_m: measured shell growth at the end of culturing; Le: expected shell growth.

A limiting factor is the small database, but in general, the present observations agree with studies that show no or little impact of acidification on the growth rates of marine calcifiers (cf., Marchant et al., 2010; Thomsen et al., 2010; Range et al., 2011, 2012; Talmage and Gobler, 2011; Dickinson et al., 2012; Fernández–Reiriz et al., 2012; Liu and He, 2012; Hiebenthal et al., 2013; Cross et al., 2015, 2016, 2018) or, even an increase in respiration, shell growth or metabolic rates after having experienced low pH condition (Wood et al., 2008; Cummings et al., 2011; Parker et al., 2012). We note however, that a combined effect of multiple stressors, such as low pH, lower dissolved oxygen and higher temperature or scarce food availability is more complex and potentially detrimental.. For instance, Steckbauer et al. (2015) reported that hypoxia and increased pCO_2 could significantly reduce the respiration rate of some marine invertebrates (Anthozoa, Gastropoda, Echinoidea and Crustacea). On the other hand, the highest growth rate in the bivalve *Macoma balthica* [= *Limecola balthica* (Linnaeus, 1758)] was observed in seawater with low O_2 and high pH (Jansson et al., 2015). Gobler et al. (2014) reported that juveniles of the bivalves *Argopecten irradians* (Lamarck, 1819) and *Mercenaria mercenaria* (Linnaeus, 1758) were not affected by and when hypoxia or acidification was applied individually, but the growth rate decreased when juveniles were exposed to both conditions simultaneously.

To explore the effects of acidification on brachiopod biomineralization, the microstructures of the specimens cultured for 214 days (#43, pH = 7.66 ±0.04; and #63, pH = 7.44 ±0.08) and the other population cultured for 335 days (#8005, pH =

28

8.0 to 8.15 $\pm$ 0.05; and #9006, pH = 7.6 to 7.35 $\pm$ 0.05) were investigated in detail. No conclusive consideration can be carried out on the specimens cultured for 214 days (#43 and #63), but in the other culturing experiments conducted for 335 days, the microstructure produced by the specimen cultured at low pH conditions was different from that produced under control condition: 1) the thickness of the primary layer increased with culturing (supplementary figure 1a-d); 2) the density and size of the endopunctae were higher (supplementary figure 1e-h); and 3) the fibres of the secondary layer were smaller. The punctal pattern detected here is different from that observed by Cross et al. (2018), who recorded no change in the punctal density of the ventral valve of *C. inconspicua* on specimens from the last 120 years. Also different is the trend in size of the endopunctae, which measured in the dorsal valve by Cross et al. (2018), seems to decrease. However, the slight environmental changes of the natural environment (refs. in Cross et al., 2018) are very different from those of our culturing experiments. Furthermore, the size of the endopunctae was measured from the dorsal valve only by Cross et al. (2018), whereas the increase in size we report was observed only from the ventral valve of *M. venosa*. A potential factor controlling this could be the duration of culturing under low-pH conditions. We note, however, that during the second phase of this acidification experiment (pH = 7.35), the seawater was strongly under-saturated with respect to calcite (Ω_{cal} = 0.6), suggesting that the observed structural changes could be also linked to the saturation state. Conversely, the duration of low-pH conditions as a controlling factor is also in line with the few data available in the literature on microstructural changes during acidification. Milano et al. (2016) reported no significant difference in the prismatic microstructure of the cockle *Cerastoderma edule* when cultured under low pH conditions for about 2 months, except for dissolution of ontogenetically younger parts of the shell. Similarly, a study by Stemmer et al. (2013) on the clam *Arctica islandica* revealed that there was no effect on the shape and size of the crystals in the homogeneous microstructure after three months of culturing at low pH (Supplementary table 1). However, the experiments conducted by Fitzer et al. (2014a, b) for six months on the blue mussel *Mytilus edulis* showed that the animals exposed to low pH and high pCO$_2$ tend to produce less organised, disorientated calcite crystals and an unordered layer structure.

Thus, in bivalves, and similar to our observations, the duration of culturing may be crucial in recording significant effects. The present results lend support to the microstructure variation observed in brachiopods during the end-Permian extinction event and concomitant ocean acidification (Garbelli et al., 2017). During this event, both Strophomenata and Rhynchonellata produced more organic rich shells to cope with the long term and protracted seawater acidification effects (Garbelli et al., 2017).

4.3 Stable isotope variation at low pH condition

Brachiopod shells are commonly used as archives for deep-time paleoenvironmental reconstructions as they potentially record the original geochemical composition of the seawater they lived in (Grossman et al., 1993; Banner and Kaufman, 1994; Mii and Grossman, 1994; Mii et al., 2001; Brand et al., 2003, 2011, 2016; Jurikova et al., in review). Several studies suggest that carbon and oxygen isotope compositions of the secondary layer of brachiopod shells, especially slow-growing species – and particularly the innermost shell parts – tend to be close to equilibrium with the ambient seawater temperature

(e.g., Popp et al., 1986; Carpenter and Lohmann, 1995; Parkinson et al., 2005; Brand et al., 2013, 2015, 2016; Takayanagi et al., 2013; Yamamoto et al., 2013). Recently, Bajnai et al. (2018) documented that brachiopods do not incorporate oxygen isotopes in thermodynamic equilibrium with ambient seawater, and appear to be subjected to taxon-specific growth-rate induced kinetic effects. The documented isotopic offset appears to be relatively constant throughout the range of brachiopod

5 shell production from cold to warm environments. Thus, the brachiopod oxygen isotope composition, when corrected for the seawater-^{18}O contribution records ambient water temperatures close to those observed for their ambient environment (Brand et al., 2013). Overall, the δ^{18}O values of brachiopods remain a mainstay and robust proxies of paleoenvironmental temperature conditions.

In general, the measured δ^{13}C (between -8.05 ‰ and +0.45 ‰) and δ^{18}O (between -3.04 ‰ and +0.21 ‰) values of the

10 secondary layer produced during growth in the natural environment (Figure 10) are similar to previous results from the shells of *M. venosa* (Penman et al., 2013; Ullmann et al., 2017; Romanin et al., 2018). Furthermore, the present results show that there are no significant differences in δ^{13}C and δ^{18}O values between the dorsal and the ventral valves (*p*–values in δ^{13}C and δ^{18}O of #8005 are 0.437 and 0.491 respectively, *p*-values in δ^{13}C and δ^{18}O of #9006 are 0.862 and 0.910 respectively), which is in agreement with previous findings (e.g., Parkinson et al., 2005; Brand et al., 2015; Romanin et al., 2018).

15 In the naturally grown shell *before–culturing*, the δ^{13}C and δ^{18}O values are relatively stable along the ontogenetic direction (Supplementary table 2), except for the depleted values at approximately mid–shell length in both #8005 and #9006. In particular, in #9006, in this part of the shell values drop to about -6 ‰ for δ^{13}C and -2 ‰ for δ^{18}O values (Figure 10). Since the samples were taken from the mid-shell layer and not from the shell interior, we can exclude that the isotope negative shift was produced by shell material added during the *during–culturing* shell thickening. This small drop may be an artefact of

20 both sampling and analytical uncertainties. However, it does not distract from the isotopic drop observed with culturing. Also, negative isotope excursions of a similar magnitude were recorded in *M. venosa* specimens from the South America shelf by Ullmann et al. (2017) and Romanin et al. (2018). Ullmann et al. (2017) implied that these variable δ^{13}C and δ^{18}O values indicate isotope disequilibrium with ambient waters in Terebratellids. In contrast, Romanin et al. (2018), who also analysed specimens collected from Comau Fjord, attributed the negative isotope excursion to environmental perturbations, in

25 particular, to changes in seawater productivity and temperature, and/or to anthropogenic activities. Negative shifts in both, δ^{13}C and δ^{18}O values during ontogeny have been also observed in the brachiopod *Terebratella dorsata*, which co–occurs with *M. venosa* and have been explained by the effect of resorption in corresponding muscle scar areas (Carpenter and Lohmann, 1995). Here, we follow the interpretation of Romanin et al. (2018) to explain the mid–shell excursion observed in our specimens.

30 The most prominent change in δ^{13}C values was observed in the secondary layer produced *during–culturing* under low pH conditions, reflecting the composition of the $\delta^{13}C_{DIC}$ (δ^{13}C VPDB: -23.63 ‰ for the low pH / high pCO$_2$ conditions and -2.03 ‰ for the control conditions, during the last culturing phase). The δ^{13}C values were significant depleted by more than 20 ‰ in the specimens cultured under low pH / high pCO$_2$ conditions (pH 7.60 and pH 7.35; #9004, #9005 and #9006) (Figure 10, Appendix, Supplementary table 2), whereas the depletion was lower and only a few per mil (about 0.9–1.2 ‰) in the control

specimens (pH 8.00 and 8.15; #8004 and #8005). This demonstrates that the $\delta^{13}C$ values of *M. venosa* to a large extent reflect the composition of the CO_2 source, and thus present a valuable geochemical archive. Similar observations have also been reported for other calcifiers cultured under controlled experimental settings with pH mediated by CO_2-bubbling. For a comparison, Hahn et al. (2014) reported a decreasing trend of about 10 ‰ in $\delta^{13}C$ values in the blue mussel *Mytilus edulis*

5 when exposed to seawater conditions of pH 8.03 (pCO$_2$ 612 µatm) and pH of 7.21 (pCO$_2$ 4237 µatm). In corals, a species– specific $\delta^{13}C$ response to high pCO$_2$ conditions was reported by Krief et al. (2010) of more negative 2.3‰ and 1.5‰ $\delta^{13}C$ values in *Porites* sp. after 14 months of culturing at low pH conditions (pH 7.49, pCO$_2$ 1908 µatm and 7.19 pCO$_2$, 3976 µatm), whereas no significant difference was found in other coral species, such as *Stylophora pistillata* (Esper, 1797).

In our culturing experiments, oxygen isotope compositions of the shells record only a minor depletion *during–culturing* at

10 different pH conditions [$\delta^{18}O$ (VPDB): -6.4 ‰ to -7.9 ‰ / (VSMOW): ~ +23.6‰ to +24.3 ‰] in comparison to the values observed in the shell parts grown under natural conditions, following the changes in the $\delta^{18}O_{H2O}$.

The fractionation of carbon and oxygen isotopes between phases – brachiopod calcite and culture seawater – is defined as $\Delta^{13}C_{cal–DIC}$ or $\Delta^{18}O_{cal–sw}$ = 1000 × ln$\alpha_{cal–DIC/sw}$, where $\alpha_{cal–DIC/sw}$ = [$^{13}C/^{12}C$]$_{cal}$ / [$^{13}C/^{12}C$]$_{DIC}$ or [$^{18}O/^{16}O$]$_{cal}$ / [$^{18}O/^{16}O$]$_{sw}$, respectively. The calculated values based on our culture measurements are presented in Table 11.

15

Table 11. Calculated carbon and oxygen fractionation factors for brachiopods based on cultured *M. venosa* and culture seawater.

Sample #ID	Treatment	Avg. $\Delta^{13}C_{cal-DIC}$	Avg. $\Delta^{18}O_{cal-sw}$	Growth temperature
#8004	Control	-4.06	29.99	10 ℃
#9005	Acidification pH 7.35	-1.21	30.92	10 ℃
#9004	Acidification pH 7.35	-2.23	30.70	10 ℃

For carbon isotopes, we observe variable $\Delta^{13}C_{cal-DIC}$ between the different specimens and culturing treatments, and it is inconclusive if this is linked to culturing conditions, differences between individuals or involves an ontogenetic component.

20 It appears that there is about a 2 ‰ difference between the control specimen and samples from the acidification treatments (pH 7.35), with the last one being, strikingly, closer to the equilibrium with seawater DIC. Possibly, this illustrates the variability in kinetic effects (Bajnai et al., 2018), but may also be linked to changes in the source $\delta^{13}C_{DIC}$ in the control treatment. More studies are needed to fully answer this question.

However, our brachiopod $\delta^{18}O$ values are offset from calcite equilibrium $\delta^{18}O$ (-4.4‰, relative to 10°C from Watkins et al.,

25 2013) by -2.2‰ to -2.7‰, for the low-pH and the control specimen, respectively. This offset is comparable to that recorded by Bajnai et al. (2018). There, the *M. venosa* specimen showed apparent equilibrium $\delta^{18}O$ relative to Kim and O'Neil (1997) which translates to a ca. -1.5‰ offset, relative to Watkins et al. (2013). In addition, alike in the experiment of Watkins et al. (2013), we observed a slight trend in pH, with higher $\Delta^{18}O_{cal–sw}$ at lower pH.

Thus, the data suggest that large part of the secondary layer isotope record may reflect the environmental conditions

30 supporting the interpretation of brachiopod shells as good archives of geochemical proxies, even when stressed by ocean acidification.

31

5 Conclusions

This study combines the analysis of shell microstructures on 6 specimens consisting of 1932 fibre size measurements, 170 primary layer thickness measurements, 256 punctal density and diameter measurements and stable isotope geochemistry on 5 specimens of 79 sample analyses, on brachiopods cultured at low pH conditions for different time intervals. The results suggest the following conclusions.

In brachiopod specimens cultured for a period of 11 months, the microstructure produced by the specimen cultured at low pH (from pH 7.60 to pH 7.35) is different from that produced under control conditions (pH 8.00 and 8.15). In particular, the microstructure of shells produced at low pH tends to be more organic rich. A result that lends strong support to brachiopod microstructure variations observed in fossil counterparts and the related effect of ocean acidification.

Brachiopod shell parts precipitated during culture conditions of low pH for about one year record a change in the microstructure but not in the growth rate.

Their $\delta^{13}C$ and $\delta^{18}O$ values are rather constant during growth but experience a sharp drop during culturing. In particular, the $\delta^{13}C$ values dropped abruptly in specimens cultured for one year at low pH conditions. This drop is related to the source of carbon dioxide gas used in the culture setup.

Brachiopods are thus faithful recorders of the ambient carbon and oxygen isotope compositions, even when stressed by environmental perturbations such as ocean acidification.

The present observations are invaluable in using proxies and shell morphologic features for studying ocean acidification events and changes in atmospheric CO_2 contents in the geologic past.

References:

Ackerly, S., Cisne, J. L., Railsback, L. B., and Anderson, T. F.: Punctal density in the Ordovician orthide brachiopod *Paucicrura rogata*: anatomical and paleoenvironmental variation, Lethaia, 26, 17–24, 1993.

Amaral, V., Cabral, H. N., and Bishop, M. J.: Moderate acidification affects growth but not survival of 6–month–old oysters, Aquatic Ecol., 46, 119–127, 2012.

Atkinson, M. J. and Bingman, C.: Elemental composition of commercial seasalts, J. Aquaricult. Aquat. Sci., 8, 39–43, 1998.

Bajnai, D., Fiebig, J., Tomašových, A., Milner G. S., Rollin-Bard, C., Raddztz, J., Löffler, N., Primo-Romos, C., and Brand, U.: Assessing kinetic fractionation in brachiopod calcite using clumped isotopes, Sci. Rep., 8, 533, 2018.

Banner, J. L. and Kaufman, J.: The isotopic record of ocean chemistry and diagenesis preserved in non-luminescent brachiopods from Mississippian carbonate rocks, Illinois and Missouri, Geol. Soc. Am. Bull., 106, 1074–1082, 1994.

5 Baumgarten, S., Laudien, J., Jantzen, C., Häussermann, V., and Försterra, G.: Population structure, growth and production of a recent brachiopod from the Chilean fjord region, Mar. Ecol., 35, 401–413, 2013.

Beniash, E., Ivanina, A., Lieb, N. S., Kurochkin, I., and Sokolova, I.: Elevated level of carbon dioxide affects metabolism and shell formation in oysters *Crassostrea virginica*, Mar. Ecol., 419, 95–108, 2010.

Berge, J. A., Bjerkeng, B., Pettersen, O., Schaanning, M. T., and Øxnevad, S.: Effects of increased sea water concentrations
10 of CO_2 on growth of the bivalve *Mytilus edulis* L, Chemosphere, 62, 681–687, 2006.

Bibby, R., Cleall–Harding, P., Rundle, S., Widdicombe, S., and Spicer, J.: Ocean acidification disrupts induced defences in the intertidal gastropod *Littorina littorea*, Biol. Lett., 3, 699–701, 2007.

Brand, U. and Veizer, J.: Chemical diagenesis of a multicomponent carbonate system-1. Trace elements, J. Sediment. Petrol., 50, 1219–1236, 1980.

15 Brand, U., Logan, A., Hiller, N., and Richardson, J.: Geochemistry of modern brachiopods: applications and implications for oceanography and paleoceanography, Chem. Geol., 198, 305–334, 2003.

Brand, U., Logan, A., Bitner, M. A., Griesshaber, E., Azmy, K., and Buhl, D.: What is the ideal proxy of Palaeozoic seawater chemistry? Mem. Assoc. Australas., 41, 9–24, 2011.

Brand, U., Azmy, K., Bitner, M. A., Logan, A., Zuschin, M., Came, R., and Ruggiero, E., Oxygen isotopes and $MgCO_3$ in
20 brachiopod calcite and a new paleotemperature equation, Chem. Geol., 359, 23–31, 2013.

Brand, U., Azmy, K., Griesshaber, E., Bitner, M. A., Logan, A., Zuschin, M., Ruggiero, E., and Colin, P. L.: Carbon isotope composition in modern brachiopod calcite: A case of equilibrium with seawater? Chem. Geol., 411, 81–96, 2015.

Brand, U., Blamey, N., Garbelli, C., Griesshaber, E., Posenato, R., Angiolini, L., Azmy, K., Farabegoli, E., and Came, R.: Methane Hydrate: Killer cause of Earth's greatest mass extinction, Palaeoworld, 25, 496–507, 2016.

25 Büscher, J. V., Form, A. U., and Riebesell, U.: Interactive effects of ocean acidification and warming on growth, fitness and survival of the cold–water coral *Lophelia pertusa* under different food availabilities, Front. Mar. Sci., 4, 101, 2017.

Caldeira, K. and Wickett, M. E.: Anthropogenic carbon and ocean pH, Nature, 425, 365, 2003.

Caldeira, K. and Wickett, M. E.: Ocean model predictions of chemistry changes from carbon dioxide emissions to the atmosphere and ocean, J. Geophys. Res., 110, C09S04, 2005.

30 Campbell, K. S. W.: Australian Permian terebratuloids, Bur. Min. Resour. Geol. Geophys. Aust. Bull., 68, l–113, 1965.

Carpenter, S. J., and Lohmann, K. C.: $\delta^{18}O$ and $\delta^{13}C$ values of modern brachiopod shells, Geochim. Cosmochim. Acta 59, 3749–3764, 1995.

Casella, L., Griesshaber, E., Simonet Roda, M., Ziegler, A., Mavromatis, V., Henkel, D., Laudien, J., Häussermann, V., Neuser, R. D., Angiolini, L., Dietzel, M., Eisenhauer, A., Immenhauser, A., Brand, U., and Schmahl, W. W.: Micro-

and nanostructures reflect the degree of diagenetic alteration in modern and fossil brachiopod shell calcite: a multi–analytical screening approach (CL, FE–SEM, AFM, EBSD), Palaeogeogr. Palaeoclimatol. Palaeoecol., 502, 13–30, 2018.

Coleman, D. W., Byrne, M., and Davis, A. R.: Molluscs on acid: gastropod shell repair and strength in acidifying oceans, Mar. Ecol. Prog. Ser., 509, 203–211, 2014.

Comeau, S., Gorsky, G., Jeffree, R., Teyssie, J. L., and Gattuso, J. P.: Impact of ocean acidification on a key Arctic pelagic mollusc (*Limacina helicina*), Biogeosciences, 6, 1877–1182, 2009.

Cowen, R.: The distribution of punctae on the brachiopod shell, Geol. Mag., 103, 269–275, 1966.

Cross, E. L., Peck, L. S., and Harper, E. M.: Ocean acidification does not impact shell growth or repair of the Antarctic brachiopod *Liothyrella uva* (Broderip, 1833), J. Exp. Mar. Biol. Ecol., 462, 29–35, 2015.

Cross, E. L., Peck, L. S., Lamare, M. D., and Harper, E. M.: No ocean acidification effects on shell growth and repair in the New Zealand brachiopod *Calloria inconspicua* (Sowerby, 1846), ICES J. Mar. Sci., 73, 920–926, 2016.

Cross, E. L., Harper, E. M., and Peck, L. S.: A 120-year record of resilience to environmental change in brachiopods, Glob. Chang. Biol., https://doi.org/10.1111/gcb.14085, 2018.

Cummings, V., Hewitt, J., Rooyen, A. V., Currie, K., Beard, S., Thrush, S., Norkko, J., Barr, N., Heath, P., Halliday, N. J., Sedcole, R., Gomez, A., McGraw, C., and Metcalf, V.: Ocean acidification at high latitudes: potential effects on functioning of the Antarctic bivalve *Laternula elliptica*, PLoS ONE, 6, e16069, 2011.

Cusack, M., Dauphin, Y., Cuif, J. P., Salomé, M., Freer, A., and Yin, H.: Micro–XANES mapping of sulphur and its association with magnesium and phosphorus in the shell of the brachiopod, *Terebratulina retusa*, Chem. Geol., 253, 172–179, 2008.

Cusack, M., Chung, P., Dauphin, Y., and Pérez–Huerta, A.: Brachiopod primary layer crystallography and nanostructure, in: Alvarez, F., and Curry, G. B., (Eds.): Evolution and Development of the Brachiopod Shell, Special Papers in Palaeontology, 84, Aberystwyth, Palaeontological Association, 99–105, 2010.

Crippa, G., Angiolini, L., Bottini, C., Erba, E., Felletti, F., Frigerio, C., Hennissen, J. A. I., Leng, M. J., Petrizzo, M. R., Raffi, I., Raineri, G., and Stephenson, M. H.: Seasonality fluctuations recorded in fossil bivalves during the early Pleistocene: Implications for climate change, Palaeogeogr. Palaeoclimatol. Palaeoecol., 446, 234–251, 2016a.

Crippa, G., Ye, F., Malinverno, C., and Rizzi, A.: Which is the best method to prepare invertebrate shells for SEM analysis? Testing different techniques on recent and fossil brachiopods, Boll. Soc. Paleontol. Ital., 55, 111–125, 2016b.

Dickinson, G. H., Ivanina, A. V., Matoo, O. B., Pörtner, H. O., Lannig, G., Bock, C., Beniash, E., and Sokolova, I. M.: Interactive effects of salinity and elevated CO_2 levels on juvenile Eastern oysters, *Crassostrea virginica*, J. Exp. Biol., 215, 29–43, 2012.

England, J., Cusack, M., and Lee, M. R.: Magnesium and sulphur in the calcite shells of two brachiopods, *Terebratulina retusa* and *Novocrania anomala*, Lethaia, 40, 2–10, 2007.

Feely, R. A., Sabine, C. L., Lee, K., Berelson, W., Kleypas, J., Fabry, V.J., and Millero, F.J.: Impact of anthropogenic CO_2 on the $CaCO_3$ system in the oceans, Science, 305, 362–366, 2004.

Fernández–Reiriz, M. J., Range, P., Alvarez–Salgado, X. A., and Labarta, U.: Physiological energetics of juvenile clams *Ruditapes decussatus* in a high CO_2 coastal ocean, Mar. Ecol. Prog. Ser., 433, 97–105, 2011.

5 Fernández–Reiriz, M. J., Range, P., Alvarez–Salgado, X. A., Espinosa, J., and Labarta, U.: Tolerance of juvenile *Mytilus galloprovincialis* to experimental seawater acidification, Mar. Ecol. Prog. Ser., 454, 65–74, 2012.

Fitzer, S., Phoenix, V. R., Cusack, M., and Kamenos, N. A.: Ocean acidification impacts mussel control on biomineralisation, Sci. Rep., 4, doi:10.1038/srep06218, 2014a.

Fitzer, S., Cusack, M., Phoenix, V. R., and Kamenos, N. A.: Ocean acidification reduces the crystallographic control in
10   juvenile mussel shells, J. Struct. Biol., 188, 39–45, 2014b.

Form, A. U., and Riebesell, U.: Acclimation to ocean acidification during long–term CO_2 exposure in the cold-water coral *Lophelia pertusa*, Glob. Chang. Biol., 18, 843–3853, 2012.Försterra, G., Häussermann, V., and Lueter, C.: Mass occurrence of the recent brachiopod *Magellania venosa* (Terebratellidae) in the fjords Comau and Renihue, northern Patagonia, Chile, Mar. Ecol., 29, 342–347, 2008.

15 Foster, M. W.: Recent Antarctic and Subantarctic brachiopods, Antarctic Research Series, 21, American Geophysical Union, Washington, D.C., pp. 183, 1974.

Garbelli, C.: Shell microstructures in Upper Permian brachiopods: implication for fabric evolution and calcification, Boll. Soc. Paleontol. Ital., 123, 541–560, 2017.

Garbelli, C., Angiolini, L., Brand, U., and Jadoul, F., Brachiopod fabric, classes and biogeochemistry: Implications for the
20   reconstruction and interpretation of seawater carbon–isotope curves and records, Chem. Geol., 371, 60–67, 2014.Garbelli, C., Angiolini, L., and Shen, S. Z.: Biomineralization and global change: A new perspective for understanding the end–Permian extinction, Geology, 45, 19–12, 2017.

Gobler, C. J., DePasquale, E. L., Griffith, A. W., and Baumann, H.: Hypoxia and acidification have additive and synergistic negative effects on the growth, survival, and metamorphosis of early life stage bivalves, PLoS ONE, 9, e83648, 2014.

25 Griesshaber, E., Schmahl1, W., Neuser, R., Job, R., Bluem, M., and Brand, U.: Microstructure of brachiopod shells–An inorganic/organic fibre composite with nanocrystalline protective layer, Mater. Res. Soc. Symp. Proc., 844, Y9.3.1– Y9.3.6, 2004.

Grossman, E. L., Zhang, C., and Yancey, T. E.: Stable–isotope stratigraphy of brachiopods from Pennsylvanian shales in Texas, Geol. Soc. Am. Bull., 103, 953–965, 1991.

30 Grossman, E. L., Mii, H., and Yancey, T. E.: Stable isotopes in Late Pennsylvanian brachiopods from the United Stated: Implications for Carboniferous paleoceanography, Geol. Soc. Am. Bull., 105, 1284–1296, 1993.

Guinotte, J. M., Orr, J., Cairns, S., Freiwald, A., Morgan, L., and George, R.: Will human–induced changes in sea water chemistry alter the distribution of deep-sea scleractinian corals? Front. Ecol. Environ., 1, 141–146, 2006.

Hahn, S., Rodolfo–Metalpa, R., Griesshaber, E., Schmahl, W. W., Buhl, D., Hall-Spencer, J. M., Baggini, C., Fehr, K. T., and Immenhauser, A.: Marine bivalve shell geochemistry and ultrastructure from modern low pH environments: environmental effect versus experimental bias, Biogeosciences, 9, 1897–1914, 2012.

Hahn, S., Griesshaber, E., Schmahl, W. W., Neuser, R. D., Ritter, A., Hoffmann, R., Buhl, D., Niedermayr, A., Geske, A., and Immenhauser, A.: Exploring aberrant bivalve shell ultrastructure and geochemistry as proxies for past sea water acidification, Sedimentology, 61, 1625–1658, 2014.

Hiebenthal, C., Philipp, E. E. R., Eisenhauer, A., and Wahl, M.: Effects of seawater pCO_2 and temperature on shell growth, shell stability, condition and cellular stress of Western Baltic Sea *Mytilus edulis* (L.) and *Arctica islandica* (L.), Mar. Biol., 160, 2073–2087, 2013.

IPCC: Climate change 2013: the physical science basis, in: Stocker, T. F., Qin, D., Plattner, G. –K., Tignor, M., Allen, S. K., Boschung, J., Nauels, A., Xia, Y., Bex, V., and Midgley, P. M. (Eds.): Contribution of working group I to the fifth assessment report of the intergovernmental panel on climate change, Cambridge University Press, Cambridge, United Kingdom and New York, NY, USA, pp. 1535, 2013.

Jansson. A., Norkko, J., Dupont, S., and Norkko, A.: Growth and survival in a changing environment: Combined effects of moderate hypoxia and low pH on juvenile bivalve *Macoma balthica*, J. Sea Res., 102, 41–47, 2015.

Jantzen, C., Laudien, J., Sokol, S., Försterra, G., Häussermann, V., Kupprat, F., and Richter, C.: In situ short-term growth rates of a cold–water coral, Mar. Freshw. Res., 64, 631–641, 2013a.

Jantzen, C., Häussermann, V., Försterra, G, Laudien, J., Ardelan, M., Maier, S., and Richter, C.: Occurrence of a cold-water coral along natural pH gradients (Patagonia, Chile), Mar. Biol., 160, 2597–2607, 2013b.

Jantzen, C., Laudien, J., Häussermann, V., Försterra, G., and Richter, C.: Seawater carbonate chemistry measured in fjord Comau, Patagonia, Chile (02-2011), Alfred Wegener Institute, Helmholtz Center for Polar and Marine Research, Bremerhaven, PANGAEA, https://doi.org/10.1594/PANGAEA.884131, 2017.

Jope, H. M.: Composition of brachiopod shell, in Moore, R. C. (Ed.): Treatise on Invertebrate Paleontology. Part H, Brachiopoda, Geological society of America and University of Kansas Press, New York and Lawrence, pp. 156–164, 1965.

Jurikova, H., Liebetrau, V., Gutjahr, M., Rollion–Bard, C., Hu, M. Y., Krause, S., Henkel, D., Hiebenthal, C., Schmidt, M., Laudien, J., and Eisenhauer, A.: Boron isotope systematics of cultured brachiopods: response to acidification, vital effects and implications for palaeo-pH reconstruction, Geochim. Cosmochim. Acta, in review.

Kim, S.T. and O'Neil, J.R.: Equilibrium and nonequilibrium oxygen isotope effects in synthetic carbonates, Geochim. Cosmochim. Acta, 61, 3461–3475, 1997.

Krief, S., Hendy, E. J., Fine, M., Yam, R., Meibom, A., Foster, G. L., and Shemesh, A.: Physiological and isotopic responses of scleractinian corals to ocean acidification, Geochim. Cosmochim. Acta, 74, 4988–5001, 2010.

Kurihara, H.: Effects of CO_2–driven ocean acidification on the early developmental stages of invertebrates, Mar. Ecol. Prog. Ser., 373, 274–284, 2008.

Lannig, G., Eilers, S., Pörtner, H. O., Sokolova, I. M., and Bock, C.: Impact of ocean acidification on energy metabolism of oyster, *Crassostrea gigas*–changes in metabolic pathways and thermal response, Mar. Drugs, 8, 2318–2339, 2010.

Laudien, J., Häussermann, V., Försterra, G., and Göhlich, H.: Physical oceanographic profiles of seven CTD casts from Gulf of Ancud into Comau Fjord in 2014, Alfred Wegener Institute, Helmholtz Center for Polar and Marine Research, Bremerhaven, PANGAEA, https://doi.org/10.1594/PANGAEA.832187, 2014.

Liu, W. and He, M.: Effects of ocean acidification on the metabolic rated of three species of bivalve from southern coast of China, Chin. J. Oceanol. Limn., 30, 206–211, 2012.

MacKinnon, D. I.: The shell structure in spiriferide brachiopoda, Bull. Br. Mus. Nat. Hist., 5, 189–258, 1974.

MacKinnon, D. I. and Williams, A.: Shell structure of terebratulid brachiopods, Palaeontology, 17, 179–202, 1974.

Marchant, H. K., Calosi, P., and Spicer, J. I.: Short–term exposure to hypercapnia does not compromise feeding, acid–base balance or respiration of *Patella vulgata* but surprisingly is accompanied by radula damage, J. Mar. Biolog. Assoc. U.K., 90, 1379–1384, 2010.

McClintock, J. B., Angus, R. A., Mcdonald, M. R., Amsler, C. D., Catledge, S. A., and Vohra, Y. K.: Rapid dissolution of shells of weakly calcified Antarctic benthic macroorganisms indicates high vulnerability to ocean acidification, Antarct. Sci., 21, 449–456, 2009.

McCulloch, M., Trotter, J., Montagna, P., Falter, J., Dunbar, R., Freiwald, A., Försterra, G., Lopez Correa, M., Maier, C., Ruggeberg, A., and Taviani, M.: Resilience of cold–water scleractinian corals to ocean acidification: Boron isotopic systematics of pH and saturation state up–regulation, Geochim. Cosmochim. Acta, 87, 21–34, 2012.

Melzner, F., Stange, P., Trübenbach, K., Thomsen, J., Casties, I., Panknin, U., Gorb, S. N., and Gutowska, M. A.: Food supply and seawater pCO$_2$ impact calcification and internal shell dissolution in the blue mussel *Mytilus edulis*, PLoS ONE, 6, e24223, 2011.

Michaelidis, B., Ouzounis, C., Paleras, A., and Pörtner H. O.: Effects of long-term moderate hypercapnia on acid–base balance and growth rate in marine mussels *Mytilus galloprovincialis*, Mar. Ecol. Prog. Ser., 293, 109–118, 2005.

Mii, H. S., and Grossman, E. L.: Late Pennsylvanian seasonality reflected in the ^{18}O and elemental composition of a brachiopod shell, Geology, 22, 661–664, 1994.

Mii, H. S., Grossman, E. L., Yancey, T. E., Chuvashov, B., and Egorov, A.: Isotopic records of brachiopod shells from the Russian Platform–evidence for the onset of mid–Carboniferous glaciation, Chem. Geol., 175, 133–147, 2001.

Milano, S., Schöne, B. R., Wang, S., and Müller, W. E.: Impact of high pCO$_2$ on shell structure of the bivalve *Cerastoderma edule*, Mar. Environ. Res., 119, 144–155, 2016.

Mingliang, Z., Jianguang, F., Jihong, Z., Bin, L., Shengmin, R., Yuze, M., and Yaping, G.: Effect of marine acidification on calcification and respiration of *Chlamys farreri*, J. Shellfish Res., 30, 267–271, 2011.

Morse, J. W., Arvidson, R. S., and Luttge, A.: Calcium carbonate formation and dissolution, Chem. Rev., 107, 342–381, 2007.

Movilla, J., Orejas, C., Calvo, E., Gori, A., López Sanz, Á., Grinyó, J., Dominguez–Carrió, C., and Pelejero, C.: Differential response of two Mediterranean cold–water coral species to ocean acidification, Coral reefs, 33, 675–686, 2014.

Navarro, J. M., Torres, R., Acuna, K., Duarte, C., Manriquez, P. H., Lardies, M., Lagos, N. A., Vargas, C., and Aguilera, V.: Impact of medium–term exposure to elevated pCO_2 levels on the physiological energetics of the mussel *Mytilus chilensis*, Chemosphere, 90, 1242–1248, 2013.

Nienhuis, S., Palmer, A. R., and Harley, C. D. G.: Elevated CO_2 affects shell dissolution rate but not calcification rate in a marine snail, Philos. Trans. R. Soc. Lond., B, Biol. Sci., 277, 2553–2558, 2010.

Orr, J. C., Fabry, V. J., Aumont, O., Bopp, L., Doney, S. C., Feely, R. A., Gnanadesikan, A., Gruber, N., Ishida, A., Joos, F., Key, R. M., Lindsay, K., Maier-Reimer, E., Matear, R., Monfray, P., Mouchet, A., Najjar, R. G., Plattner, G. K., Rodgers, K. B., Sabine, C. L., Sarmiento, J. L., Schlitzer, R., Slater, R. D., Totterdell, I. J., Weirig, M. F., Yamanaka, Y., and Yool, A.: Anthropogenic ocean acidification over the twenty–first century and its impact on calcifying organisms, Nature, 437, 681–686, 2005.

Parker, L. M., Ross, P. M., and O'Connor, W. A.: Comparing the effect of elevated pCO_2 and temperature on the fertilization and early development of two species of oysters, Mar. Biol., 157, 2435–2452, 2010.

Parker, L. M., Ross, P. M., and O'Connor, W. A.: Populations of the Sydney rock oyster, *Saccostrea glomerata*, vary in response to ocean acidification, Mar. Biol., 158, 689–697, 2011.

Parker, L. M., Ross, P. M., O'Connor, W. A., Borysko, L., Raftos, D. A., and Pörtner, H. –O.: Adult exposure influences offspring response to ocean acidification in oysters, Glob. Chang. Biol., 18, 82–92, 2012.

Parkinson, D., Curry, G. B., Cusack, M., and Fallick, A. E.: Shell structure, patterns and trends of oxygen and carbon stable isotopes in modern brachiopod shells, Chem. Geol., 219, 193–235, 2005.

Payne, J. L. and Clapham, M. E.: End–Permian mass extinction in the oceans: an ancient analog for the twenty-first century? Annu. Rev. Earth Planet. Sci., 40, 89–111, 2012.

Peck, L. S., Clarke, A., and Holmes, L. J.: Size, shape and the distribution of organic matter in the Recent Antarctic brachiopod *Liothyrella uva*, Lethaia, 20, 33–40, 1987.

Penman, D. E., Hönisch, B., Rasbury, E. T., Hemming, N. G., and Spero, H. J.: Boron, carbon, and oxygen isotopic composition of brachiopod shells: Intra–shell variability, controls, and potential as a paleo–pH recorder, Chem. Geol., 340, 32–39, 2013.

Pérez-Huerta, A., Cusack, M., McDonald, S., Marone, F., Stampanoni, M., and MacKay, S.: Brachiopod punctae: a complexity in shell biomineralisation, J. Struct. Biol., 167, 62–67, 2009.Popov, L. E., Egerquist, E., and Holmer, L. E.: Earliest ontogeny of Middle Ordovician rhynchonelliform brachiopods (Clitambonitoidea and Polytoechioidea): implications for brachiopod phylogeny, Lethaia, 40, 85–96, 2007.

Popp, B. N., Anderson, T. F., and Sandberg, P. A.: Brachiopods as indicators of original isotopic compositions in some Paleozoic limestones, Geol. Soc. Am. Bull., 97, 1262–1269, 1986.

Range, P., Chícharo, M. A., Ben-Hamadou, R., Piló, D., Matias, D., Joaquim, S., Oliveira, A. P., and Chícharo, L.: Calcification, growth and mortality of juvenile clams *Ruditapes decussatus* under increased pCO$_2$ and reduced pH: Variable responses to ocean acidification at local scales? J. Exp. Mar. Biol. Ecol., 396, 177–184, 2011.

5 Range, P., Piló, D., Ben-Hamadou, R., Chícharo, M. A., Matias, D., Joaquim, S., Oliveira, A. P., and Chícharo, L.: Seawater acidification by CO$_2$ in a coastal lagoon environment: Effects on life history traits of juvenile mussels *Mytilus galloprovincialis*, J. Exp. Mar. Biol. Ecol., 424–425, 89–98, 2012.

Ries, J. B., Cohen, A. L., and McCorkle, D. C.: Marine calcifiers exhibit mixed responses to CO$_2$–induced ocean acidification, Geology, 37, 1131–1134, 2009.

Romanin, M., Crippa, G., Ye, F., Brand, U., Bitner, M. A., Gaspard, D., Häussermann, V., and Laudien J.: A sampling
10 strategy for recent and fossil brachiopods: selecting the optimal shell segment for geochemical analyses, Riv. Ital. Paleontol. Stratigr., 124, 343–359, 2018.

Shirayama, Y. and Thornton, H.: Effect of increased atmospheric CO$_2$ on shallow water marine benthos, J. Geophys. Res. Oceans, 110, C09S08, doi:10.1029/2004jc002618, 2005.

Smirnova, T. N. and Popiel–Barczyk, E.: Characteristics of the shell ultrastructure in Terebratellacea, in: Brachiopods
15 through time, MacKinnon, D. I., Lee, D. E., and Campbell, J. D. (Eds.): Brachiopods through time, Balkema, Rotterdam, pp. 159–165, 1991.

Steckbauer, A., Ramajo, L., Hendriks, I. R., Fernandez, M., Lagos, N. A., Prado, L., and Duarte, C. M.: Synergistic effects of hypoxia and increasing CO$_2$ on benthic invertebrates of the central Chilean coast, Front. Mar. Sci., 2, https://doi.org/10.3389/fmars.2015.00049, 2015.

20 Stemmer, K., Nehrke, G., and Brey, T.: Elevated CO$_2$ levels do not affect the shell structure of the bivalve *Arctica islandica* from the Western Baltic, PLoS ONE, 8, e70103, 2013.

Suckling, C. C., Clark, M. M., Richard, J., Morley, S. A., Thorne, M. A., Harper, E. M., and Peck, L. S.: Adult acclimation to combined temperature and pH stressors significantly enhances reproductive outcomes compared to short–term exposures, J. Anim. Ecol., 84, 773–784, 2015.

25 Takayanagi, H., Asami, R., Abe, O., and Miyajima, T.: Intraspecific variations in carbon–isotope and oxygen–isotope compositions of a brachiopod *Basiliola lucida* collected off Okinawa–jima, southwestern Japan, Geochim. Cosmochim. Acta, 115, 115–136, 2013.

Talmage, S. C., and Gobler, C. J.: Effects of elevated temperature and carbon dioxide on the growth and survival of larvae and juveniles of three species of northwest Atlantic bivalves, PLoS ONE, 6, e26941, 2011.

30 Thomsen, J., and Melzner, F.: Moderate seawater acidification does not elicit long-term metabolic depression in the blue mussel *Mytilus edulis*, Mar. Biol., 157, 2667–2676, 2010.

Thomsen, J., Gutowska, M. A., Saphörster, J., Heinemann, A., Trübenbach, K., Fietzke, J., Hiebenthal, C., Eisenhauer, A., Körtzinger, A., Wahl, M., and Melzner, F.: Calcifying invertebrates succeed in a naturally CO$_2$–rich coastal habitat but are threatened by high levels of future acidification, Biogeosciences, 7, 3879–3891, 2010.

Tukey, J. W.: Exploratory data analysis. Reading, PA: Addison–Wesley, 1977.

Ullmann, C. V., Frei, R., Korte, C., and Lüter, C.: Element/Ca, C and O isotope ratios in modern brachiopods: Species–specific signals of biomineralization, Chem. Geol., 460, 15–24, 2017.

Watkins, J. M., Nielsen, L. C., Ryerson, F. J., and DePaolo, D. J.: The influence of kinetics on the oxygen isotope composition of calcium carbonate, Earth Planet. Sci. Lett., 375, 349–360, 2013.

Watson, S., Peck, L. S., Tyler, P. A., Southgate, P. C., Tan, K. S., Day, R. W., and Morley, S. A.: Marine invertebrate skeleton size varies with latitude, temperature and carbonate saturation: implications for global change and ocean acidification, Glob. Chang. Biol., 18, 3026–3038, 2012.

Williams, A.: The calcareous shell of the Brachiopoda and its importance to their classification, Biol. Rev., 31, 243–287, 1956.

Williams, A.: Growth and structure of the shell of living articulate brachiopods, Nature, 211, 1146–1148, 1966.

Williams, A.: Evolution of the shell structure of articulate brachiopods, Spec. Pap. Palaeontol., 2, 1–55, 1968.

Williams, A.: The secretion and structural evolution of the shell of thecideidine brachiopods, Philos. Trans. R. Soc. Lond., B, Biol. Sci., 264, 439–478, 1973.

Williams, A.: Shell structure, in: Kaesler, R. L. (Ed.): Treatise on Invertebrate Paleontology, Part H, Revised, Brachiopoda, vol. 1, Geological Society of America Inc., and The University of Kansas, Boulder, Colorado, USA, pp. 267–320, 1997.

Williams, A. and Cusack, M.: Chemicostructural diversity of the brachiopod shell, in: Selden, P. A. (Ed.): Treatise on Invertebrate Paleontology, Part H, Brachiopoda Revised, vol. 6, Geological Society of America Inc., and The University of Kansas, Boulder, Colorado, USA, pp. 2396–2521, 2007.

Wood, H. L., Spicer, J. I., and Widdicombe, S.: Ocean acidification may increase calcification rates, but at a cost, Proc. R. Soc. Lond., B, Biol. Sci., 275, 1767–1773, 2008.

Yamamoto, K., Asami, R., and Iryu, Y.: Correlative relationships between carbon–and oxygen–isotope records in two cool-temperate brachiopod species off Otsuchi Bay, northeastern Japan, Paleontol. Res., 17, 12–26, 2013.

Ye, F., Crippa, G., Angiolini, L., Brand, U., Capitani, G., Cusack, M., Garbelli, C., Griesshaber, E., Harper, E., and Schmahl, W.: Mapping of recent brachiopod microstructure: a tool for environmental studies, J. Struct. Biol., 201, 221–236, 2018a.

Ye, F., Crippa, G., Garbelli, C., and Griesshaber, E.: Microstructural data of six recent brachiopod species: SEM, EBSD, morphometric and statistical analyses, Data in Brief, 18, 300–318, 2018b.